

## DISCLAIMER

SGP-TR--110

DE88 012262

This report was prepared as an account of work sponsored by an agency of the United States Government. Neither the United States Government nor any agency thereof, nor any of their employees, makes any warranty, express or implied, or assumes any legal liability or responsibility for the accuracy, completeness, or usefulness of any information, apparatus, product, or process disclosed, or represents that its use would not infringe privately owned rights. Reference herein to any specific commercial product, process, or service by trade name, trademark, manufacturer, or otherwise does not necessarily constitute or imply its endorsement, recommendation, or favoring by the United States Government or any agency thereof. The views and opinions of authors expressed herein do not necessarily state or reflect those of the United States Government or any agency thereof.

SGP-TR-110

## Injection Through Fractures

Robert Anthony Johns

May 1987

Financial support was provided through the Stanford Geothermal Program under Department of Energy Contract No. DE-AS07-84ID12529 and by the Department of Petroleum Engineering, Stanford University



Stanford Geothermal Program  
Interdisciplinary Research in  
Engineering and Earth Sciences  
STANFORD UNIVERSITY  
Stanford, California

MASTER

*Go*  
DISTRIBUTION OF THIS DOCUMENT IS UNLIMITED

## **DISCLAIMER**

**This report was prepared as an account of work sponsored by an agency of the United States Government. Neither the United States Government nor any agency Thereof, nor any of their employees, makes any warranty, express or implied, or assumes any legal liability or responsibility for the accuracy, completeness, or usefulness of any information, apparatus, product, or process disclosed, or represents that its use would not infringe privately owned rights. Reference herein to any specific commercial product, process, or service by trade name, trademark, manufacturer, or otherwise does not necessarily constitute or imply its endorsement, recommendation, or favoring by the United States Government or any agency thereof. The views and opinions of authors expressed herein do not necessarily state or reflect those of the United States Government or any agency thereof.**

## **DISCLAIMER**

**Portions of this document may be illegible in electronic image products. Images are produced from the best available original document.**



## TABLE OF CONTENTS

LIST OF FIGURES .....	v
ABSTRACT .....	vii
SECTION 1. INTRODUCTION .....	1
SECTION 2. PREVIOUS WORK .....	3
SECTION 3. EXPERIMENTAL APPARATUS.....	7
3.1 Flow Systems .....	7
3.2 Tracer Detection Systems.....	9
3.3 Data Collection System .....	11
3.4 Core Description.....	12
SECTION 4. EXPERIMENTAL PROCEDURE .....	15
4.1 Flow System Operation.....	15
4.2 Data Collection Methods .....	17
4.3 Data Processing Methods .....	19
SECTION 5. EXPERIMENTAL RESULTS .....	20
5.1 Unfractured Core Samples.....	20
5.2 Fractured Core Tests .....	24
SECTION 6. MODELING THE EXPERIMENTAL DATA.....	30
6.1 Conventional Analytical Models .....	32
6.1.1 Taylor Dispersion Model .....	33
6.1.2 Matrix Diffusion Model.....	36
6.2 Inlet Dispersion Mechanism .....	39
6.3 Modified Conventional Analytical Models.....	47
6.3.1 Matrix Diffusion Model with Dispersed Inlet Boundary Condition.....	47
6.3.2 Taylor Dispersion Model with Dispersed Inlet Boundary Condition.....	52
SECTION 7. MATRIX DIFFUSION MODEL MATCH PARAMETERS .....	54
7.1 Datum Time Correction.....	54
7.2 Breakthrough Time.....	55
7.3 Dimensionless Dispersion Coefficient .....	57
7.4 Discussion of Fracture Aperture Estimates from Model Match Parameters .....	63
SECTION 8. TRACER ADSORPTION: CALCULATED AND MEASURED TRACER RETENTION IN THE CORE .....	65
8.1 Tracer Retention for a Sorbing Tracer .....	65
8.2 Tracer Retention for a Non-Sorbing Tracer .....	69
8.3 Tracer Retention for Low Flowrate Tests .....	71
SECTION 9. INLET BOUNDARY CONDITION EFFECTS ON TEST RESULTS.....	74

SECTION 10. CORE FRACTURE APERTURE:CALCULATED VS. MEASURED .....	77
SECTION 11. SUMMARY AND CONCLUSIONS .....	80
SECTION 12. RECOMMENDATIONS .....	81
SECTION 13. NOMENCLATURE .....	82
REFERENCES .....	84
APPENDIX A: Derivation of the Continuous Injection Case Solution to Matrix-Diffusion Model .....	87
APPENDIX B: Derivatives of the Solutions of the Matrix Diffusion Model With Respect to the Nonlinear Parameters .....	98
APPENDIX C: Derivatives of the Solutions of the Convection-Dispersion Model With Respect to the Nonlinear Parameters .....	101
APPENDIX D: Listing of Programs to Perform Nonlinear Curvefitting of the Matrix Diffusion Model With a Sample Input and a Corresponding Output .....	137
APPENDIX E: Listing of Programs to Perform Nonlinear Curvefitting of the Convection Dispersion Model With a sample Input and a Corresponding Output .....	148
APPENDIX F: Complete Data Set for Test Number 11 .....	153

## LIST OF FIGURES

Fig. 1 Photograph of Core Holder, Switching Valves and Inlet and Outlet Electrodes

Fig. 2 Electrode Circuit and Flow Tee Diagram

Fig. 3 Schematic of Pipe Length Test Section

Fig. 4 Graphical Representation of Voltage Pulsing Procedure

Fig. 5 Core Photographs Before and After Tracer Tests

Fig. 6 Pore Volume Plots for Unfractured Core Tests

Fig. 7 Fractured Core Tracer Test using 80 Mesh Fracture Proppant

Fig. 8 Voltage Profile for Step Up at 3.7 cc/min

Fig. 9 Concentration Profile for Step Up at 3.7 cc/min

Fig. 10 Equivalent Slug Test for Step Up at 3.7 cc/min

Fig. 11 Voltage Profile for Step Down at 3.7 cc/min

Fig. 12 Concentration Profile for Step Down at 3.7 cc/min

Fig. 13 Equivalent Slug Test for Step Down at 3.7 cc/min

Fig. 14 Pore Volume Plots for Fractured Core Tests

Fig. 15 Fossum Model Match of 1.4 cc/min Test

Fig. 16 Fossum Model Match of 1.4 cc/min Test using Datum Correction as a Regression Variable

Fig. 17 Jensen Model Match of 1.4 cc/min Test

Fig. 18 Jensen Model Match of 16 cc/min Test

Fig. 19 Inlet Electrode Response to Tracer Front at 1.4 cc/min

Fig. 20 Inlet Electrode Response to Tracer Front at 16 cc/min

Fig. 21 Tubing Dispersion Test: Tracer Front at 1st Electrode

Fig. 22 Tubing Dispersion Test: Tracer Front at 2nd Electrode

Fig. 23 Tubing Dispersion Test: Tracer Front at 3rd Electrode

Fig. 24 Tubing Dispersion Test: Tracer Front Matched with Error Function at 1.2 cc/min

Fig. 25 Tubing Dispersion Test: Tracer Front Matched with Error Function at 4.0 cc/min

Fig. 26 Tubing Dispersion Test: Tracer Front Matched with Error Function at 8.0 cc/min

Fig. 27 Tubing Dispersion Test: Tracer Front Matched with Error Function at 16. cc/min

Fig. 28 Tubing Dispersion Correlation

Fig. 29 Matrix Diffusion Model with Error Function Inlet Boundary Condition: Match of 1.75 cc/min Test

Fig. 30 Matrix Diffusion Model with Error Function Inlet Boundary Condition: Match of 3.7 cc/min Test

Fig. 31 Taylor Dispersion Model with Error Function Inlet Boundary Condition: Match of 0.8 cc/min Test

Fig. 32 Taylor Dispersion Model with Error Function Inlet Boundary Condition: Match of 16 cc/min Test

Fig. 33 Core Inlet and Outlet Tracer Concentration Profiles at 16 cc/min

Fig. 34 Core Inlet and Outlet Tracer Concentration Profiles at 1.4 cc/min

Fig. 35 Core Inlet and Outlet Tracer Concentration Profiles at 0.8 cc/min

Fig. 36 Cumulative Tracer Mass Retained in Core as a Function of Pore Volumes Injected

Fig. 37 Tracer Concentration for Sorbing Tracer in Matrix Pore Fluid after 16 cc/min Test

Fig. 38 Tracer Mass Retained in Core for Sorbing Tracer after 16 cc/min Test

Fig. 39 Tracer Concentration for Non-Sorbing Tracer in Matrix Pore Fluid after 16 cc/min Test

Fig. 40 Tracer Mass Retained in Core for Non-Sorbing Tracer after 16 cc/min Test

Fig. 41 Tracer Concentration for Sorbing Tracer in Matrix Pore Fluid after 1.4 cc/min Test

Fig. 42 Tracer Mass Retained in Core for Sorbing Tracer after 1.4 cc/min Test

## ABSTRACT

Tracer tests are conducted in geothermal reservoirs as an aid in forecasting thermal breakthrough of reinjection water. To interpret tracer tests, mathematical models have been developed based on the various transport mechanisms in these highly fractured reservoirs. These tracer flow models have been applied to interpret field tests. The resulting matches between the model and field data were excellent and the model parameters were used to estimate reservoir properties. However, model fitting is an indirect process and the model's ability to estimate reservoir properties cannot be judged solely on the quality of the match between field data and model predictions. The model's accuracy in determining reservoir characteristics must be independently verified in a closely controlled environment.

In this study, the closely controlled laboratory environment was chosen to test the validity and accuracy of tracer flow models developed specifically for flow in fractured rocks. The laboratory tracer tests were performed by flowing potassium iodide (KI) through artificially fractured core samples. The tracer test results were then analyzed with several models to determine which best fit the measured data. A Matrix Diffusion model was found to provide the best match of the tracer experiments. The core properties, as estimated by the Matrix Diffusion model parameters generated from the indirect matching process, were then determined. These calculated core parameters were compared to the measured core properties and were found to be in agreement. This verifies the use of the Matrix Diffusion flow model in estimating fracture widths from tracer tests.

## SECTION 1: INTRODUCTION

In many geothermal developments it is necessary to reinject low temperature fluids as a means of waste disposal. Reinjection is also desirable as a means to provide pressure maintenance and to enhance recovery by extracting heat left behind when fluids originally in place have been produced. Unfortunately reinjection can also have detrimental effects if premature breakthrough of cold reinjection water occurs. Horne (1982) noted several cases in which production wells were adversely impacted in response to the start of reinjection operations. Tracer tests were subsequently conducted in the reinjection wells to identify the cold fluids' path to the production wells. These tests revealed extremely fast breakthrough between injection and production wells. This was believed to be due to the highly permeable fractures which are the primary fluid conduits in these geothermal systems.

In order to quantitatively interpret these tracer tests, a reservoir flow model is required to represent the mechanisms controlling tracer transport. Due to the extensive fracturing, conventional convection/dispersion models for flow in uniform porous media were not considered applicable. Field test results were also far different than those seen before in more uniformly porous reservoirs. These test results confirmed the need for a model which considers the extreme contrast between fracture and matrix properties in these reservoirs.

In response to this need, several models have recently been developed specifically to interpret these tracer tests. Generally, these models relate the test response to fracture aperture and tracer dispersivity. However, some of the model parameters are difficult to measure when matching field tests. Thus, the model accuracy in predicting reservoir properties cannot be directly verified. This uncertainty turns out to be critical in any further quantitative predictions. For example, thermal breakthrough calculations

are extremely sensitive to the fracture width used in forecast models. This indicates the importance of assessing the models accuracy in estimating fracture properties.

To test the accuracy of the tracer model, a test must be conducted in which reservoir characteristics are known precisely. The heterogeneity and uncertainty found in nature makes field scale verification of the tracer flow models impractical. However, the models can be tested in experimental tracer tests conducted in a closely controlled laboratory environment where reservoir parameters can be directly measured on the core sample. Flow models verified in this way can then be applied to interpret field tests, generating reliable reservoir property estimates for use in thermal breakthrough calculations.

Thus, the objective of this study is divided into five tasks, namely; (1) Develop experimental techniques to simulate field tracer tests in a laboratory environment, (2) Conduct tracer tests on fractured cores, (3) Analyze test results with analytical models to evaluate the ability to match experimental results, (4) Measure core properties and compare with estimates from model match parameters, and (5) Modify existing models and/or propose new ones to accurately estimate core properties from tracer test results.

## SECTION 2: PREVIOUS WORK

Previous experimental and analytical work has been conducted to address specific flow mechanisms active in fractured reservoirs during tracer tests. The mathematical models subsequently developed for tracer flow in fractures were based on the physical mechanisms observed in the experimental work. However, laboratory tests which truly emulate a fractured geothermal reservoir tracer test have only recently been undertaken. The experimental results from this work can be incorporated into calibrating specific models for fractured reservoir tracer tests.

Tracer flow models for fractured systems evolved from the classical convection-dispersion model. Johnston and Perkins (1963) presented correlations for using the convection-dispersion model to analyze tracer tests in uniform porous media. Coats and Smith (1964) later modified the model to include mass transfer to an immobile phase from a mobile phase flowing through the porous medium. Dean (1963) also presented a model to reflect interaction between a flowing and non-flowing fraction. However, fracture transport is different from flow in a porous medium and these models are not well suited for use in geothermal environments. Models specifically developed for fractured reservoirs have more recently developed. These models are generally of two types depending on the physical reservoir description. One description assumes discrete matrix blocks in a parallelepiped fracture network. The other common description considers only a single fracture and the adjacent matrix rock which makes up the fracture walls.

Bibby (1980) presented a finite element model for a fracture network depicting transport in the fractures and diffusion into the matrix. This model concluded that diffusion between mobile fracture fluids and static matrix pore fluid retards solute transport. Sudicky et al. (1982) also modelled a fracture network and concluded that frac-

ture spacing can influence solute retardation. However, he noted fracture spacing effects are less important at wider fracture spacings and higher flow rates. Although the reservoir description in a fractured geothermal reservoir may be somewhat different from the description used in these models, the results of the two studies provide insight into the types of tracer models required for a geothermal system. For example, in Wairakei, New Zealand, tracer tests were studied by McCabe et al (1983) concluding flow from injection wells is at relatively high rates and predominantly associated with a single fracture. The conclusions of Sudicky's fracture network analysis suggest that a single fracture flow model, which is less complex, should provide accurate results in this reservoir since it has such high flow rates and only a few, major fracture zones.

Many investigators have proposed models for and conducted experimental studies of solute transport in a single fracture. Several studies were conducted to investigate radionuclide migration in a nuclear waste repository. Neretnieks (1980) presented an analytical model for solute transport in a fissure and adjacent matrix. Diffusion and adsorption were the only mechanisms governing transport in the rock matrix. Neretnieks concluded that diffusion is an important mechanism retarding solute movement. Later, Neretnieks (1982) conducted laboratory experiments using both sorbing and non-sorbing solutes and verified his earlier flow model. Grisak and Pickens (1980) developed a more complicated finite difference model also for modeling nuclear waste movement in a repository. Their model considered not only matrix diffusion but also hydrodynamic dispersion within the fracture. Tang et al. (1981) also developed a model with hydrodynamic dispersion within the fracture and used the model to match experimental data. The results of these studies showed that diffusion into the rock matrix is a significant retardation mechanism and also indicated that hydrodynamic

dispersion within the fracture only effects solute transport at low flow velocities. The experiments of Grisak et al.(1980) added further evidence to support these conclusions.

Studies more specifically aimed at tracer movement in geothermal systems have also been conducted concurrent with much of the waste disposal work. Rodriguez and Horne (1981) proposed a single fracture flow nuclear model in which Taylor diffusion was the mechanism responsible for fluid mixing in the fracture. This Taylor dispersion flow model was subsequently verified by a series of experiments in a Hele-Shaw cell by Gilardi(1984) and Bouett(1986) and was incorporated into a tracer test analysis model by Fossum and Horne(1982). The model was used to match Wairakei field test data. The early time field test response was matched by this flow model but the late time response observed in the field tests could not be precisely represented. This suggested that some additional mechanism lead to tracer retention within the fracture system.

The question of the tracer retention mechanism was investigated experimentally by Breitenbach (1982) in a series of laboratory core tests. Motivated by Breitenbach's experimental findings Jensen and Horne (1983) later applied a matrix diffusion approach incorporating the Neretnieks (1980) model. This model matched Wairakei field data well. In particular it showed a good match of the late time tracer arrivals which the earlier Taylor dispersion model could not match. Unfortunately, this diffusion model did not provide a direct estimate of fracture aperture. The fracture aperture was coupled with the matrix diffusivity in one of the two dimensionless variables used by the model, so in order to estimate fracture aperture a value for matrix diffusivity needed to be known. Neretnieks (1980) earlier had also reported difficulty in estimating tracer diffusivity without a calibration basis.

To develop a model which provided a unique fracture aperture estimate, Walkup and Horne (1985) later presented another matrix diffusion model based on a more complex retention mechanism. This model considered convection, diffusion, dispersion and absorption processes. The result was the decoupling of the fracture aperture from other system variables. The fracture aperture could therefore be determined uniquely from the model parameters generated by a match of field test data.

Pulskamp (1985) conducted laboratory experiments to test the validity of these matrix diffusion models. The results of his tests were not conclusive, however, due the data collection methods employed in his study. Pulskamp made tracer concentration measurements of discrete core effluent samples in a manner similar to field test sampling procedures. Pulskamp later noted that the sampling frequency did not adequately define the tracer response under laboratory conditions. Pulskamp's work was subsequently used to establish the criteria for tracer concentration measurements adopted in this study.

In summary, a significant amount of work has been conducted, suggesting that matrix diffusion is a dominant transport mechanism in fractured, low matrix permeability rocks. The studies also indicate that hydrodynamic dispersion within the fracture may not be an important factor at the high flow rates in geothermal reinjection operations. This study investigated these two propositions by comparing the model responses to closely controlled laboratory experiments.

## SECTION 3: EXPERIMENTAL APPARATUS

### Section 3.1 Flow Systems

The experimental equipment consisted of a core holder suspended in a high temperature air bath with three primary control systems. A confining pressure system consisted of a hydraulically pressurized sleeve around the core plug providing a simulated overburden as well as a tight seal around the core. A water flow system, including a pump, an excess flow loop and a constant pressure accumulator, regulated the flow of distilled water through the core. Tracer, contained in a pressurized vessel, was flowed through the core under the control of a pressure regulator and a pressurized nitrogen bottle. This equipment was initially designed and constructed by Sageev (1980), modified by Breitenbach (1982) and subsequently used by Pulskamp (1985). This setup had been used on all unfractured core samples, however, it was found less suitable for the fractured cores due to the low pressure drops across the core. For fractured samples, the flow loops were modified to take advantage of the low head requirements.

The fractured cores utilized a simple gravity flow system for controlling flow. Distilled water and tracer solutions were stored in constant pressure reservoirs. Pressure was kept constant on the fluid exiting the vessel by locating the air suction at a point below the water surface. The air suction elevation was held at the same position for the duration of a run. These constant pressure vessels were constructed by Gilardi (1984) and later used also by Bouett (1986). The flow rate was controlled by adjusting the elevation difference between the air suction port in the vessel and the core outlet. This system was found to provide extremely steady flows through the core at the 1-3 psi pressure drops required for the various runs. This constant, steady rate was desired not only to simplify model analyses but also to allow a high frequency of tracer concentration measurements.

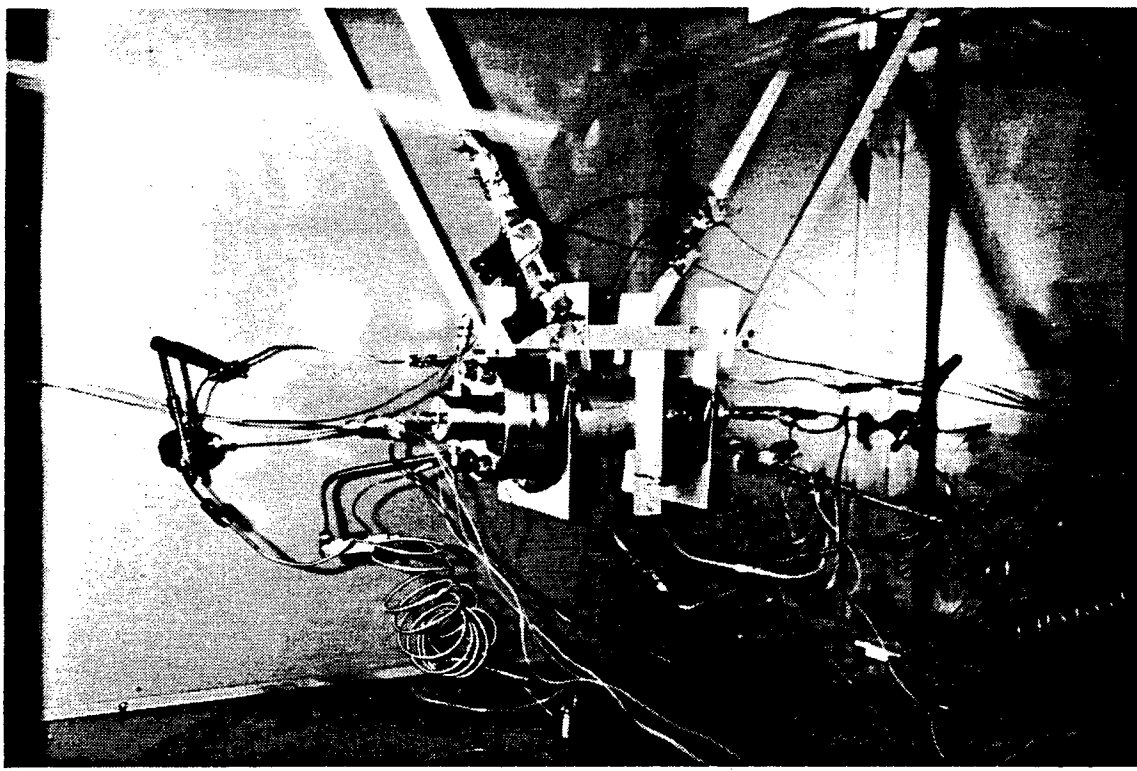


Figure 1. Photograph of core holder, switching valves, and inlet and outlet electrodes

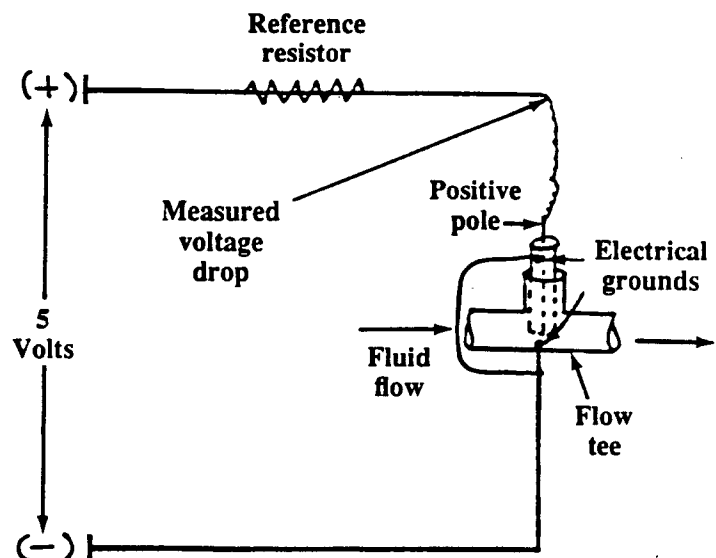


Figure 2. Electrode circuit and flow tee diagram

### Section 3.2 Tracer Detection Systems

Tracer concentrations measurements were made at two locations in the core flow loop. At these locations electrodes were installed in the flow system to provide the very high sampling frequency that previous work by Pulskamp(1985) had indicated was necessary. As shown in Figure 1, these two electrodes and their reference resistors were installed immediately outside the core holder inlet and outlet. The locations were chosen so that the tracer could be detected as it entered the core and the tracer concentration in the effluent was measured as it left the core.

The gold plated electrodes were identical to those previously used by Gilardi (1984) and Bouett (1986) in their Hele-Shaw cell. They were installed in brass flow tees connected directly into the flow loop. The measurement end of the electrode, positioned perpendicular to and in the center of the flow stream, was grounded to the brass tee (see Figure 2). The electrodes were held in the tees by snug brass fittings with teflon packing to provide a pressure seal. A common electrical ground was established between the flow tees and the data measurement equipment to assure a similar reference voltage.

These same electrodes were also used to measure tracer flow through a pipe loop assembled to test dispersion in the flow system. A 1.75 meter pipelength was assembled with electrodes located 13, 65 and 165 cm from the three way inlet valve at the start of the pipe loop. The apparatus was actually assembled with the same tubings, tees and valves previously used in the core holder circuit. The same gravity flow system consisting of the constant pressure vessels was used to regulate flow through the network. A schematic of the equipment (Figure 3) illustrates this system.

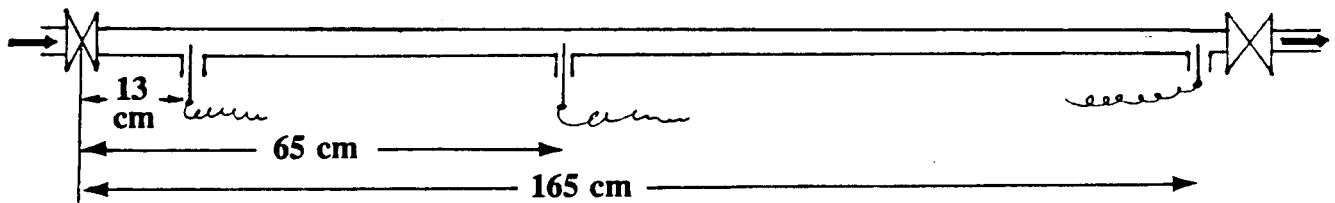


Figure 3. Schematic of pipe length test section

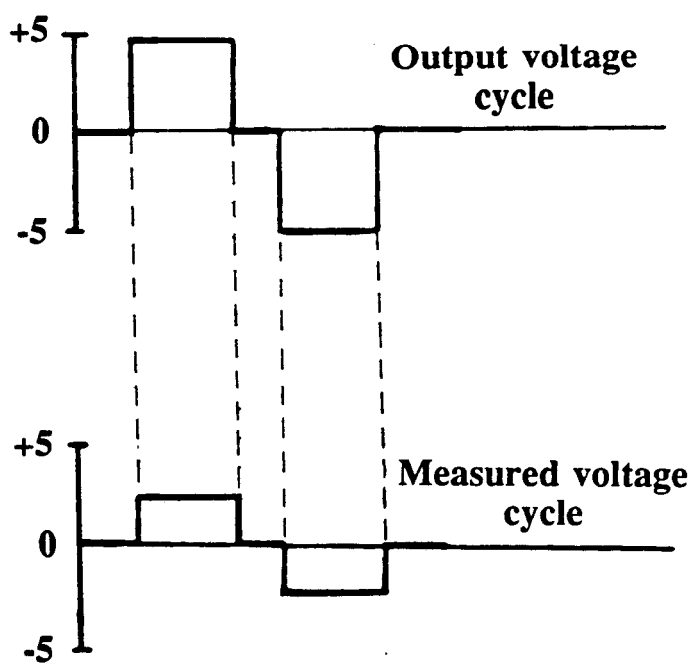


Figure 4. Graphical representation of voltage pulsing procedure

### Section 3.3 Data Collection System

The voltage drop across the electrode (and hence the tracer concentration) was monitored by a KEITHLEY/das Series 500 Measurement and Control System. This unit is capable of analog input and output of conditioned signals, switching and 12 bit analog to digital conversion. The KEITHLEY unit is also capable of digital input and output which serves as a communication pathway for receiving instructions from and sending data to a command controller. The command unit used was a COMPAQ personal computer. The personal computer contained the real time clock for sequencing tracer measurement requests and referencing data measurements. The unit also stored data accumulated for the entire run. The same command unit and controller was used earlier by Bouett (1986) to sequence and collect voltage measurements for electrodes in a Hele-Shaw cell.

The electrode voltage was measured in the following way. A positive five volt analog output signal was driven across the resistors and electrodes to the common ground. The voltage drop was then measured between the positive electrode pole and the ground. Immediately after taking measurements at all locations, a negative five volt output signal was driven for the same length of time as the positive voltage pulse. The voltage was then set to zero until the next data measurement request was made. Using this method (see Figure 4), there is no average net charge on the electrode preventing a buildup of ions on the electrode surface. The software driver for this routine, in BASIC, and can be found in Appendix E. The program does the following: (1) Sets the real time clock, (2) Reads the clock, sends output voltages and requests data at predetermined elapsed times, (3) Receives the measured data and (4) Stores the measured data.

### Section 3.4 Core Description

The cores for these experiments were cut from a Bandera sandstone from Redfield, Kansas. This finely grained uniform sandstone was determined to have 17% porosity (as measured from the core dry weight and water saturated core weight). A liquid permeability was measured from tests on the unfractured core and found to be 13 millidarcy.

Several 2.5 cm diameter and 15.25 cm length cores were cut for use in the tracer experiments. To simulate fractures, cores were sawed in half down the central axis and then reassembled with a fracture proppant to prevent fracture closure under confining pressure. Photographs of a sawed core are shown in Figure 5. One core used an 80-100 mesh sand applied sparingly as a proppant. The proppant for the other core was a 20-40 mesh sand applied liberally in the fracture. Apertures created with the 20-40 mesh proppant were on the order of 0.05 cm. Those for the 80-100 mesh sand were only 0.01 cm.

The actual core fracture width was measured in a destructive test conducted after all tracer experiments were completed. A clear epoxy resin was mixed with an oil based red dye and a hardening catalyst and then injected into the core under gas pressure. The core was released from overburden 24 hrs later and the hardened fracture cast removed. Photographs of the core and cast are in Figure 5. Some areas were observed to be unfilled by the resin, but this is most likely due to channelling low pressure gas through the core, as gas breakthrough was observed in the core effluent. Using this fracture cast, twenty fracture width measurements were made using a micrometer and the average aperture was found to be 0.0817 cm. The standard deviation for the twenty observations was 0.0116 cm.

The tracer used in the experiments was potassium iodide (KI), selected because of its extensive use in geothermal reservoir field tests. The tracer solution was made by mixing a 1 molar KI solution with distilled water to create a concentration of 105 ppm.

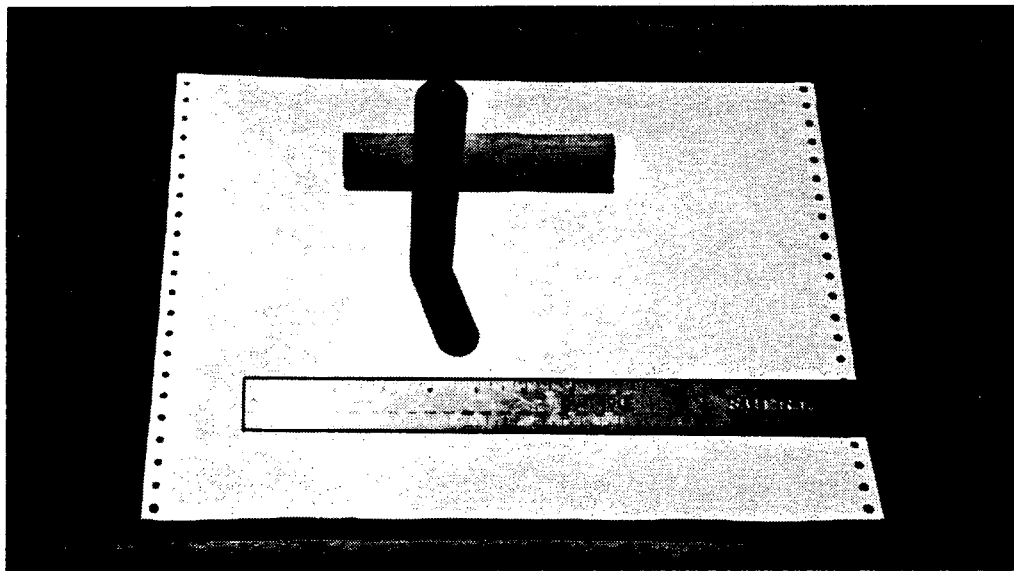
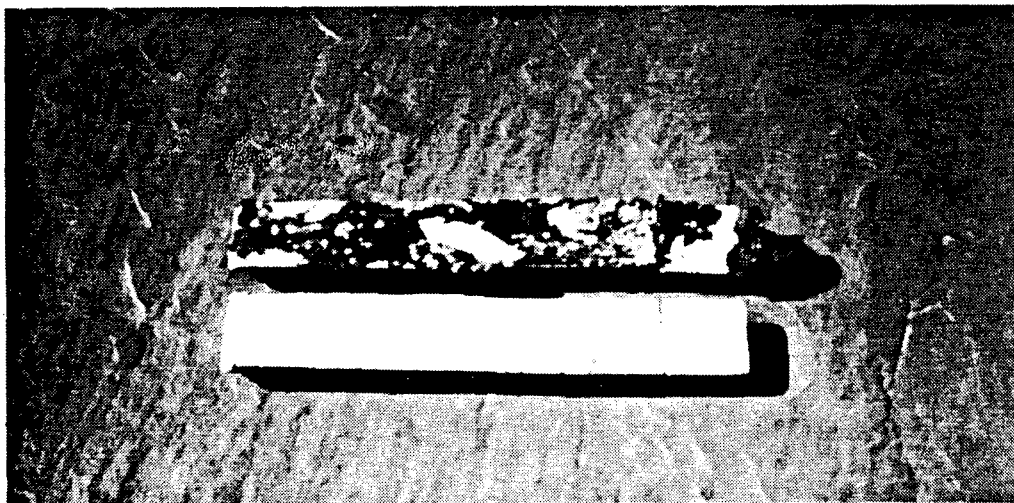


Figure 5. Photograph of sawed core before assembly with proppant



Photographs of core and epoxy fracture cast after tracer tests

## SECTION 4: EXPERIMENTAL PROCEDURE

There were three primary tasks required in conducting the tracer tests namely, (1) flowing the background distilled water, (2) switching to the tracer solution and (3) measuring the tracer concentrations in the core effluent.

### Section 4.1 Flow System Operation

Prior to conducting the tracer test, it was necessary to flush 5-10 pore volumes of distilled water through the core. The flushing was required to stabilize the ions dissolved in the core effluent. The ions in the effluent were due to a non-equilibrium exchange between the core and distilled water. This exchange was a function of flow rate and the outlet fluid concentration ranged from 2 to 10 ppm dissolved ionic solids at rates of 16 to 1 cc/min, respectively. This pre-flow stabilization period had an additional benefit. The pre-flow period and the constant pressure at the core inlet and outlet assured a steady rate through the core. The inlet pressures were controlled by maintaining a constant suction port elevation in the liquid vessel. The outlet pressures were held constant by a constant elevation atmospheric discharge. Only after all conditions such as flow rate, pressure and effluent composition had stabilized would the actual test begin.

When the core effluent had stabilized in rate and background concentration, the inlet valve of the core holder was switched to accept inlet from the tracer solution vessel. The tracer vessel was identical in size, location and suction port elevation to the distilled water vessel to assure identical flow rates from each vessel. Tracer flow was then continued until breakthrough occurred and the tracer concentration at the core outlet stabilized. Thus, the tracer input was in the form of a step change maintaining continuous tracer injection until the completion of the test. In contrast to continuous

injection tests, slug or spike tests are another type of tracer test commonly used in the field. In a slug test, a single pulse of tracer is sent through the system. Since small volumes of fluid are used in the laboratory, it is obviously difficult to introduce a discrete slug into the core. For this reason, step tests are more practical in the laboratory.

After first flowing distilled water followed by continuous injection of the tracer solution, the process was reversed. This determined the reversibility of the test. The reverse test consisted of a step change from tracer solution back to distilled water long after the tracer solution flow conditions had stabilized. This reverse procedure should have generated a response similar in shape but exactly opposite in direction to the initial step change from distilled water to tracer solution. By comparing the shape of these two tests, the reversibility of the tracer retention process could be evaluated.

Flow rates and pressure gradients for the tests were chosen to represent conditions typical of those in geothermal reservoirs. The flow rates varied between 0.75 and 16 cc/min and the pressure drop across the core varied from 0.1 to 2.0 psi. This corresponds to flow velocities of 4 to 80 m/hr and a pressure gradient of up to 4 psi/ft. The purpose in considering such a wide range of flow rates was to generate a sharp contrast between the tracer response curves for the tests. This was necessary as the shape of the tracer curve does not vary linearly with velocity. For most of the dispersion flow models, the dimensionless dispersion coefficient varies with the square root of the velocity. Thus, a 50% change in velocity results in only a 25% change in the dispersion characteristics of the system. By covering one and a half orders of magnitude, a five fold change in the dimensionless dispersion coefficient could be observed.

## Section 4.2 Data Collection Methods

Using the data collection system described earlier, the voltage drop across the electrode was measured 15-30 times per minute. The data collection frequency varied with flow rate. The highest sampling rate was for the highest flow rates. During the first trial tests, it was observed that immediately after initiating the voltage pulses the electrode response would drift for a short time until the system capacitance was charged. The drift problem was resolved by simply pulsing the electrodes for several minutes during the pre-flow stabilization period prior to beginning the tracer test. Actual data collection began one minute before switching the flow to the tracer solution and continued for several minutes after the tracer in the core effluent had stabilized. Following these procedures, data collection lasted anywhere from five to forty minutes depending on the flow rates. The entire data set collected during each run was stored in the microcomputer memory and later transferred to disk.

The measured data is in the form of voltage vs. time. In order to generate tracer concentration profiles it was necessary to correlate the measured electrode voltage to fluid tracer concentration. The correlation was made by first mixing several test samples to a known concentration by diluting an Iodide Standard solution with distilled water. Solution concentrations were mixed to cover the range of 4-100 ppm. The voltage drop across the electrode was then measured in the various solutions and plotted to establish a correlation between sample concentration and electrode voltage. The calibration sample voltage measurements were found to be semi-log linearly dependent on the tracer concentration as Gilardi(1984) had noted in his work. The followong semi-log relation was used to convert all tracer test voltage measurements into effluent tracer concentrations.

$$\frac{C_e}{C_i} = 10^{4.1 - \text{Volts}} - 2.0 \quad (1)$$

where

$C_e$  = Effluent Tracer Concentration ppm

$C_i$  = Injected Concentration ppm

Volts = Measured Electrode Voltage volts

4.1 = Effluent Background Voltage volts

2.0 = Effluent Background Concentration ppm

A copy of the FORTRAN code which made this conversion is included in the Appendix E.

### Section 4.3 Data Processing Methods

The test data collected represents the core response to continuous tracer injection. This step function response is easily converted into a slug test response by differentiating the continuous injection measurements with respect to time. The resulting response is then directly comparable to the standard spike injection well to well tracer test conducted in the field. This slug response also has more sensitivity than the step response during the transient flow period so critical to model analyses. For both these reasons the slug test data presentation was preferred for analysis of the experimental data.

The slug test response was generated from the continuous injection test data by differentiating the tracer concentration measurements with respect to time. Two methods were evaluated for differentiating the continuous injection test data to determine which gave the best results. A finite difference method was attempted, however the results generally had a high noise level. A least squares method was used and proved superior to the finite difference algorithm. The least squares technique used a number of adjacent points and fit a straight line through them. The slope of the fitted straight line was then used to represent the derivative at the central point. The optimum number of adjacent points was found to be five. Less points left some signal noise and more points removed some of the definition of the curve. A copy of the program used to generate the slug test data (by differentiation) is contained in the Appendix E.

## SECTION 5: EXPERIMENTAL RESULTS

Several experiments with an unfractured core were conducted first. The unfractured core tracer response is well known and thus it served as a test of the experimental procedures and tracer detection techniques employed. The tests also provided an estimate of rock permeability to distilled water when fully saturated with water and a method of determining the tubing volume between the measurement electrodes. After evaluating the testing procedures using the unfractured samples, fractured cores were tested next. The fractured core tracer response, which is not as well known as the response of unfractured samples, could then be determined with confidence.

### Section 5.1 Unfractured Core Samples

The unfractured core tests were conducted with the original distilled water pump and pressurized tracer vessel that Pulskamp (1985) had used. The core permeability was calculated from Darcy's law, where

$$k = 14.7 \frac{q}{A} \frac{L}{p_i - p_e} \quad (2)$$

where

$k$  = core permeability darcy's

$q$  = flowrate  $\frac{cm^3}{sec}$

$A$  = core cross sectional area  $cm^2$

$L$  = core length  $cm$

$p_i$  = core inlet pressure psia

$p_e$  = core exit pressure psia

The measured flowrates and pressures and the calculated permeabilities for the four tests of the unfractured core sample are summarized in Table 1. Average permeability was found to be 13 md with good agreement between all the cases. The equivalent slug test responses for four of these cases are plotted in Figure 6. The data is plotted

**Table 1**  
**Unfractured Core Test Summary**

TEST	Date	Pressures		Rates and Permeability			
				Measured Data		Calculated Data	
		Upstream PSIG	Downstream PSIG	Delta P PSIG	Flow Rate CC/MIN	Calc K (md)	Deviation Error
1	Jul 22	285	80	205	3.0	12.0	-8.4%
2	Jul 23	335	50	285	4.0	11.5	-12.2%
3	Jul 24	460	60	400	7.6	15.5	+18.3%
4	Aug 4	180	150	30	0.5	13.6	+3.8%

$$\text{Mean Permeability} = 13.1$$

on a pore volume basis to allow for a direct comparison of results on a dimensionless time scale. As the plots show, the curves are almost symmetrical and effectively collapse to one curve indicating that the response is independent of flow velocity. In this plot the symmetrical tracer concentration profile reflects a common property of dispersion often found for uniform porous media. This property is reflected in the dimensionless dispersion coefficient, the Peclet number.

The Peclet number is defined as

$$P_e = \frac{u L}{D_p} \quad (3)$$

where

$P_e$  = dimensionless Peclet number

$u$  = flow velocity  $\frac{\text{cm}}{\text{sec}}$

$L$  = flow length  $\text{cm}$

$D_p$  = total porous media dispersion coefficient  $\frac{\text{cm}^2}{\text{sec}}$

where

$D_p = D_m + D_h$  = molecular diffusion coefficient + media hydrodynamic dispersion coefficient

It has generally been observed for porous media that the medium hydrodynamic dispersion coefficient increases linearly with flow velocity. Also, the hydrodynamic dispersion is much greater than the molecular diffusion allowing the total media dispersion coefficient to be calculated ignoring molecular diffusion effects. Thus, the ratio of the total media dispersion coefficient to the flow velocity, termed the medium dispersivity, is a constant for a uniform porous medium. This constant media dispersivity has been observed to remove flow velocity as a system variable when test results are displayed in dimensionless form. The experimental data from this study exhibits this property and therefore agrees with these observations. This result is a good indication that the experimental procedures, data collection and data analysis methods used are reliable.

The unfractured test results were further examined to obtain a direct measurement of the tubing volume between the inlet and outlet electrodes. The slug response in Figure 6 should reach a peak value at a pore volume of one. The volume used in generating these plots, corresponding to both pore and tubing volume, can be treated as a variable to adjust the x-axis. By shifting this curve slightly to the right, the correct combined core and tubing volume can be estimated as 13.6 cc. The 11 cc core pore volume is then subtracted from the 13.6 cc used to shift the test data so the peak coincides with a pore volume of one. This leaves 2.6 cc for the tubing volume which agrees well with calculations made from equipment drawings.

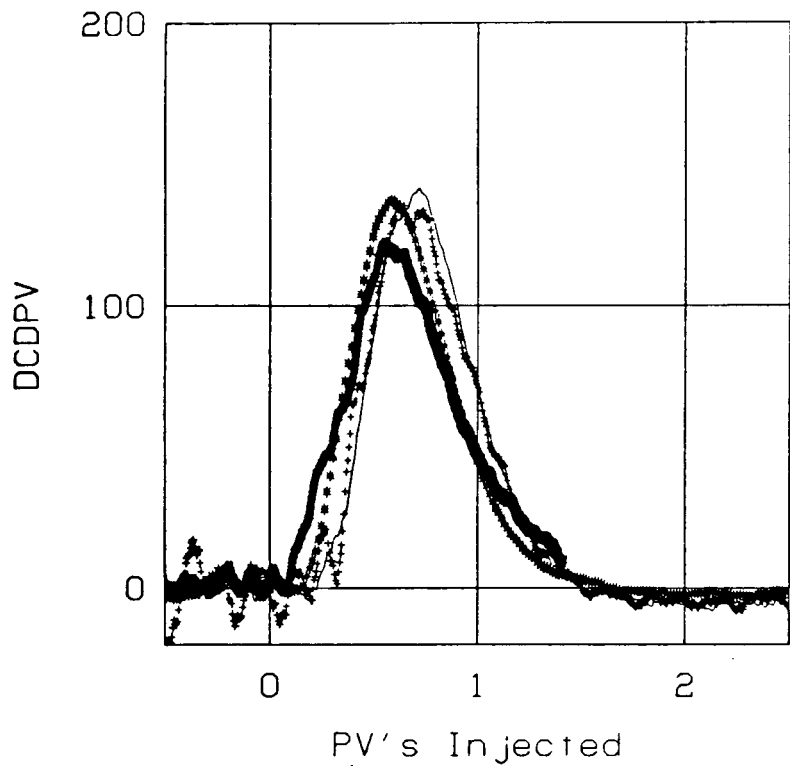


Figure 6. Pore volume plots for unfractured core tests  
 (-) 3 cc/min (+) 4 cc/min (\*) 7.6 cc/min (#) 0.5 cc/min

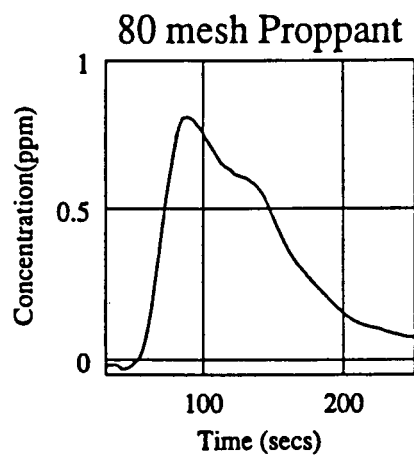


Figure 7. First fractured core test with both fracture and matrix response

## Section 5.2 Fractured Core Tests

The initial fractured core tests were conducted with an 80-100 mesh sand as a fracture proppant. The volume of proppant was deliberately kept as small as possible to minimize any flow restrictions within the fracture. Unfortunately this proppant was only partially effective in keeping the fracture open. The equivalent slug test response for this core (Figure 7) shows the response indicative of two flow paths. This is probably due to the separate responses of the fracture and core matrix. A total flow rate of 4.5 ml/min was measured at a 185 psi pressure drop. This indicates that the total core permeability has been enhanced from 13 to only 20 md. Matrix flow at this pressure drop is calculated to be 3.0 cc/min leaving 1.5 cc/min as fracture flow. This degree of matrix flow agrees with the two peak concentration profile where the low storage fracture responds first and the matrix later. Although these results are interesting, the core is obviously not representative of flow in most geothermal reservoirs. For example, at Wairakei matrix permeability is responsible for only a small percentage of total flow directly into wells and fractures are the dominant flow corridors. This type of system could be better emulated if the fracture size (and thus permeability) were increased substantially so the flow through the core matrix is negligible.

To increase the fracture width, a 20-40 mesh sand was chosen as proppant and inserted liberally in a new fractured core sample. Only one layer of proppant was inserted into the fracture as two layers would be unstable under overburden pressure. The initial flow tests using this new core indicated that the larger proppant was effective. The fracture totally dominated the flow through the core and calculated average permeability increased to 7800 md. Matrix flow was estimated at only 0.1% of the total flow. The tracer response profiles later confirmed the lack of matrix flow as no secondary matrix pulse was seen in the core effluent tracer concentration curves.

This sample was used in all subsequent fractured core tests.

The data measured for the fractured core tests is summarized in Table 2. As examples of the tracer concentration data handling procedures, the entire suite of tracer profiles generated for the 3.7 cc/min test are shown in Figures 8 through 13. This includes the actual measured voltage data, the corresponding tracer concentration profiles and also the equivalent slug test response. The voltage responses measured during the step change injection tests for both the "step up" and "step down" tests are in Figures 8 and 11, respectively. The "step up" refers to the stabilized flow of distilled water as the background fluid followed by the switch to tracer solution. This case is representative of a continuous injection tracer test. The "step down" is the reverse test resulting from flow of tracer as the background fluid followed by a change back to distilled water. The voltage data of Figures 8 and 11 was then used to convert to tracer concentration generating Figures 9 and 12. These tracer concentrations are in response to continuous tracer injection and they were differentiated to yield the equivalent slug test responses shown in Figures 10 and 13. This entire series of plots was generated for each test, however they are not all shown here in the interest of brevity. Only the reservoir equivalent slug test is shown for the other tests in appendix A. One complete tabular data set for the 3.7 ml/min test is contained in Appendix F.

In general, the resolution of the data was good. Repeat tests were conducted at similar flow rates and near identical results were observed, indicating the repeatability of the test. Test reversibility was evaluated by comparing the step up and step down data in Figures 8 through 13. Although the curve shape and peak values are similar, the plots are not mirror images of each other. This suggests some hysteresis in the tracer transport mechanism. However, the remainder of the analyses in this report

**Table 2**  
**Fractured Core Test Summary**

TEST	Date	Measured Data		Calculated Parameters				
				Permeabilities		Fracture Estimate		
		1986	Delta P	Flow Rate	Bulk Core (md)	Fracture (darcy)	Aperature MM	Deviation Error
PSIG	CC/MIN							
1	Oct 29	NA	16.0		NA	NA	NA	NA
2	Oct 30	NA	4.0		NA	NA	NA	NA
3	Nov 3	NA	1.4		NA	NA	NA	NA
4	Nov 5	0.379	8.7		9372	1323	0.126	+10.5%
5	Nov 6	1.011	9.7		7837	1180	0.119	+4.4%
6	Nov 6	0.408	3.7		7407	1121	0.116	+1.7%
7	Nov 8	0.238	1.75		6000	990	0.109	-4.4%
8	Nov 8	1.697	16.3		7846	1180	0.119	+4.4%
9	Nov 13	0.108	0.7		5278	874	0.099	-13.2%
10	Nov 18	0.108	0.75		5655	936	0.106	-7.0%

Mean Fracture Width = 0.114 mm

Most Likely Value = 0.119 mm  
(ignoring low rates)

Fracture Pore Volume =(0.0119cm)(2.36cm)(15.24cm)=0.46 cc

Core Matrix Pore Vol =(0.7854)(15.24cm)(2.36 cm)(2.36cm)(0.17)=11.35 cc  
Total Pore Vol =11.81 cc

centered on the reservoir equivalent slug test data (the "step up" slug tests) and the reverse test results are left as a subject for further study.

Reviewing the fractured core slug tests, results are seen to be quite different from the unfractured core tests. The slug test response, the highest resolution plot, shows a great degree of asymmetry, similar to the field results observed in Wairakei. These responses show the same early steep rise and late time "tails" characteristic of the field

test responses. The similarity between the laboratory and field test results indicates that the experimental geometry adequately emulates reservoir conditions. It was therefore considered justifiable to begin quantitative analysis of the experimental results.

Before any further analysis of the data was possible, it was necessary to adjust the time datum of the measured response to reflect the actual time of tracer entry into the core. It is important to note the time scale for Figures 8 through 13 and the plots in Appendix A reflects the start of the data collection clock and it is NOT time measured from when the tracer entered the core. Thus, a shift of time datum by 20-200 secs was required depending on the flow rate. This time datum correction was estimated using the inlet electrode response as follows:

$$t_{dc} = t_{ie} + \frac{V_t}{q} \quad (4)$$

where

$t_{dc}$  = calculated time datum correction secs

$t_{ie}$  = measured inlet electrode first tracer arrival time secs

$V_t$  = tubing volume between electrodes  $\text{cm}^3$

$q$  = flowrate  $\frac{\text{cm}^3}{\text{sec}}$

This time datum correction was then subtracted from the measured times correcting the plots to a true time scale.

$$t_a = t_{oe} - t_{dc} \quad (5)$$

where

$t_a$  = actual test time reflecting tracer entry into the core secs

$t_{oe}$  = measured clock time at outlet electrode secs

These shifted plots were later used to develop pore volume plots and in the model analyses. In fact, model analyses were found to be sensitive to the actual test start time and the shift parameter was often used as a system variable. This is discussed in more detail in the modeling section.

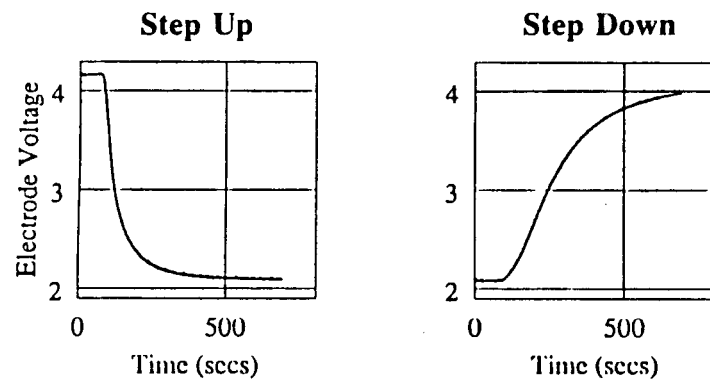


Figure 8. Voltage profile for step up at 3.7 ml/min

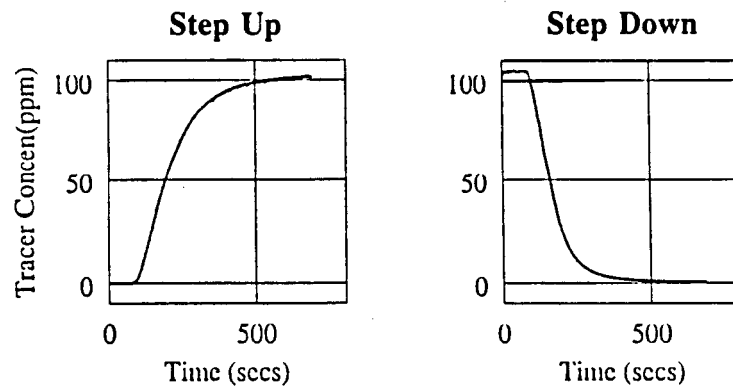


Figure 9. Concentration profile for step up at 3.7 ml/min

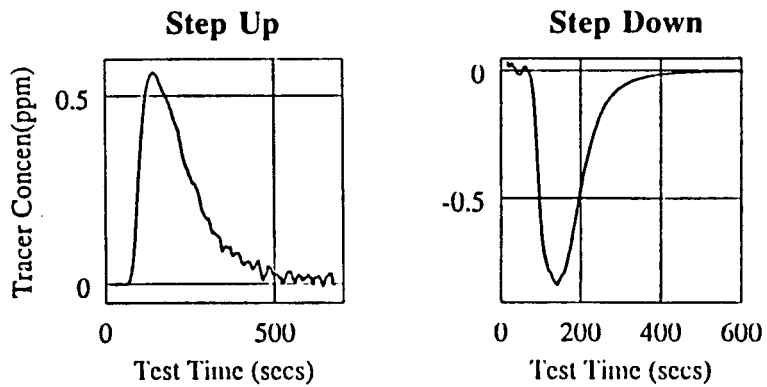


Figure 10. Equivalent slug test for step up at 3.7 ml/min

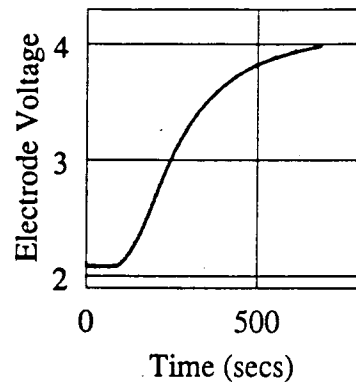


Figure 11. Voltage profile for step down at 3.7 ml/min

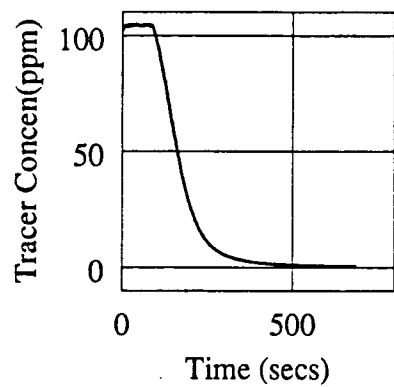


Figure 12. Concentration profile for step down at 3.7 ml/min

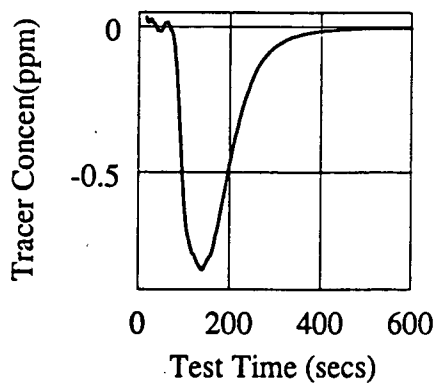


Figure 13. Equivalent slug test for step down at 3.7 ml/min

## SECTION 6: MODELING THE EXPERIMENTAL DATA

The experiments conducted on the fractured core resulted in an asymmetrical tracer breakthrough profile characteristic of the Wairakei field tracer tests. It should be possible to match this profile shape using the models which have been applied to the Wairakei field test data. However, before attempting any mathematical analysis of the experimental data, a pore volume plot was made so that the results from all of the runs could be viewed on a single plot. The fractured core results (Figure 14) are quite different from those obtained earlier using the unfractured core (Figure 6). The curves for different flow rates no longer collapse to a single uniform shape on this dimensionless scale, indicating that the mechanisms controlling tracer dispersion in the fractured core are velocity dependent. This velocity dependent dispersivity, which was not observed in the uniform core, was further investigated using several analytical fracture flow models.

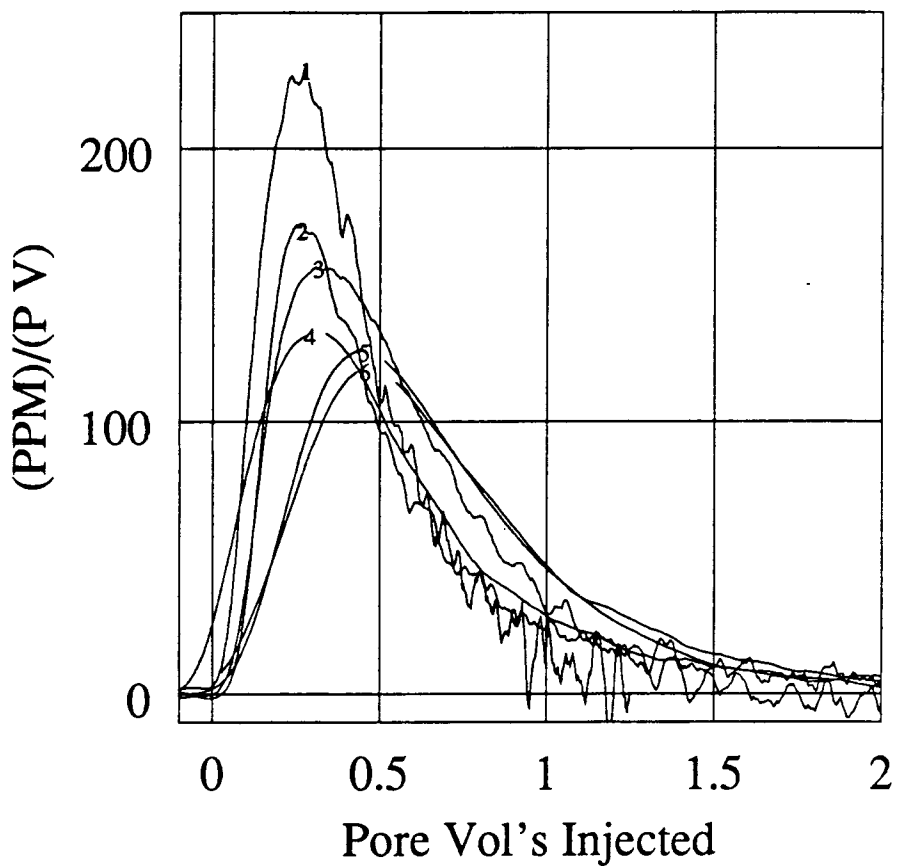


Figure 14. Pore volume plots for fractured cores  
1 = 0.75 cc/min 2 = 1.25 cc/min 3 = 1.4 cc/min  
4 = 8.70 cc/min 5 = 9.70 cc/min 6 = 16.0 cc/min

## Section 6.1 Conventional Analytical Models

Several models are available for analysis of flow in fractured porous media. However, only models which are representative of the physical system constructed in the laboratory were deemed relevant for analyses. In the laboratory, as in real geothermal reservoirs, the flow was almost totally in the fracture and the matrix acted only through exchange with the fluid in the fracture. This restricted the choice of models to those considering 1) the matrix impermeable to fluid flow 2) linear flow in a single fracture and 3) fracture/matrix exchange only at the fracture wall. The models in this category vary greatly in terms of complexity and the mechanisms they consider. As the goal of this work was partly to evaluate the dominant tracer transport mechanism, several models were considered even though they were expected to be shown to be inappropriate. The philosophy used was to start with the simplest model. Complexity was only added as required to better match experimental results. Models which consider complex mechanisms which could not be precisely quantified were not investigated. The additional complexities of these models were thought to risk clouding the evaluation of the dominant mechanisms by introducing transport phenomena that were not well understood.

Interpretation of the experimental results required solution of an inverse problem in which the stimulus and response are known and are used to identify the system. In order to decide whether a particular model is appropriate for the system and also estimate the most likely model parameters, several methods can be used. The simplest and most time consuming is trial and error. Slightly more complicated analyses use dimensionless type curves to identify the effects of system variables on the output response. Another more quantitative method uses non-linear optimization methods. The greatest accuracy and lowest error is associated with these optimization methods and thus one

was chosen to fit the models to the results. A least squares non-linear regression program named VARPROM, which is based on a paper by Golub and Pereya (1973), was used to fit the experimental results with all the various flow models.

#### Section 6.1.1 Taylor Dispersion Model

Horne and Fossum (1982) developed a model for fracture flow in which planar Taylor Dispersion is the only tracer dispersion mechanism. No interaction is considered with the matrix in this model and thus results are almost symmetrical about the peak concentration. Using this model, attempts were made here to fit the experimental data from several runs. The FORTRAN code and equations for the model can be found in Fossum's report (1982).

The attempts at model regression were not successful. The asymmetrical experimental data resulted in a poor match with this model, just as field test data had. The strong asymmetry of the curves indicates that in an equivalent spike injection tracer would be held up in the core and released again at a later time, producing the long tailing effect observed in the data. This caused predictions with the model to be inaccurate, as shown in Figure 15.

However, it was noted that the model could match the experimental data by allowing the optimization routine to also treat the test start time as a variable. The resulting match of the experimental data (Figure 16) is better, but the start time used in the match does not correspond with the measured start time. Furthermore, the Taylor diffusion solution as presented by Fossum is most likely not valid at these early times for two reasons.

First, the true Taylor solution is

$$\frac{C_e}{C_i} = erfc \frac{x - ut}{2 \sqrt{\eta t}} + e^{\frac{ux}{\eta t}} erfc \frac{x + ut}{2 \sqrt{\eta t}} \quad (6)$$

However, Fossum's model uses an approximation of Equation 5 which ignores the second term in the equation. This approximation is valid at late times as the second term diminishes to zero rapidly as time increases. The time scale for the test match in Figure 16 and the fast breakthrough of tracer in the laboratory cores, however, results in conditions where the late time approximation is not appropriate. Thus, Fossum's model is not valid for the times shown in much of Figure 16.

A second reason for discounting this match again relates to the small values of time in Figure 16. The dimensionless time for this model

$$t_d = 4 \frac{D_m}{W^2} t \quad (7)$$

where

$t_d$  = dimensionless time

$D_m$  = tracer molecular diffusion coefficient  $\frac{cm^2}{sec}$

$t$  = time secs

$W$  = fracture aperture cm

must be greater than one half for the tracer concentration to equalize across the fracture aperture. Prior to a dimensionless time of one half, the Taylor solution given in Equation 5 is not actually valid. As Figure 16 clearly shows, some of the solution occurs at a time when the proper velocity profile has not yet developed.

Considering the two points above, if matching experimental data requires shifting the test start time close to the origin where: (1) the solution deviates from the differential equations describing the system and (2) the model uses an approximate solution not valid at such early times, then the model is inappropriate for describing the system.

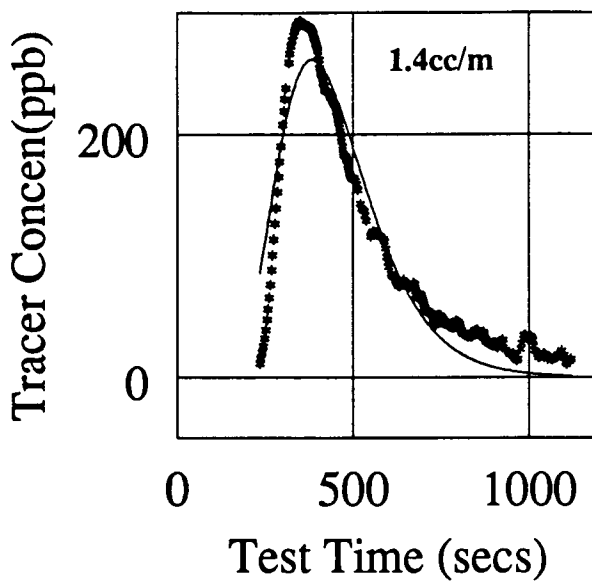


Figure 15. Match with fossum model without adjusting start time  
Model (-) and data (\*)

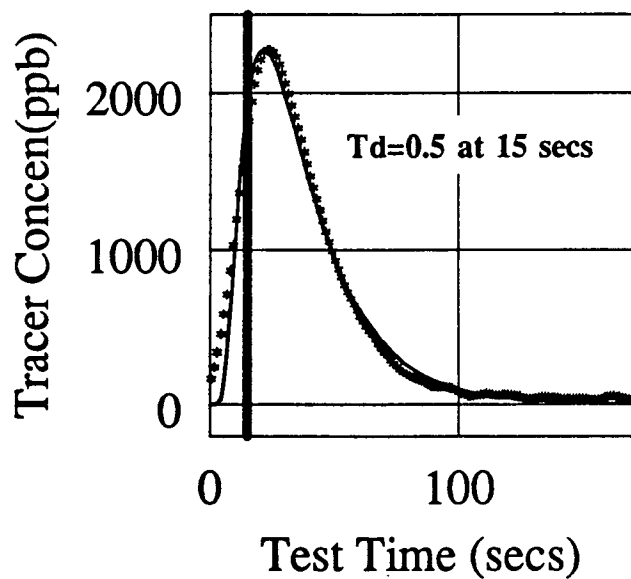


Figure 16. Match with fossum model using start time as a regression variable  
(calculated start time draws data so close to origin that an insufficient  
time has elapsed for Fossum solution to be valid)  
Model (-) and data (\*)

### Section 6.1.2 Matrix Diffusion Model

The tracer diffusion model presented by Jensen and Horne (1983) was the second model used to match experimental results. The solution for this model and the corresponding computer code is presented in Jensen's report (1983). The regression attempts using this model were more successful than those with Fossum's model and resulted in less error between calculated and measured values. As shown in Figures 17 and 18, the match was still only fair. However, during the early time period, the model was in error, showing later tracer breakthrough at a higher concentration than the experimental data. Before abandoning the model, the possibility of some deviation from ideality in the laboratory tests was considered.

Reviewing the model match, the early time predictions indicated a later first tracer arrival than the test results. The model also predicted higher peak concentrations at breakthrough. The early time error could be caused by a deviation from the unit step change assumed to occur at the core inlet face. A less abrupt change in the inlet concentration would result in lower breakthrough tracer concentrations and lower values in the curve peak. The cause of a ramp increase tracer solution concentration (as opposed to a sudden step change) could be mixing of the distilled water and tracer solutions in the volume of pipework between the tracer valve and the core.

To reveal the magnitude of any mixing before the core inlet, the inlet electrode responses for the 16 and 1.75 cc/min tests (Figures 19 and 20) were examined. The tracer front as it passed the inlet electrode is obviously not an ideal step change and is closer to an exponential rise. The time duration of the transient response period is short, however, in comparison to the total test time it is still significant. The mixing occurring before the core entrance must, therefore, be considered in the boundary conditions of any model solution.

This upstream mixing is apparently due to dispersion in the tubing between the three way valve and the core inlet. The dispersion mechanism for laminar flow in a pipe has been studied by Taylor (1956). The model developed by Taylor was tested to determine its applicability to the data measured at the inlet electrode.

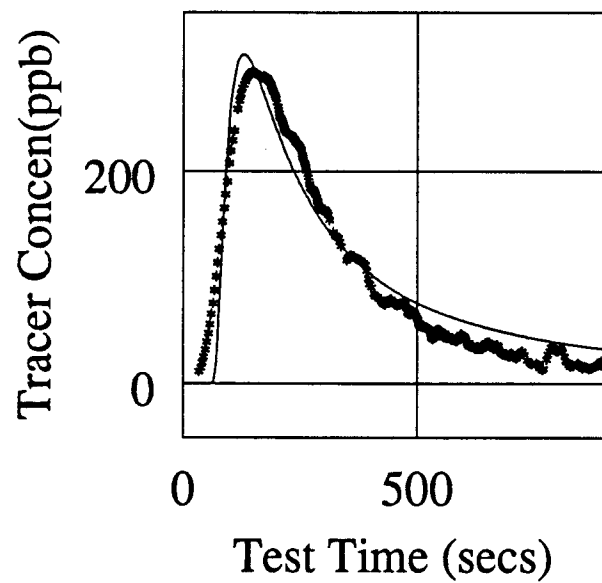


Figure 17. Jensen model match at 1.4 cc/min: Fair agreement with data but late breakthrough  
Model (-) and data (\*)

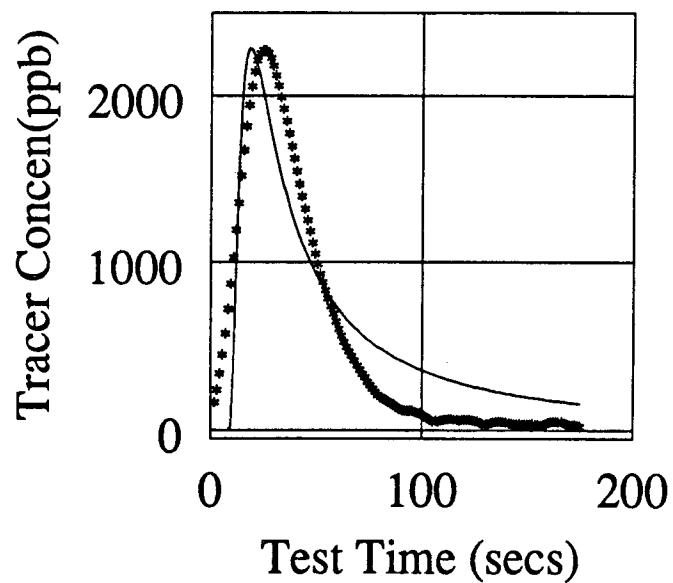


Figure 18. Jensen model match at 16 cc/min : Again later tracer breakthrough  
Model (-) and data (\*)

## Section 6.2 Inlet Dispersion Mechanism

With the goal of developing the functionally correct form of the tracer front at the core inlet, experiments were carried out to properly characterize the mechanism of dispersion in the inlet tubing. This was then used as the boundary condition to obtain the general solution of the tracer models by developing a new model solution including the new modified inlet boundary condition. Initially the inlet front in Figures 19 and 20 was represented by an exponential function. This generated a solution capable of matching experimental results fairly well, however the results were not consistent between the various experiments. It became obvious that the solution for the inlet boundary must be consistent with the forces causing the mixing and that more data would be required to better define the tracer front as it enters the core.

Two problems had to be overcome in determining the correct inlet boundary condition. First, the tracer concentration was needed exactly as the tracer front entered the core rather than at the inlet electrode location. Installing an electrode within the core holder was not possible. Second, the shape of the front previously measured at the inlet electrode location did not reflect the Taylor solution. These problems were overcome by making a series of experiments in a length of pipe. The tracer front was observed as it traveled down the tubing and this data was used to predict the front shape as it enters the core.

The tracer fronts observed at a 1.2 cc/min flow rate at distances of 13, 65 and 165cm from the inlet valve are plotted in Figures 21, 22 and 23, respectively. The 13 cm location corresponds to the 13 cm distance between inlet electrode and the tracer inlet in the actual core flow loop. As before the front at the 13 cm location does not have the symmetry observed for Taylor Dispersion and the data matches an exponential function. However, the fronts further downstream do have the symmetrical shape

associated with Taylor dispersion in a pipe and do not fit the exponential function (see Figures 22 and 23). Subsequent runs at other flow rates also revealed that the first location deviated from Taylor's model. This is either due to the effects of the inlet valve or because sufficient time had not elapsed to develop a Taylor front (dimensionless time is roughly one-half). The locations further downstream, which correspond to the core inlet location (and beyond), all conformed to Taylor's model.

Thus, the data from several runs were fit to the following complimentary error function solution initially developed by Taylor(1956).

$$\frac{C_i}{C_o} = \operatorname{erfc} \frac{x - ut}{2\sqrt{\eta} t} \quad (8)$$

where

$x$  = measurement electrode location cm

$u$  = flow velocity  $\frac{cm}{sec}$

$t$  = time sec

$\eta$  = Taylor Dispersion Coefficient  $\frac{cm^2}{sec}$

$C_o$  = inlet concentration ppm

The match for all runs, with flow rates ranging from 0.7 to 16 cc/min, were quite good. Figures 24 through 27 show examples of the model match of the tracer front at the 65 cm location. The calculated dispersivity values for all of the pipe flow experiments are shown in Table 3. The conclusion was that the mixing did agree with a Taylor dispersion model by the time the front reached the core inlet face and an error function solution (Equation 5) was the correct core inlet boundary condition.

Having successfully described the mixing of tracer and distilled water before the core inlet, a correlation (Figure 28) was developed between injection rate, tubing mixing length and the dispersion coefficient. The correlation was used to determine the appropriate tubing dispersion parameter at a mixing length equivalent to the core inlet.

**Table 3**  
**Tubing Dispersion Test Summary**

TEST	Date	Measured Data		Calculated Dispersion Parameters			
				Second Electrode		Third Electrode	
		1986	Flowrate CC/MIN	1st Electrode Correlation Number	Location CM	Dis. Param. SQ-CM/SEC	Location CM
16	Jan 26	1.25		2	65	12.5	165
17	Jan 26	16.0		8	65	121.5	165
18	Feb 3	15.5		7	65	121.9	165
19	Feb 3	11.0		6	65	83.6	165
20	Feb 3	4.1		3	65	48.9	165
21	Feb 3	5.5		4	65	59.9	165
22	Feb 5	0.7		1	65	2.6	165
23	Feb 5	8.5		5	65	52.5	165
							473

The actual core inlet face is only some 35 cm from the tracer switching valve, however, the equivalent mixing length is longer due the mixing head in the core holder apparatus. An estimate of the mixing length was made from the tubing volume and cross sectional area as follows:

$$L_m = \frac{V_t}{A_p} = \frac{2.7 \text{ cm}^3}{0.27 \text{ cm}^2} = 100 \text{ cm} \quad (9)$$

The Taylor Dispersion coefficient for each flowrate was then estimated from Figure 28 at the core inlet mixing length of 100 cm. This generated the constants in Equation 5 which were then used to develop a new solution for the Matrix Diffusion model with a dispersed boundary condition.

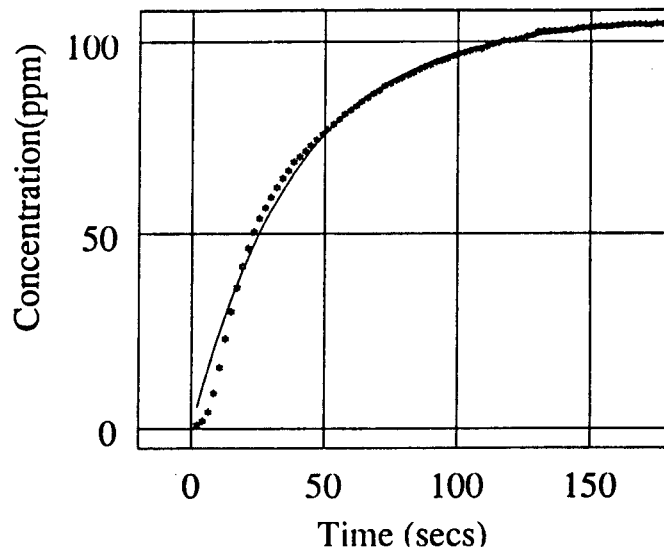


Figure 19. Inlet electrode measurement of tracer front prior to entering the core - front resembles exponential  
Exponential (-) and data (\*) at 1.4 cc/min

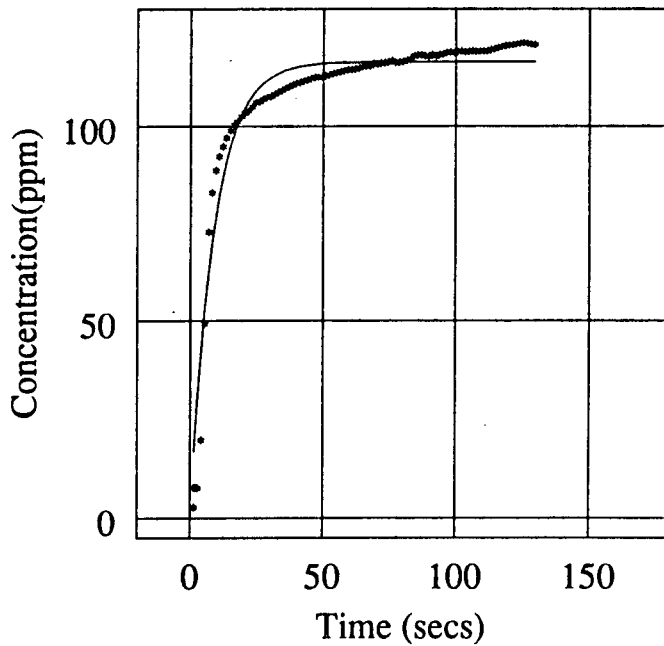


Figure 20. Inlet electrode measurement of tracer front prior to entering the core - front resembles exponential  
Exponential (-) and data (\*) at 16 cc/min

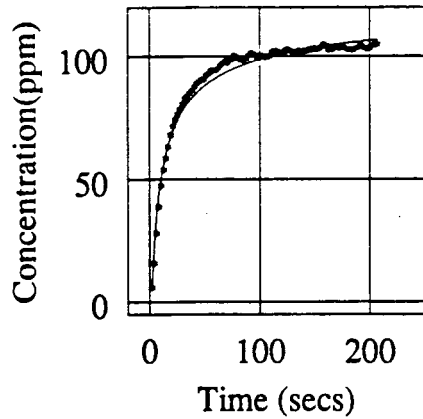


Figure 21. Tracer front at 1st electrode (13 cm): Note lack of symmetric profile  
Flowrate = 1.2 cc/min

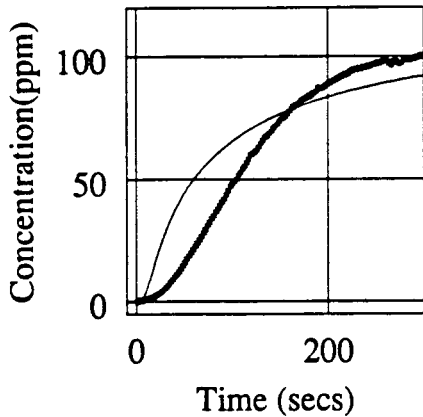


Figure 22. Tracer front at 2nd electrode (65 cm): Taylor dispersion profile poorly matched by exponential. Flowrate = 1.2 cc/min

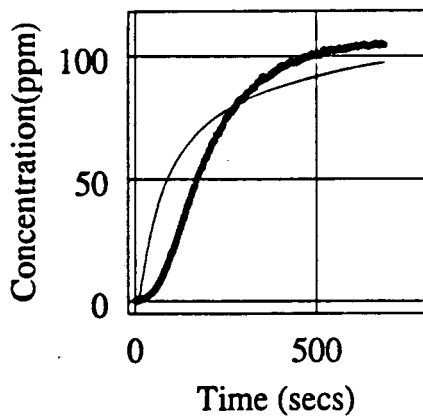


Figure 23. Tracer front at 3rd electrode (165 cm): Taylor dispersion profile poorly matched by exponential. Flowrate = 1.2 cc/min

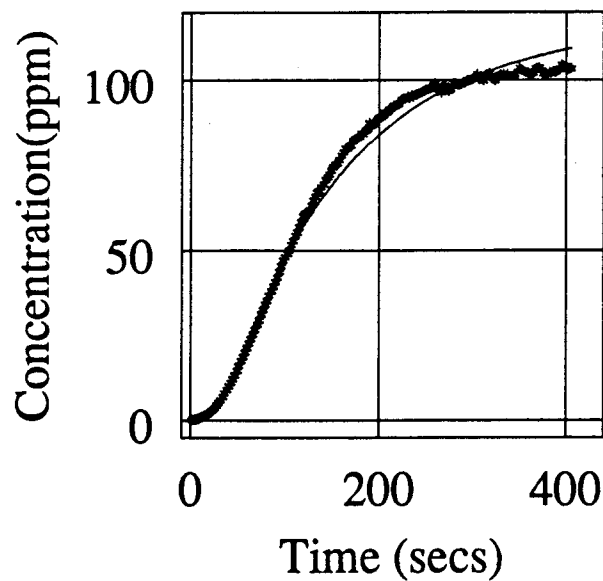


Figure 24. Tracer front at 2nd electrode : Data (\*) and matched error function (-)  
Flowrate = 1.2 cc/min

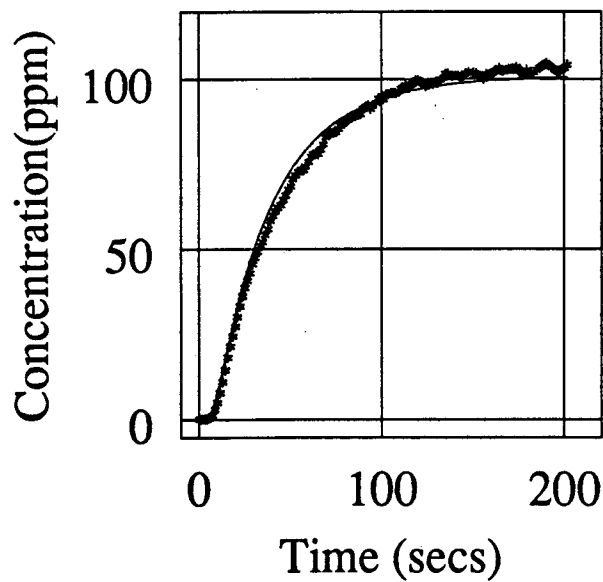


Figure 25. Tracer front at 2nd electrode : Data (\*) and matched error function (-)  
Flowrate = 4 cc/min

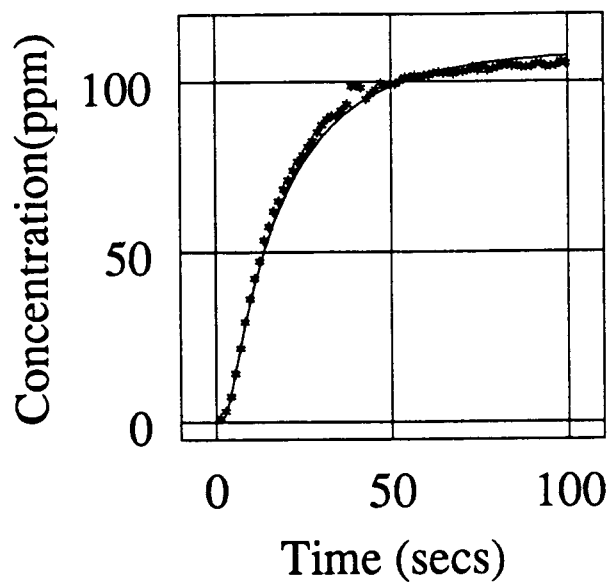


Figure 26. Tracer front at 2nd electrode : Data (\*) and matched error function (-)  
Flowrate = 8 cc/min

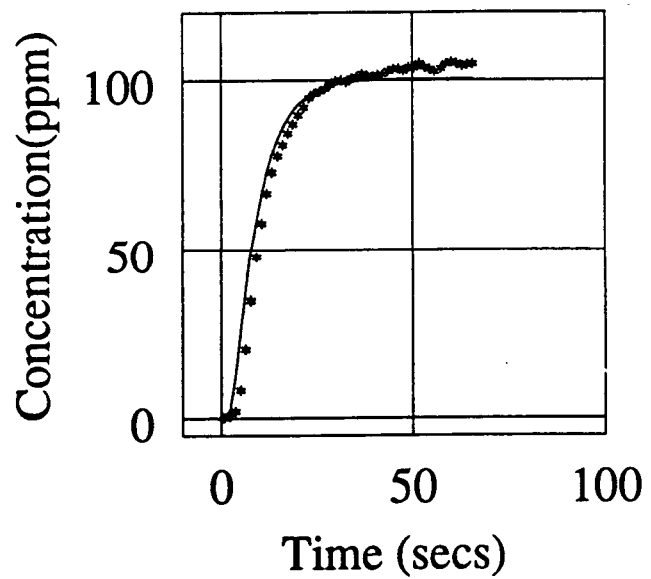


Figure 27. Tracer front at 2nd electrode : Data (\*) and matched error function (-)  
Flowrate = 16 cc/min

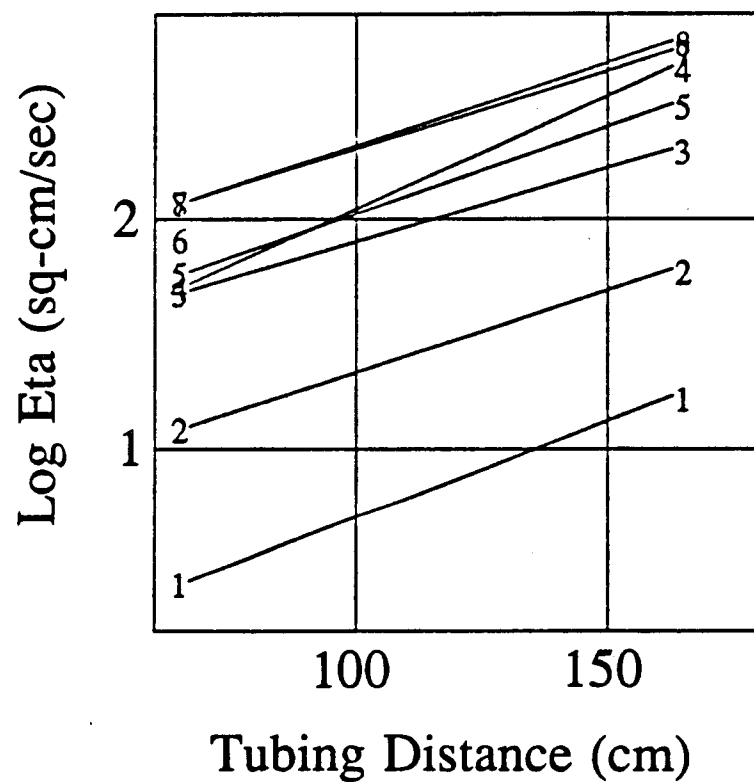


Figure 28. Correlation between dispersion coefficient and distance from tubing inlet  
 1 = 0.7 ml/min 2 = 1.25 ml/min 3 = 4.1 ml/min 4 = 5.5 ml/min  
 5 = 8.5 ml/min 6 = 11.0 ml/min 7 = 15.5 ml/min 8 = 16. ml/min

## Section 6.3 Modified Conventional Analytical Models

### Section 6.3.1 Matrix Diffusion Model with Dispersed Inlet Boundary Condition

The Matrix Diffusion Model solution previously applied to the test data was developed assuming a unit step change inlet boundary condition. This solution was modified for an error function inlet boundary condition to reflect Taylor dispersion in the inlet tubing. The solution was obtained by transforming the error function inlet boundary condition into Laplace space and applying it to the Laplace transform of the solution to the matrix diffusion model. This generated the specific solution for the error function inlet condition. The continuous injection solution was then multiplied by the Laplace variable  $s$  to differentiate the continuous solution into the slug test solution. The Laplace space solution was found to be:

$$C_f = s e^{-2b\frac{\sqrt{s+a}-\sqrt{a}}{\sqrt{s+a}(\sqrt{s+a}-\sqrt{a})}} e^{-\frac{s}{\beta}} e^{-2\alpha\frac{\sqrt{s}}{\sqrt{\beta}}} \quad (10)$$

where

$$a = \frac{u^2}{4\eta} \quad \text{inlet dispersion parameter sec}^{-1}$$

$$b = \frac{x}{2\sqrt{\eta}} \quad \text{inlet dispersion parameter sec}^{-0.5}$$

$$\eta = \text{Taylor Dispersion Coefficient inlet parameter} \frac{\text{cm}^2}{\text{sec}}$$

$$\alpha = \frac{D_e}{W\sqrt{D_a\beta}} = \text{dimensionless dispersion coefficient}$$

$$\beta = \text{reciprocal breakthrough time} \quad \frac{1}{\text{sec}}$$

$$D_a = \text{apparent diffusivity} \quad \frac{\text{cm}^2}{\text{sec}}$$

$$D_e = \text{effective diffusivity} \quad \frac{\text{cm}^2}{\text{sec}}$$

$$x = \text{core inlet location} \quad 100 \text{ cm}$$

$$u = \text{tubing flow velocity} \quad \frac{\text{cm}}{\text{sec}}$$

$$t = \text{time sec}$$

$$W = \text{fracture width cm}$$

Detailed derivation of this equation is in Appendix B.

This slug test solution could not be inverted from Laplace space to real space analytically and the equation was inverted into real space using the Stehfest numerical inversion method (Stehfest 1970). The VARPRO nonlinear regression was used to fit the new model (Equation 9) to experimental data. A listing of the FORTRAN program which was used and a sample output is given in Appendix C.

Three variable parameters were used in the VARPRO nonlinear regression routine. The nonlinear variables were: (1) the tracer breakthrough time, (2) the dimensionless core dispersion parameter, and (3) the time datum correction reflecting tracer entry into the core. The first two regression parameters were truly unknowns and a function of the core properties. These same core parameters were used as regression variables in the unmodified Matrix Diffusion model. The third regression parameter, the datum time correction, was actually not an unknown. The datum correction could be determined from the inlet electrode response to the tracer front and the tubing volume between the two electrodes. However, the regression analysis treated the datum time correction as a possible variable, allowing a better fit of the data. The regressed values for the time datum corrections were found to be generally consistent with measured values, but the regression procedure provided a small adjustment to the datum corrections accounting for any errors in the measured time datum correction. The slight variations between measured and regressed time datums most probably reflect actual tubing volume changes due to small flow system modifications made during the course of the experiments. The regression method, therefore, provided a better match of the data with only a minor adjustment in the test start time.

The only terms in Equation 9 not treated as regression parameters were the inlet dispersion terms. These test constants were fairly well known from the tubing disper-

sion experiments. Regression on these boundary condition terms was attempted but without success. The coupling of the tracer dispersion in the tubing and the tracer dispersion in the core presented a problem whose solution was nonunique. Thus, the regression routine could not converge on a unique set of model parameters when the tubing dispersion terms were included as regression parameters.

The tracer profiles for the seven fractured core tests were fitted to the modified matrix diffusion model and the calculated regression variables are listed in Table 4. The measured and calculated tracer profiles are shown for two cases in Figures 29 and 30. The agreement between the calculated and observed response is excellent, indicating that the model is applicable to the system. Plots for all the test matches are in Appendix D. They generally show the same excellent agreement between model predictions and experimental data depicted in the two examples shown here. The modified inlet boundary condition model correctly matched the early time period where the step boundary condition model lead to considerable errors. A summary of model match variables and input parameters is in Table 4.

The model match parameters listed in Table 4 represent the following system variables,

$$\alpha = \frac{D_e}{W\sqrt{D_a}\beta} \quad (11)$$

where

$$\beta = \text{reciprocal breakthrough time} \quad \frac{1}{\text{sec}}$$

$$D_e = \text{effective diffusivity} \quad \frac{\text{cm}^2}{\text{sec}}$$

$$D_a = \text{apparent diffusivity} \quad \frac{\text{cm}^2}{\text{sec}}$$

$$W = \text{fracture width} \quad \text{cm}$$

**Table 4**  
**Diffusion Model Match Parameters**

TEST	Flowrate cu-cm/min	Inlet Dispersion Parameters		Model Parameters and Fracture Aperatures			
				Start Time Match	Reciprocal Beta Match	Time 0	Tub Vol
		Inlet Length CM	Dispersion Parameter SQ-CM/SEC	Seconds	CC	Model Secs	Aperture MM
6	16.0	100	270	23.4	2.8	8.61	0.65
7	4.0	100	60	125	4.1	10.35	0.19
8	1.4	100	10	189	2.11	12.42	0.08
9	8.7	100	90	141	4.4	1.0	0.04
10	9.7	100	100	87	3.3	7.7	0.35
11	3.7	100	60	59.4	2.6	15.3	0.26
12	1.75	100	15	174	3.0	14.7	0.12
13	16.3	100	270	57.0	4.3	8.18	0.606
14	0.7	100	3	214	2.3	28.8	0.093
15	0.75	100	3.5	267	2.6	18.9	0.06

Mean Aperture using Breakthrough Time = 0.25 mm  
Standard Deviation = 87%

The estimated fracture apertures can thus be calculated using the model match parameters, providing that values for the molecular diffusivity, matrix porosity and apparent dispersion coefficient can be obtained.

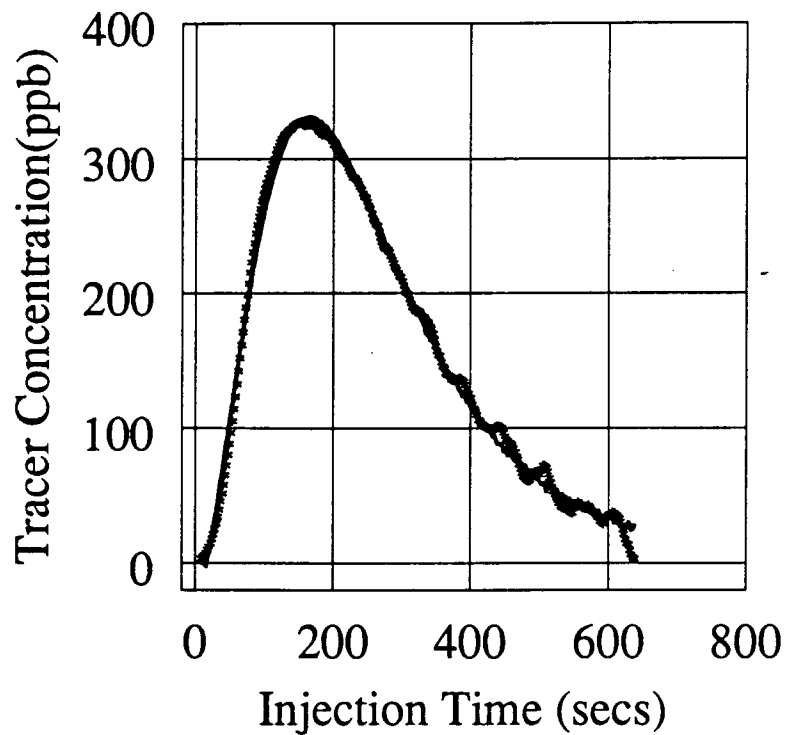


Figure 29. Matrix diffusion model with error function inlet boundary condition  
Model (-) and data (\*) at flowrate = 1.75 cc/min

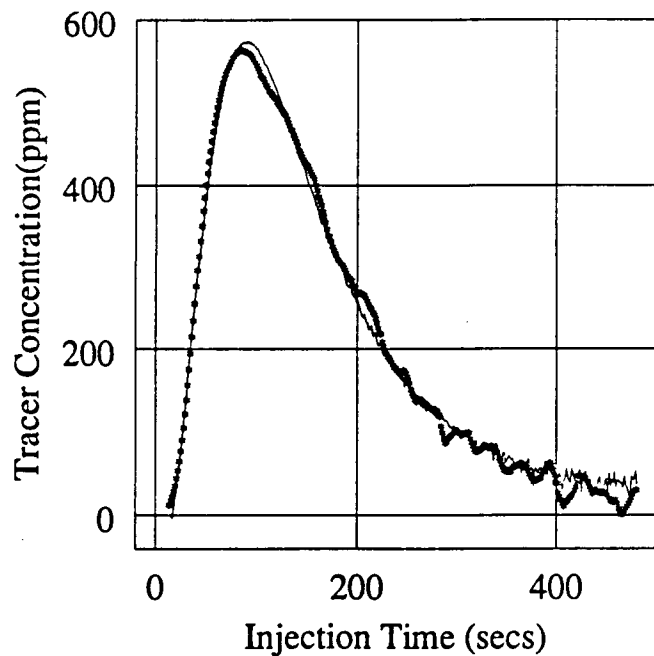


Figure 30. Matrix diffusion model with error function inlet boundary condition  
Model (-) and data (\*) at flowrate = 3.7 cc/min

### Section 6.3.2 Taylor Dispersion Model with Dispersed Inlet Boundary Condition

Although the Matrix Diffusion model as modified for an error function inlet boundary condition had already matched the experimental data well, the Taylor Dispersion model was also modified and fitted to the data. Detailed derivation of the modified solution is not presented, however, it is similar in principal to that for the Matrix Diffusion model modification and the final solution is shown in Appendix B.

The resulting match with this model (Figures 31 and 32) is worse than the unmodified version. Fitting the data shifted the test start time some 20-50 seconds AFTER the tracer had already broken through in the core effluent. The model is obviously not practical for matching experimental test data, however, this negative result is presented for completeness.

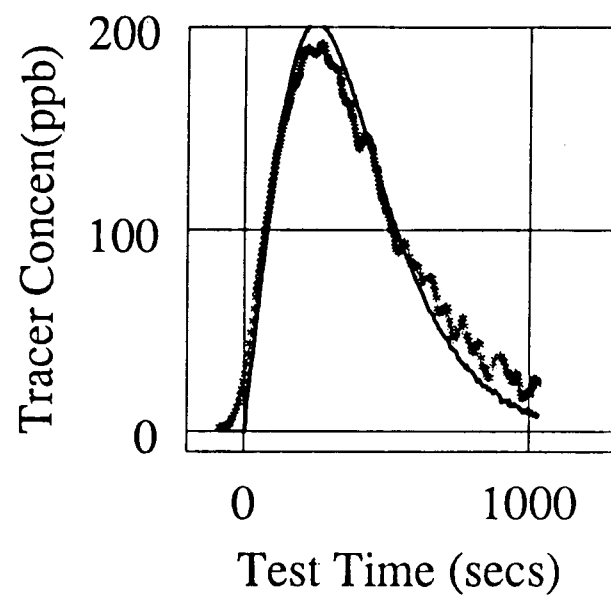


Figure 31. Fossum model with modified boundary condition: Note breakthrough before start time. Model (-) and data (\*) at 0.8 cc/min flowrate.

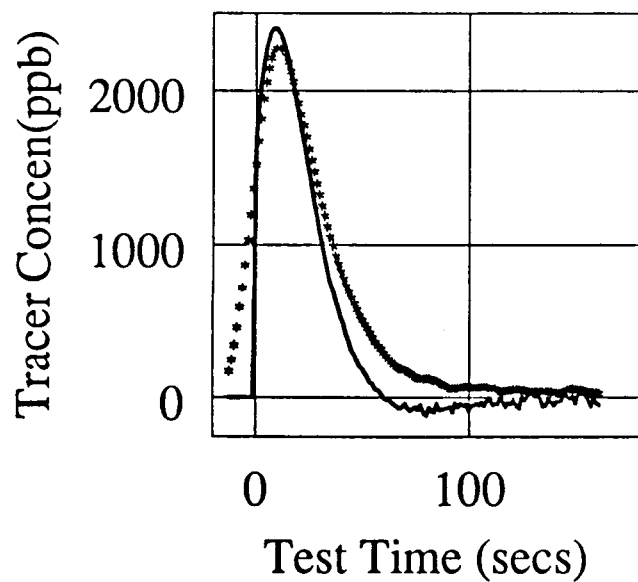


Figure 32. Fossum model with modified boundary condition: Note breakthrough before start time. Model (-) and data (\*) at 16 cc/min flowrate.

## SECTION 7: MATRIX DIFFUSION MODEL MATCH PARAMETERS

The three parameters matched with the modified Matrix Diffusion model were used to estimate core properties and checked for consistency with other experimental observations. The matched datum time correction was used to calculate the tubing volume between the two electrodes. The matched breakthrough time was used to calculate a unique fracture width. The third parameter, the dimensionless dispersion coefficient, provided another fracture width estimate and also characterized the tracer matrix diffusion and absorption mechanisms.

### Section 7.1 Datum Time Correction

The model matched datum correction times for all runs are listed in Table 4. These datum corrections were used in Equation 4 together with the inlet electrode tracer arrival time and the measured test fluid flow rate to calculate the tubing volume between the electrodes. The calculated tubing volumes are shown in Table 4 for all the runs. The estimates generally show little scatter and agree with the tubing volume estimates previously made. The average value is 2.6 cc with only a few cases deviating more than 5-10%.

Although the tubing volume has no bearing on deriving core property estimates, the figures are included because they provide a quality control check on the experimental data. Generally, the runs significantly deviating from the 2.6 cc average are suspect and the quality of the experimental data should be scanned for any errors. The model predictions for these runs (nos. 9 and 10) actually do not fit the measured data very well, further indicating a problem with the data. These test results are most likely skewed by a changing flow rate during the course of the run. In any respect, these test results should be weighed lightly when evaluating core properties.

## Section 7.2 Breakthrough Time

The model matched core effluent breakthrough times provided a unique opportunity to estimate the fracture aperture directly. In field tests, the areal (or vertical) extent of the fracture is seldom known. Even if some approximation can be made, the degree to which the tracer actually flows within the full areal extent is never known. The laboratory test differs from field tests as the core is confined and a direct estimate of the fracture length and cross-section is available. Using the measured core dimensions and the flow rates a simple formula for fracture width can be derived.

$$W = \frac{q}{L D \beta} \quad (12)$$

where

$W$  = fracture width cm

$\beta$  = matched reciprocal breakthrough time  $\frac{1}{\text{sec}}$

$q$  = flow rate  $\frac{\text{cm}^3}{\text{sec}}$

$L$  = core length = 15.24 cm

$D$  = core diameter = 2.36 cm

The fracture width values calculated using this equation are listed in Table 4 along with the matched tracer breakthrough times. Values range from 0.06 cm down to 0.004 cm. The estimates vary widely, but not randomly. There is an obvious correlation between rate and estimated aperture, with larger apertures inferred at the higher flow rates. It may be that results at low rates suffer from an uncertainty similar to that which exists at field scale; that is the unknown flow distribution across the fracture width. At higher rates the flow may fully distribute across the core diameter, however, at low flow rates a preferential flow path within the fracture may inhibit the flow from fully developing across the full fracture width. The actual cause of the variation remains uncertain, however the fracture aperture estimates from the core cast (0.08 cm)

and the hydraulic calculations (0.012 cm) generally bound the model estimates, indicating the approximation is fairly good.

### Section 7.3 Dimensionless Dispersion Coefficient

After evaluating the fracture aperture using the matched breakthrough time, the dimensionless dispersion parameter was used to provide a second estimate of the fracture aperture and to investigate the tracer diffusion and adsorption within the core. The coupling of these effects into one parameter prevents a unique estimate of the effects of any single parameter unless other information is available. As stated earlier, the dimensionless dispersion parameter represents the following:

$$\alpha = \frac{D_e}{W\sqrt{D_a \beta}} \quad (13)$$

Of the five terms in this equation, three are unknown. Only the first breakthrough time and the dimensionless dispersion parameter are known from the model match. Thus, estimates for the effective and apparent diffusivities must be made to calculate the fracture aperture. The tracer effective diffusivity is difficult to precisely estimate, however, it is usually taken as the product of molecular diffusion and the matrix porosity. Thus,

$$D_e = D_m \Phi \quad (14)$$

or, more specifically for these tests:

$$D_e = 2.1 \times 10^{-5} \frac{cm^2}{sec} \times 0.17 = 3.57 \times 10^{-6} \frac{cm^2}{sec}$$

The effective diffusivity is generally found to be within an order of magnitude of this estimate for a porous medium.

The fourth parameter, the apparent diffusivity is more difficult to estimate mainly because such a wide range of values are observed in field and laboratory situations. Generally,

$$D_a = \frac{D_e}{K_d \rho_p} \quad (15)$$

where

$K_d \rho_p$  = the dimensionless solid/liquid partition coefficient

For non-sorbing solutes, Neretnieks (1980) has shown this parameter is equal to the matrix porosity. He also indicates that for strongly sorbing solutes values up to 10000 are not uncommon. This wide range of possible values (0.01-10000) for the adsorption parameter usually far outweighs the uncertainty in the effective diffusion coefficient and thus warranted more investigation into the appropriate value for the laboratory tests. The specific solute of interest, KI, is usually considered non-sorbing in geothermal rocks, but the core sample in this study is an unfired sandstone. As the sandstone may contain some clays with adsorption sites available to the solutes, the adsorption of KI was investigated using the experimental data already available and by means of a laboratory adsorption experiment.

The degree of any tracer adsorption was initially evaluated by integrating the effluent tracer concentration profiles (minus the influent profile) to calculate the cumulative volume of tracer retained in the core. Results for several runs were reviewed and the results from three typical runs are shown in Figures 33 through 36. Figures 33, 34 and 35 show the core inlet and outlet tracer concentration as a function of pore volume for three different flow rates. The area between the curves can be integrated to determine the volume of tracer actually retained within the core. The integration results (Figure 36) indicates the cumulative tracer mass retained in the core as a function of pore volumes injected. In some cases up to 0.8 mg of KI has been retained in the core. Using the 11.5 cc core pore volume, this suggests an average core fluid concentration of 52 ppm or 50% of the injected tracer concentration. However, this is not possible if diffusion (a very slow process) is the only process considered to be retaining tracer within the core. Rough calculations show that an average tracer concentra-

tion of only 3-5 ppm would exist in the matrix if diffusion were solely responsible for the tracer retained within the matrix. This 3-5 ppm tracer concentration can only account for some 0.05 mg of tracer in the core matrix. Summing the tracer mass retained in the core matrix with the 0.10-0.15 mg in the fracture results in only 0.15 to 0.20 mg of total tracer mass in the core. This figure falls far short of the tracer mass indicated by Figures 33 through 36. Adsorption, or another similar process, must be the cause of this additional tracer retention in the core.

The adsorption parameter was quantified by means of a simple experiment. A 6.4 cc bulk volume piece of core was crushed to its 5.34 cc granular volume. The rock was then mixed with 170 cc of a 105 ppm tracer solution. The tracer solution subsequently decreased in concentration to 69 ppm. Using this data, a dimensionless sorption parameter of 17 was calculated. This is indicative of a very weakly sorbing solute, which is reasonable for KI in a low porosity sandstone.

Finally, all the terms in the dimensionless dispersion parameter have been quantified except the fracture aperture. The adsorption and diffusion terms and the two model match parameters were then used to make a second estimate of the fracture aperture. The following values for the coefficients in Equation 13 were used in estimating the fracture aperture:

$$D_e = 3.57 \times 10^{-6} \frac{cm^2}{sec}$$

$$D_a = 2.1 \times 10^{-7} \frac{cm^2}{sec}$$

$\alpha$  = known model match parameter dimensionless

$\beta$  = known model match parameter  $sec^{-1}$

Calculated values are tabulated with the match parameters in Table 4. The calculated apertures all range from 0.01 to 0.09 cm, which agrees well with other estimates.

Another method for estimating the fracture aperture from the model dimensionless dispersion parameter was also evaluated. The reciprocal breakthrough time was treated as an unknown and Equation 12 was substituted into equation 13. The result is the following equation for fracture aperture based on the model matched dimensionless dispersion parameter, the apparent and effective diffusivities, and the injection flow rate:

$$W = \frac{D_e^2}{\alpha} \frac{L D}{q D_a} \quad (16)$$

Using this formula, the fracture apertures shown in Table 5 were estimated. These estimates are the more consistent than the previous estimates, with an average value of 0.073 cm and a 33% standard deviation from the average value. If the two suspect cases (8 and 13) are disregarded, the average is 0.068 cm with an 18% standard deviation. This fracture aperture determination is by far the most accurate of the three methods used. Unfortunately, this method is difficult to use in a field test analysis where the fracture areal extent is not known.

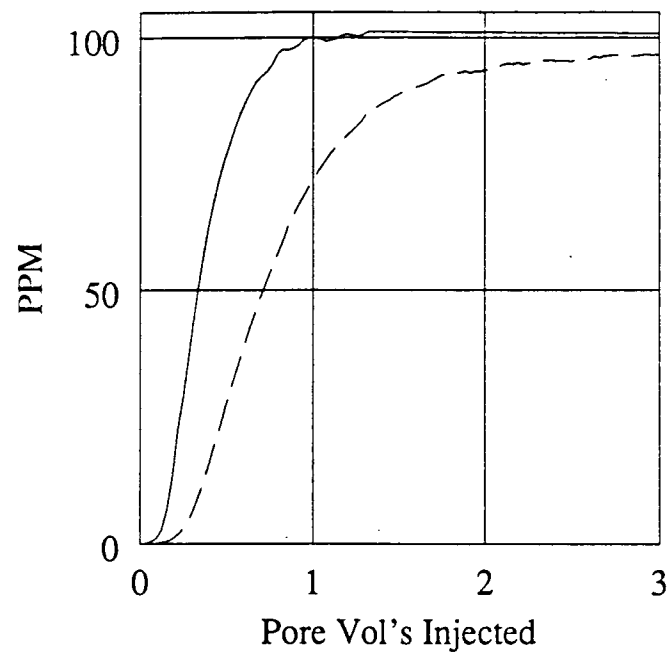


Figure 33. Core inlet (-) and outlet (--) profiles showing tracer retained in core.  
Flowrate = 16 cc/min

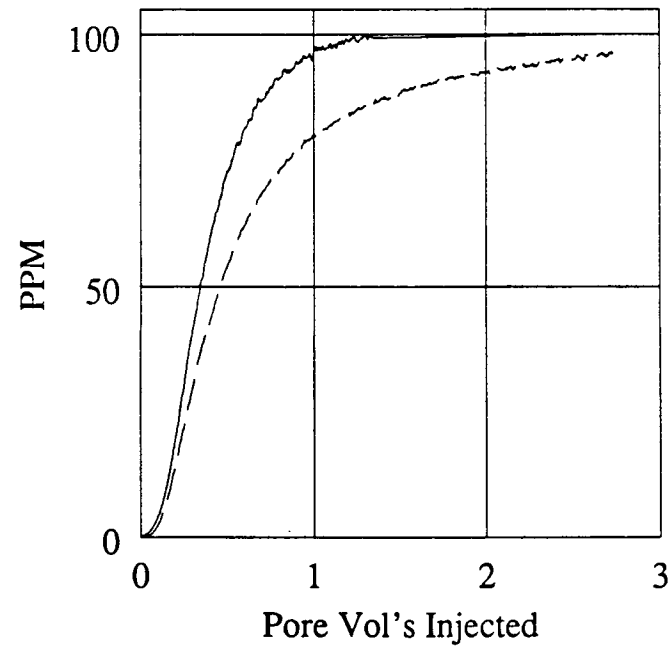


Figure 34. Core inlet (-) and outlet (--) profiles showing tracer retained in core:  
Note less area between curves as rate decreases.  
Flowrate = 1.4 cc/min

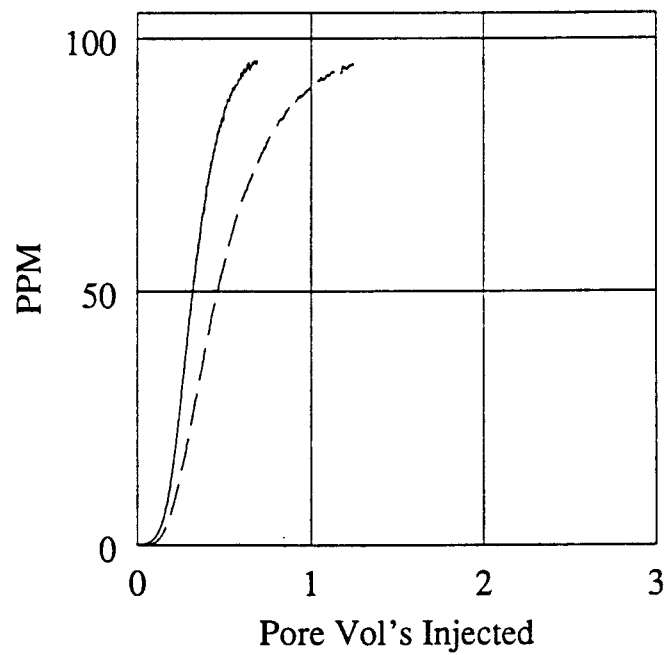


Figure 35. Core inlet (-) and outlet (--) profiles showing tracer retained in core:  
Note less area between curves as rate decreases  
Flowrate = 0.8 cc/min

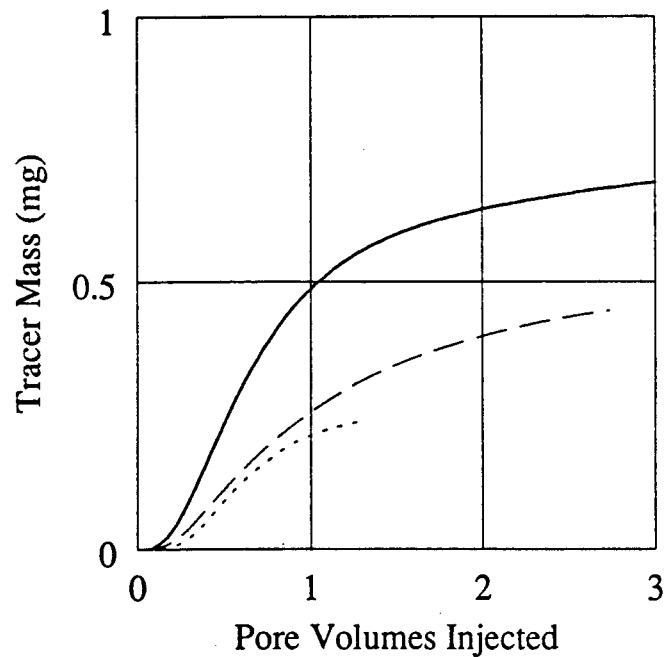


Figure 36. Cumulative tracer mass retained in core at 3 flowrates: Note tracer retention decreases with flowrate  
16 cc/min (-), 1.4 cc/min (--) and 0.8 cc/min (---)

## Section 7.4 Discussion of Fracture Aperture Estimates from Model Match Parameters

In the preceding two sections, the two diffusion model parameters were used to generate fracture aperture estimates ranging from 0.005 to 0.090 cm. The average estimate using the breakthrough time parameter is 0.0245 cm with a standard deviation of 0.0212 cm or 87% of the predicted value. The average value derived with both parameters is 0.0463 cm with a standard deviation of 0.025 cm, or 53% of the predicted value. The average value derived using only the dimensionless dispersion parameter is 0.07 cm with a 33% standard deviation. If runs 9 and 13 are disregarded (discrepancy between measured and regressed time datum corrections and a poor model match of the measured data), the standard deviation for aperture estimates using only the breakthrough time parameter drops to 83%, 44% when using both parameters and 18% when using only the dimensionless dispersion parameter. All aperture estimates of 0.025 cm, 0.046 cm and 0.07 cm are reasonable, however, the third value is obviously more reliable based on the standard deviation parameters. The greater precision in the estimate made with only the dimensionless match parameter suggests 0.07 cm is the best estimate of the actual fracture aperture.

The cause of the increased precision in the second and third aperture estimates may be due to errors in the breakthrough parameter. This lower precision in aperture values estimated from the tracer breakthrough time could be due to errors introduced into the model through the inlet dispersion function. Slight changes were made to the constants in the inlet dispersion function to reflect the degree of uncertainty associated with the inlet dispersion correlation (Figure 28). These changes were found to have far less effect on the regressed dimensionless dispersion parameter than the regressed value for the breakthrough time. Thus, errors inherent in an empirical correlation such

as Figure 28 would have a greater impact on the aperture values derived from only the breakthrough time, which is far more sensitive to the inlet boundary condition. The possible errors in the inlet boundary condition, therefore, would result in the widest range of apertures derived from the breakthrough time parameter alone. The error would be reduced when using both parameters and almost eliminated if the breakthrough term was ignored. This is parameters and eliminated when the breakthrough term was ignored.

The exact cause of the greater error in the apertures derived using only the breakthrough time remains a subject for further work. It is clear, though, that the dimensionless dispersion coefficient provides a more reliable fracture aperture estimate and should be given far greater weight in any field test analyses.

## SECTION 8: TRACER ADSORPTION: CALCULATED AND MEASURED TRACER RETENTION IN THE CORE

The previous fracture aperture calculations from model match parameters noted the significance of the adsorption and diffusion terms in estimating fracture aperture. If a totally non-sorbing solute had been assumed, the fracture aperture calculated from the match parameters would have been an order of magnitude below the estimate made from the breakthrough times and the aperture observed in the epoxy fracture cast. This stresses the importance of quantifying tracer adsorption when interpreting test results. Even if the tracer is very weakly sorbing, assuming no adsorption can lead to considerable errors in estimating fracture aperture. As adsorption has such a significant impact on the model aperture estimate, the tracer retained within the core due to adsorption was modelled to determine whether model calculations agreed with the measured values from the core inlet and outlet tracer concentration profiles (Figures 33 through 36).

### Section 8.1 Tracer Retention for a Sorbing Tracer

The tracer retention within the core was determined in two steps. First, the tracer concentration distribution was determined. Second, the distribution was integrated over the core to determine the total mass within the core. To accomplish the first step, the flow model, match parameters and dispersion and adsorption terms were used to calculate the final tracer concentration distribution within the core when the tracer test was terminated. The concentration distribution was determined using the following Laplace space equation for the modified Matrix Diffusion model derived in Appendix B:

$$C_m = e^{-\frac{2b}{\sqrt{s+a}(\sqrt{s+a}-\sqrt{a})}} e^{-\frac{s}{\beta}} e^{-2\alpha\frac{\sqrt{s}}{\sqrt{\beta}}} e^{-z\frac{\sqrt{s}}{D_a}} \quad (17)$$

where

$C_m$  = concentration within the core at  $z$

$$z = \text{distance fracture wall cm}$$

The concentration within the fracture is obtained by setting  $z$  to zero.

Equation 17 was inverted from Laplace to real space with the Stehfest algorithm (1970), and used to calculate the tracer concentration distribution away from the fracture wall at locations 2, 4, 6, 8, 10, 12 and 15 cm from the core inlet. The calculations were made for the end of the 16 cc/min run (400 seconds). The tracer concentration distributions determined using Equation 17 (Figure 37) were found to vary little with the distance from the core inlet. The test time was found to be far more important in determining the tracer distribution within the rock matrix. Thus, the tracer concentration distribution calculated at only one location (Figure 37) was used to represent the entire core length. The calculated distribution was then used in the following numerical integration scheme to determine the cumulative mass retained within the core matrix:

$$M_m = \frac{C_z + C_{z+dz}}{2} dz L D \phi + K_d \rho_p \quad (18)$$

where

$$C_z = \text{tracer concentration at } z \frac{mg}{cm^3}$$

$$C_{z+dz} = \text{tracer concentration at } z + dz \frac{mg}{cm^3}$$

$$dz = \text{increment in } z \text{ direction cm}$$

$$D = \text{core diameter } 2.5 \text{ cm}$$

Using equation 18, the total mass was summed over the core matrix. The total mass in the core was then determined as

$$M_t = M_m + M_f = M_m + W L D C_f \quad (19)$$

where

$$M_t = \text{total mass in core mg}$$

$$M_f = \text{mass in fracture mg}$$

$$C_f = \text{tracer concentration in fracture } \frac{mg}{cm^3}$$

Using Equations 18 and 19, the cumulative mass retained in the core was calculated as a function of matrix penetration depth (Figure 38). The model estimates a total of 0.9 mg is retained within the entire core. This figure agrees with the 0.76 mg estimate made using the core inlet and outlet tracer concentration profiles (Figures 33 and 36). Of the 0.9 mg calculated, 0.173 mg is estimated to be in the fracture, only 0.007 gm is dissolved in the matrix pore fluid and 0.72 gm is adsorbed onto the rock.

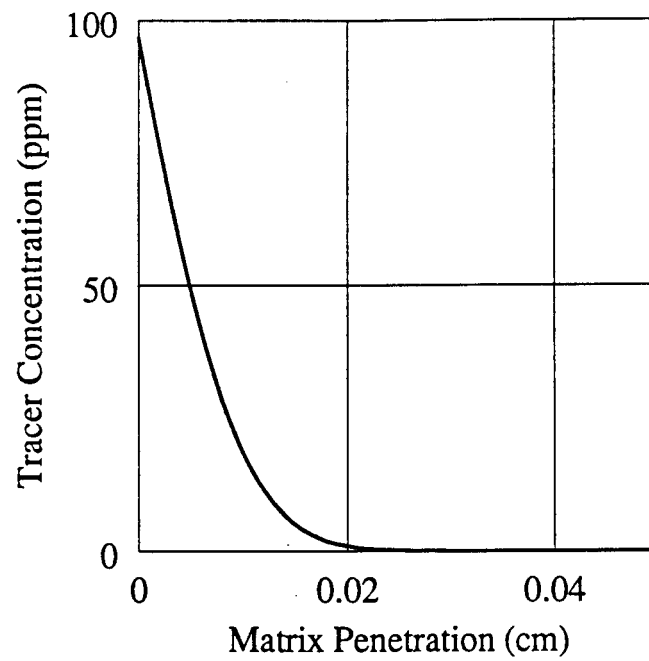


Figure 37. Tracer concentration in the matrix pore fluid after 16 cc/m test

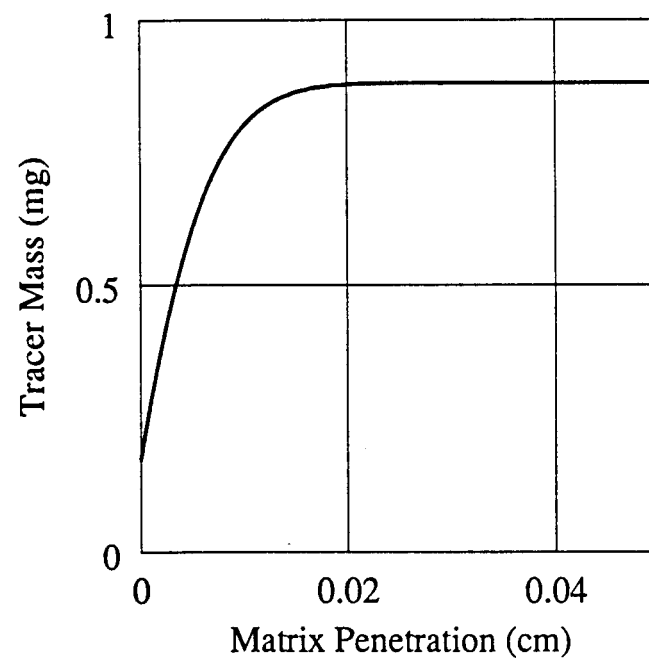


Figure 38. Total tracer mass in the core at a given matrix penetration depth

## Section 8.2 Tracer Retention for a Non-Sorbing Tracer

The previous tracer retention calculations used the adsorption coefficients derived in Section 7. If, however, no tracer adsorption occurred in the core (i.e. a non-sorbing solute as a tracer), diffusion alone into the matrix could act as a tracer retardation mechanism. An estimate of the tracer concentration distribution and total tracer mass retained within the core assuming a non-sorbing tracer was possible using Equations 17-19 by using the following definition for the dimensionless adsorption parameter:

$$K_d \rho_p = \phi$$

Using this modification, the tracer concentration distribution for a non-sorbing tracer was calculated from Equation 17 at the end of the 16 cc/m flowrate test (Figure 39). As expected, the non-sorbing tracer is retarded less and penetrates deeper into the core. These non-sorbing tracer concentrations (Figure 39) were then used in Equations 18 and 19 to estimate the total mass retained in the core for a non-sorbing tracer (Figure 40). The non-sorbing tracer resulted in only 0.24 mg of tracer retained in the core. Of this 0.24 mg, roughly 0.06 is within the matrix pore fluid and 0.17 mg is within the fracture. This low retention within the matrix reflects the slow diffusion of tracer into the rock pore volume. Thus, tracer retained with a non-sorbing solute is significantly lower than the 0.76 mg actually calculated previously using influent and effluent data. Considering the large discrepancy between the non-sorbing tracer calculations and the experimental observations, and the fair agreement between the adsorption model estimates and the experimental data, tracer adsorption at the levels assumed in the fracture aperture calculations are justified. Tracer retention due only to matrix diffusion (0.24 mg) can not account for the 0.8 mg of tracer retained in the core during the test.

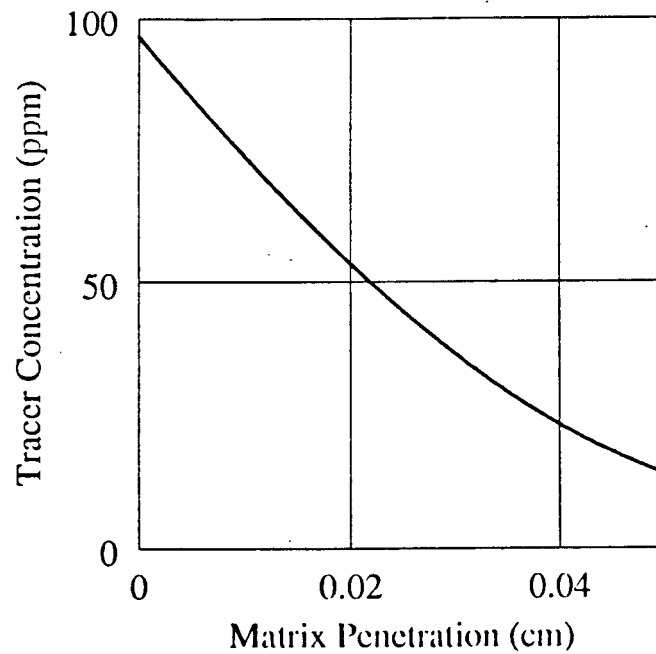


Figure 39. Tracer concentration in the matrix for a non-sorbing tracer

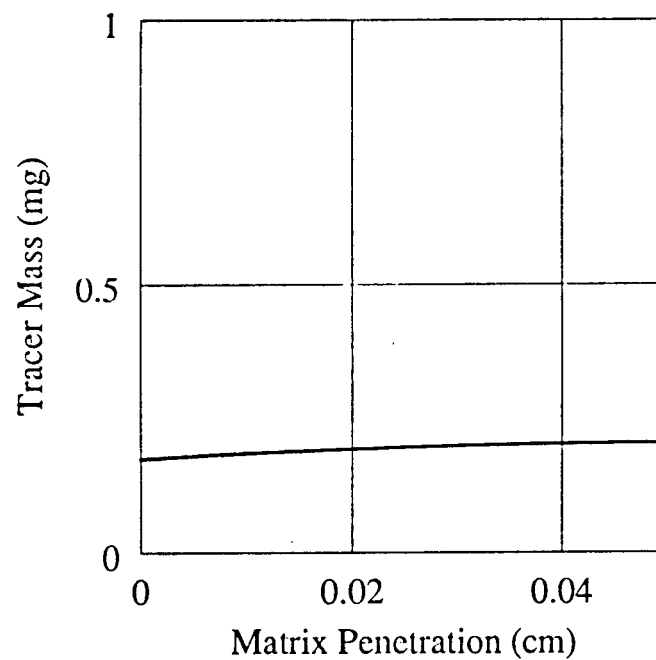


Figure 40. Total tracer mass retained in the core for a non-sorbing tracer:  
Note the majority of the tracer is within the fracture

### Section 8.3 Tracer Retention for Low Flowrate Tests

To further test the above conclusions, core tracer concentration profiles (Figure 41) and core mass retention estimates (Figure 42) for a sorbing solute using the effective and apparent diffusivities from Section 7 were made for the end of the 1.4 cc/min flow rate test (900 seconds). These calculations actually show larger tracer masses retained in the core at the end of the test than the tracer retention estimates for the 16 cc/min case. The higher retention for the lower rate case predicted by the model occurs because the test time at lower flowrates is longer. The actual test flowrate is a significant factor effecting tracer retention within the core until tracer breakthrough in the core effluent. After breakthrough, tracer concentrations rise rapidly reaching 50 to 60% of the injected tracer concentration in a short time. The effect of flowrate, therefore, diminishes rapidly after only 0.3-0.4 pore volumes injected. After 0.4 pore volumes are injected, tracer concentrations within the fracture are high enough regardless of flowrate to allow effective diffusion into the rock matrix and the most important parameter effecting tracer mass retained in the core is time, as diffusion is the limiting process. Therefore, according to the model the lower rate case, which takes twice as much time to run as the higher rate test, should retain more tracer.

These calculations predicting a larger tracer mass retained in the core at the lower flowrates, however, contradict the experimental data from the tracer retention plots (Figures 33 through 36). The experimental data shows a decrease in tracer mass retained in the core as flowrate decreases. The cause for this discrepancy remains unknown. A concentration dependent adsorption parameter which decreases with concentration could, perhaps, explain the reduced tracer mass retention at the lower flowrate. The longer time period when the low flowrate case has a lower effluent tracer concentration would then be more significant, reducing the total mass adsorbed in the core.

However, if a lower adsorption parameter were assumed for the lower rate case, the model matched fracture aperture for the low flowrate cases (already below average) would drop more than an order of magnitude. Also, if a concentration dependent adsorption parameter existed, one would expect the adsorption parameter to increase (rather than decrease) with decreasing concentration as more adsorption sites would be available to the solute on a unit mass basis.

Considering the anomalous tracer breakthrough times and the unexplained adsorption characteristics of the lowest flowrate tests, some deviation from the flow model is apparent in the laboratory tests. A reduced core flow area due to channeling within the fracture could cause premature breakthrough and also lower tracer retention by reducing the surface area for mass transfer into the rock matrix. The possibility of hydrodynamic dispersion within the fracture also could explain the experimental results. The cause for the discrepancy remains uncertain and is the subject for further work.

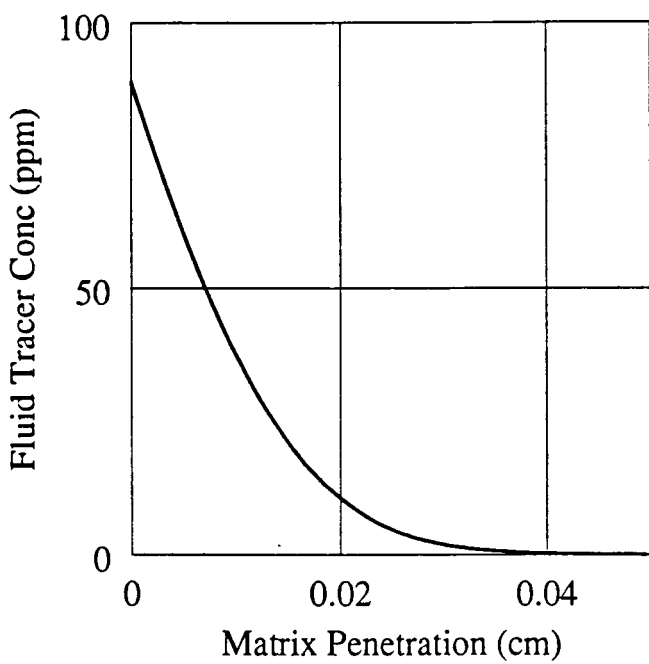


Figure 41. Tracer concentration in the matrix pore fluid after the 1.4 cc/m test

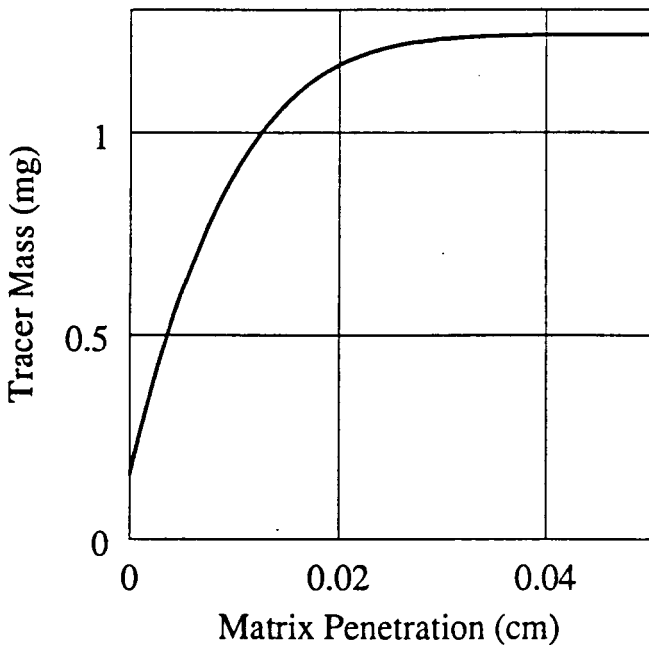


Figure 42. Total tracer mass in the core after the 1.4 cc/m test

## SECTION 9: INLET BOUNDARY CONDITION EFFECTS ON TEST RESULTS

The dispersed inlet boundary condition obviously had an effect on test results as modification of the tracer flow model was necessary to accurately match the laboratory data. To evaluate the effects of tracer dispersion in the inlet tubing on the experimental results, the model match parameters generated for the various core tests were used in the standard slug injection Matrix Diffusion model to estimate the core response without the dispersed inlet condition. Taking the model match parameters for the reciprocal breakthrough time and the dimensionless dispersion coefficient from the runs at 16 cc/min and 0.8 cc/min, the core response to a uniform tracer slug at the core inlet was simulated (Figures 43 and 44). Comparing the ideal slug test results with the actual experimental data, the inlet dispersion effects on test results is significant. The simulated test indicates a higher peak value and steeper early time response would occur without any tracer dispersion before entry into the core. A pore volume plot of the simulated test data was also generated (figure 45). The pore volume plot for the simulated test more clearly shows breakthrough at near peak concentration levels after a pore volume on the order of the fracture volume has been injected. The pore volume plot also shows a change in the trend seen in the actual experimental data (Figure 14). The simulated pore volume plot shows similar peak arrival concentrations for both rates, whereas, a higher peak was observed at the lower rates in figure 14. This result is more consistent with expectations, as the breakthrough times for both tests are so small, the effect of diffusion on the slug peak should be relatively insignificant. Thus, the somewhat anomalous result seen in the actual data is an artifact of the mixing in the inlet tubing prior to the tests.

Comparing the simulated slug tests with the experimental data collected in the laboratory, the laboratory test conditions could be improved to provide a laboratory

test which is more similar to field tests. The two simulated cases (Figure 43 and 44) show the experimental data deviates from the standard slug test response more than indicated by the initial match attempted with the unmodified Matrix Diffusion model (Figures 19 and 20). The simulated slug test response has a much stronger asymmetry than the laboratory tests and, thus, actually better emulates the asymmetry of the field test response seen in Wairakei. A preliminary review of the data collected in this study was conducted before detailed modeling efforts were undertaken. The review (as well as the initial model match attempts in Figures 19 and 20) had indicated the laboratory tests were responding similarly to the Wairakei tests. However, the final analysis indicates the laboratory conditions had a significant impact on the tracer test results. The impact of the mixing of the tracer solution with the background distilled water before entering the core is greater than initially expected. As the real goal of this work was to emulate the field test conditions, it is recommended that the mixing effects be eliminated in any further testing efforts. This could be accomplished by using a longer core, reducing the effects of the tracer mixing zone at the core inlet until they were negligible. Calculations based on the experiences in this study could be made to determine the required core length for the new test apparatus so that the dispersed zone in the core effluent would not impact the test response.

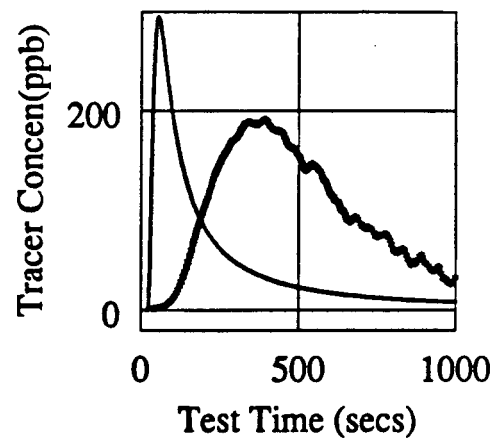


Figure 43. Simulated core response (-) compared with experimental results (\*)  
Flowrate = 0.8 cc/min

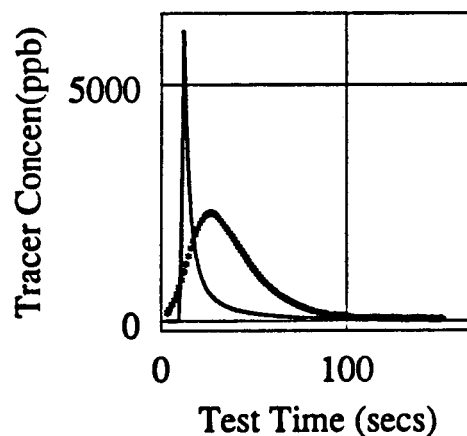


Figure 44. Simulated core response (-) compared with experimental results (\*)  
Flowrate = 16 cc/min

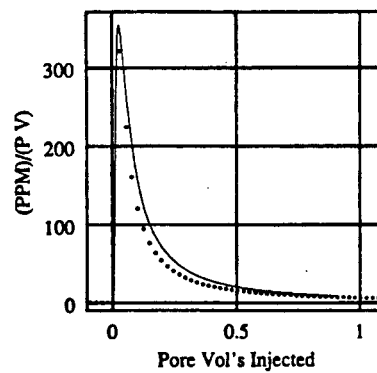


Figure 45. Pore volume plot for simulated core tests, 16 cc/min (-) & 0.8 cc/min (\*)

## SECTION 10: CORE FRACTURE APERTURE: CALCULATED VS. MEASURED

One of the objectives of this study was to verify the accuracy of the tracer model in estimating fracture aperture. Three estimates of the fracture aperture were made during the course of this work. Fracture permeability calculations were made using the following cubic fracture flow equation:

$$q = \frac{W^3}{12} \frac{P_i - P_e}{L} \quad (19)$$

The results of these calculations provided an estimate of the fracture aperture (0.012 cm). An estimate of the fracture aperture was also available from physical observations of the fracture cast. The fracture cast, created with epoxy resin, indicated a mean aperture of 0.08 cm. Finally, the tracer model match parameters were used to obtain two fracture aperture estimates. Fracture aperture estimated from the breakthrough time was 0.025 cm, with a 85% standard deviation. Using both match parameters, an average aperture of 0.047 cm with a 45% standard deviation in the data was calculated. Using only the dimensionless dispersion parameter, an average value of 0.07 cm was calculated with a 33% standard deviation. The differences between the various estimates and the fairly broad range in the tracer model estimates can be explained by comparing the physical conditions of the tests to the assumptions inherent in the models used to evaluate the fracture aperture.

The aperture estimate determined using flow rate and pressure drop measurements in the cubic fracture aperture equation assumes that a uniform fracture exists throughout the core. In reality, proppant within the fracture creates substantial restrictions impeding flow. It is not surprising, then, that a lower value is predicted using this simple equation. The equation could be adjusted to account for the fracture proppant by modifying the flow area to reflect this flow restriction. This roughly works out to a

25% increase in fracture aperture for a 50% reduction in flow area. Using this order of magnitude approximation and the visual observation that as much as 80-90% of the fracture area is blocked by sand grains in the epoxy cast, a fracture aperture on the order of 0.05 cm is more likely. Another unknown, influencing the fracture permeability estimate of fracture aperture, is the pressure drop in the laboratory flow system. The pressure drops across the fracture were initially anticipated to be 10 to 20 psi and the 0.2 to 0.5 psi head losses in the flow system were considered negligible. However, at the lower pressure drops (0.3 to 1.5 psi) required to minimize matrix flow, the flow system losses cannot be ignored. Considering this factor, the actual pressure drop occurring within the core would be reduced, increasing the aperture estimate by as much as 50%. The actual pressure drop within the flow system is, however, difficult to calculate due to the complex mixing heads used in the core holder. For this reason, a quantitative impact of flow system head losses is not possible. In summary, the 0.012 cm aperture estimate represents a likely lower bound on the true aperture as all of the errors inherent in this estimate tend to lower the calculated values.

The fracture aperture indicated by the epoxy cast is, perhaps, a good estimate of the true fracture aperture. The low standard deviation of the measured values suggests little error in the measurements, however, the error in this estimate is not due to the physical measurement system. The main uncertainty is whether the fracture cast actually represents the overburden core conditions, or, if the fracture cast swelled when released from the core holder. The cast could not totally dry without air in the core holder and it is possible the aperture (and the cast) expanded once released from overburden pressure. Considering this possibility, the core cast is most likely a good upper bound on the fracture aperture.

The fracture aperture estimate from the tracer flow model, which is the main rea-

son for this study, has a fairly wide range of variability. However, errors apparent when estimating the fracture aperture from the first breakthrough time alone actually are responsible for the majority of the uncertainty in the model estimates. The variation in apertures arising when only the second match parameter is used to determine the aperture is not extreme and the range of error in the estimate is well within 20 % of the average value. This result would suggest the aperture as derived by the tracer analysis model is roughly 0.07 cm, fitting extremely well into the above upper and lower bounds on the actual fracture aperture from physical measurements.

## SECTION 11: SUMMARY AND CONCLUSIONS

1. Tracer tests on fractured cores were conducted in the laboratory resulting in tracer response profiles similar to those observed in fractured geothermal reservoirs such as Wairakei.
2. Laboratory tracer tests were analyzed with two analytical flow models. The Taylor Dispersion model was found to be inappropriate for matching the data even after adjusting the model for experimental conditions. The Matrix Diffusion model was found to match the test data reasonably and, once modified for the tracer dispersion in the inlet of the laboratory equipment, gave a very accurate match of the measured data.
3. Parameters arising from the match of the data to the Matrix Diffusion model were used to estimate core properties. Estimated average fracture apertures was found to be 0.07 cm which, agrees well with other estimates. The tracer/rock adsorption characteristics were also defined. A value of 17 for the dimensionless partition coefficient was estimated.
4. The Matrix Diffusion model realistically reflects tracer transport mechanisms in fracture dominated, low porosity reservoirs. The model's parameters can be used to provide reliable estimates of reservoir properties such as the fracture aperture and tracer adsorption and diffusion characteristics.
5. Adsorption effects, even for very weakly sorbing tracers, are significant and these effects should be included in fracture aperture estimates.

## SECTION 12: RECOMMENDATIONS

1. Further studies of the reverse tracer tests and the adsorption characteristics of the lower flowrate tests should be conducted to gain insight into the diffusion/adsorption of tracer in field slug tests.
2. Future tests in laboratory samples should use a longer core length (200-300 cm) to minimize the effects of tracer mixing prior to entering the core. Samples of lower matrix porosity and permeability should be used as they will be more representative of flow rates, pressure drops and fracture widths observed in the field.
3. Tracer test models which can provide a unique fracture estimate in field tests should be investigated to model the laboratory tests from this study. The uncertainty in the effects of diffusion and adsorption effects on tracer transport could thus be eliminated.
4. Until the development of a model which decouples diffusion and adsorption effects from the mechanisms which characterize the fracture aperture, the Matrix Diffusion model can be used to give a good estimate of fracture aperture. When estimating the fracture width, reservoir adsorption properties should be considered due to the strong coupling of these two terms in the model solution.

## SECTION 13: NOMENCLATURE

$C_f$	Tracer concentration in fracture <i>ppm</i>
$C_m$	Tracer concentration in matrix <i>ppm</i>
$C_o$	Tracer concentration in injected tracer solution <i>ppm</i>
$p_i$	Core inlet pressure <i>psia</i>
$p_e$	Core outlet pressure <i>psia</i>
$P_e$	Peclet number, dimensionless
$D_a$	Apparent diffusion coefficient $\frac{cm^2}{sec}$
$D_m$	Molecular diffusion coefficient $\frac{cm^2}{sec}$
$D_p$	Porous media dispersion coefficient $\frac{cm^2}{sec}$
$D_h$	Porous media hydrodynamic dispersion coefficient $\frac{cm^2}{sec}$
$D_e$	Effective diffusion coefficient $\frac{cm^2}{sec}$
$t_a$	Actual test time relative to tracer entry into core sec
$t_{da}$	Datum time correction from clock time to actual test time sec
$t_d$	Dimensionless time
$t_{ie}$	Measured inlet electrode tracer arrival time sec
$t$	Time sec
$V_t$	Tubing volume between electrodes $cm^3$
$M_m$	Tracer mass in core matrix <i>mg</i>
$M_f$	Tracer mass in core fracture <i>mg</i>
$M_t$	Total tracer mass in core <i>mg</i>
$K$	Permeability <i>darcy</i>

$q$	Flowrate $\frac{cm^3}{sec}$
$A$	Cross sectional area $cm^2$
$L$	Core length $cm$
$u$	Flow velocity $\frac{cm}{sec}$
$x$	Tubing length $cm$
$D$	Core diameter $cm$
$W$	Fracture aperture $cm$
$a$	Inlet dispersion parameter = $\frac{u^2}{4\eta} \text{ sec}$
$b$	Inlet dispersion parameter = $\frac{x}{2\sqrt{\eta}} \text{ sec}^{\frac{1}{2}}$
$\eta$	Taylor dispersion coefficient $\frac{cm^2}{sec}$
$\beta$	Reciprocal breakthrough time $\frac{1}{sec}$
$\phi$	Matrix porosity <i>void fraction</i>
$\alpha$	Dimensionless dispersion coefficient

## REFERENCES

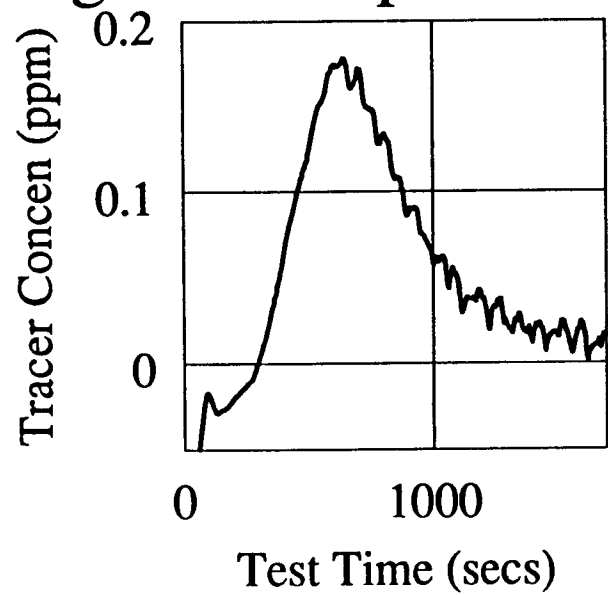
1. HORNE, R. N., "Geothermal ReInjection Experience in Japan," Journal of Petroleum Technology, March 1982.
2. FOSSUM, M. P., Tracer Analysis in a Fractured Reservoir: Field Results From Wairakei, New Zealand, Stanford Geothermal Program, SGP-TR-56 Stanford CA, June 1982.
3. FOSSUM, M. P. and HORNE, R. N., "Interpretation of the Tracer Return Profiles at Wairakei Geothermal Field Using Fracture Analysis," Geothermal Resources Council, Transactions, Vol. 6, October 1982.
4. HORNE R. N. and RODRIGUEZ, F., "Dispersion in Tracer Flow in Fractured Geothermal Systems," Geophysical Research Letters, Vol. 10, No. 4 , 289-292, 1983.
5. GRISAK, G.E. and PICKENS, J.F., "Solute Transport Through Fractured Media , " Water Resources Research, Vol. 16, no. 4, 719-739, 1980.
6. NERETNIEKS, I., "Diffusion in the Rock Matrix: An Important factor in Radionuclide Retardation ?," J. Geophysical Research, Vol. 85, no.B8, 4379,4397, 1980.
7. NERETNIEKS, I., ERIKSEN,J. and TAHTINEN, P., "Tracer Movement in a Single Fissure Granitic Rock: Some Experimental Results and Their Interpretation," Water Resources Research, Vol. 18, No. 4, 849-858, 1982.

8. DEANS, H. A., "A Mathematical Model for Dispersion in the Direction of Flow in Porous Media," *Trans. AIME* Vol.228,49-52, 1963.
9. PERKINS, R. K. and JOHNSTON, O. C., " A Review of Diffusion and Dispersion in Porous Media," *Trans. AIME* Vol.228,70-84, 1963.
10. COATS, K. H. and SMITH, B. D., "Dead End Pore Volume and Dispersion in Porous Media," *SPE of AIME Trans.*, 73-84, March 1964.
11. CARSLAW, H. S., and JAEGER, J. C., "Conduction of Heat in Solids", 2nd Edition, Oxford University Press, 1959.
12. JENSEN, C. L., " Matrix Diffusion and Its Effect On the Modeling of Tracer Returns from the Fractured Geothermal Reservoir at Wairakei, New Zealand," Stanford Geothermal Program, SGP-TR, Stanford CA, December 1983.
13. TAYLOR, G.I., " Dispersion of Soluble Matter in Solvent Flowing Slowly Through a Tube," *Proc. Royal Society London*, Vol. 219,186-203, 1953.
14. GOLUB, G. H. and PEREYA, V., "The Differentiation of Pseudo-Inverses and Non-linear Least squares Problems Whose Variables Separate," *SIAM J. Numerical Analysis*, Vol. 10, No. 2, 413-431, 1973.
15. STEHFEST, H., "Algorithm 368 Numerical Inversion of Laplace Transforms," *Communications of the ACM*, January 1970.
16. VARPRO, Computer Science Department, Stanford CA.

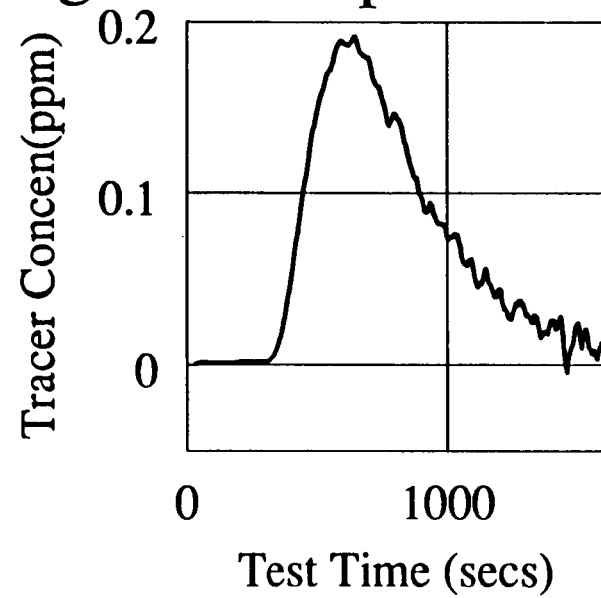
17. GILARDI, J. R., "Experimental Determination of the Effective Dispersivity in a Fracture," Stanford Geothermal Program, SGP-TR-78, Stanford, CA, 1984.
18. BOUETT, L. W., "The Effect of Transverse Mixing on Tracer Dispersion in a Fracture," Stanford Geothermal Program, SGP-TR-103, Stanford, CA, 1986.
19. BIBBY, R., "Mass Transport in Dual Porosity Media," Water Resour. Res. 17, 1075-1081, 1981.
20. GRISAK, G. E. and PICKENS, J. F., "An Analytical Solution for Solute Transport through Fractured Media with Matrix Diffusion," J. Hydrol. 52, 47-57, 1981.
21. SUDICKY, E. A., and FRIND, E. O., "Contaminant Transport in Fractured Porous Media: Analytical Solutions for a System of Parallel Fractures," Water Resour. Res. 18, 1634-1642, 1982.
22. TANG, D. H., et al., "Contaminant Transport in Fractured Porous Media: Analytical Solutions for a Single Fracture," Water Resour. Res. 17, 555-564, 1981.
23. KOCABAS, I., "Analysis of Injection-Backflow Tracer Tests," Stanford Geothermal Program, SGP-TR-96, Stanford, CA, 1986.
24. MCCABE, W. J. et al., "Radioactive Tracers in Geothermal Underground Water Flow Studies," Geothermics, vol. 12, no 2/3, pp. 83-110, 1983.

**APPENDIX A: Reservoir Equivalent Slug Test Plots for Laboratory  
"Step Up" Tracer Tests**

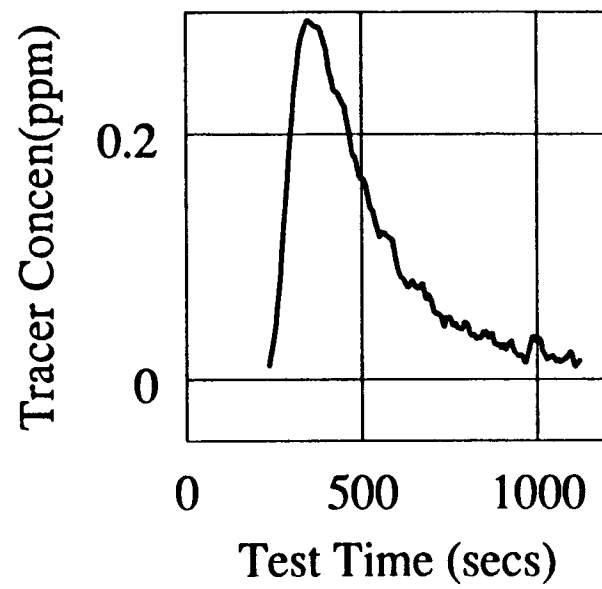
## Slug Test Response 0.7 cc/m



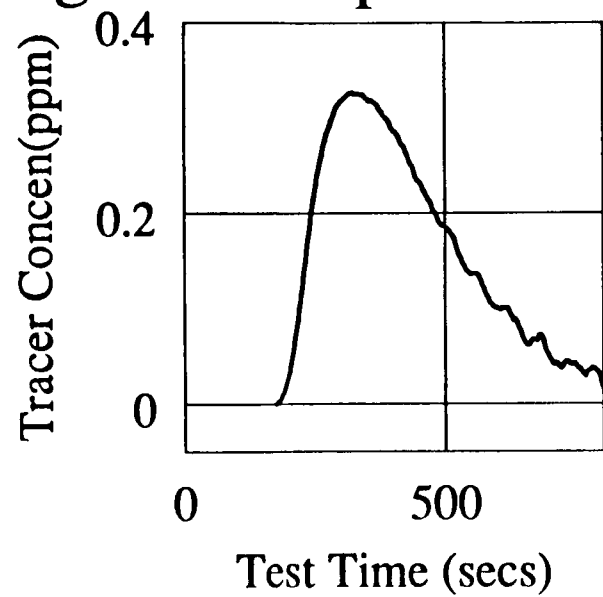
## Slug Test Response 0.75 cc/m



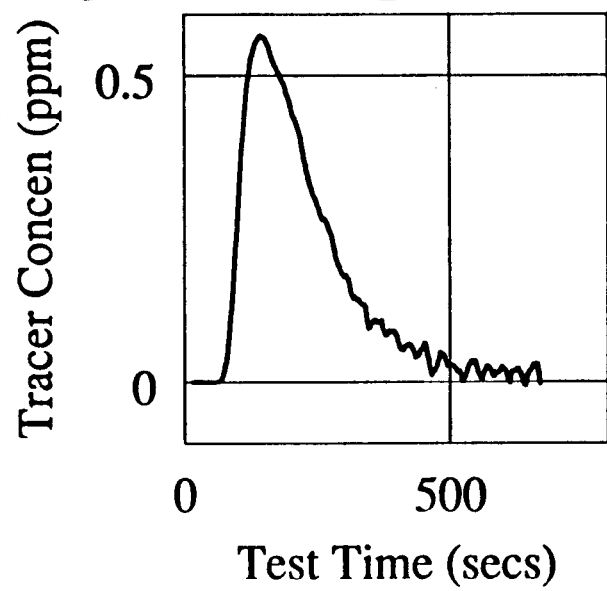
## Slug Test Response 1.4 cc/m



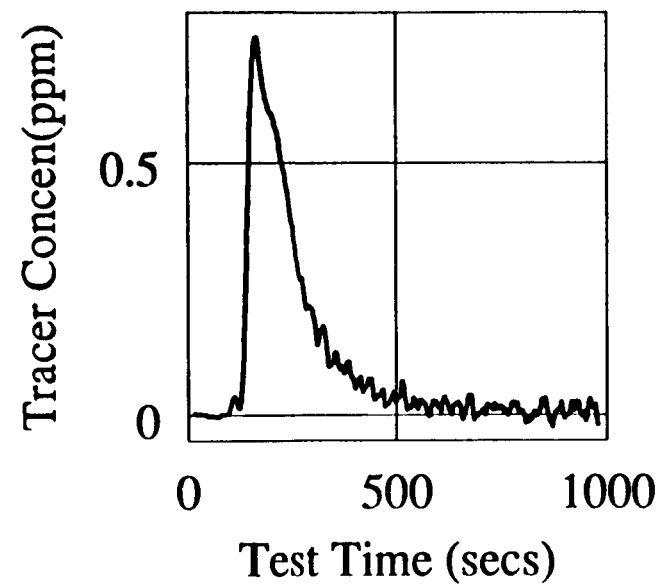
## Slug Test Response 1.75 cc/m



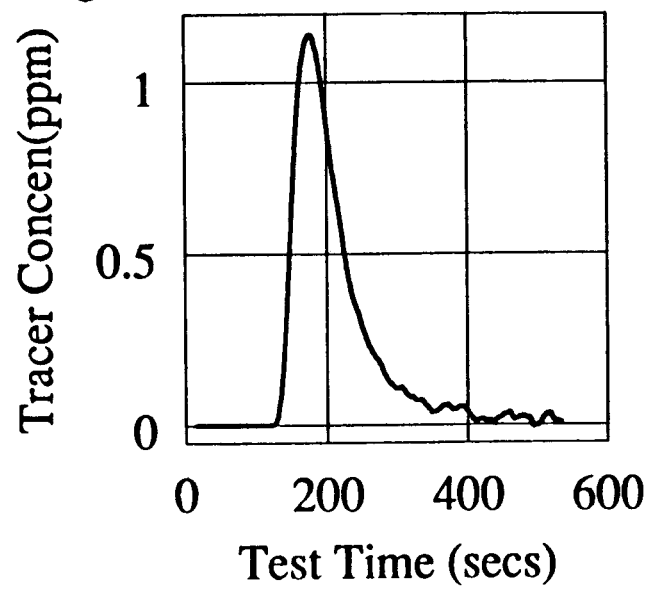
## Slug Test Response 3.7 cc/m



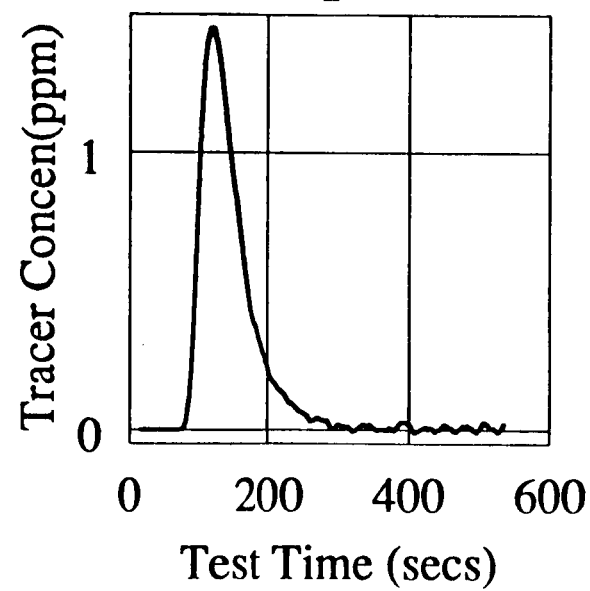
## Slug Test Response 4 cc/m



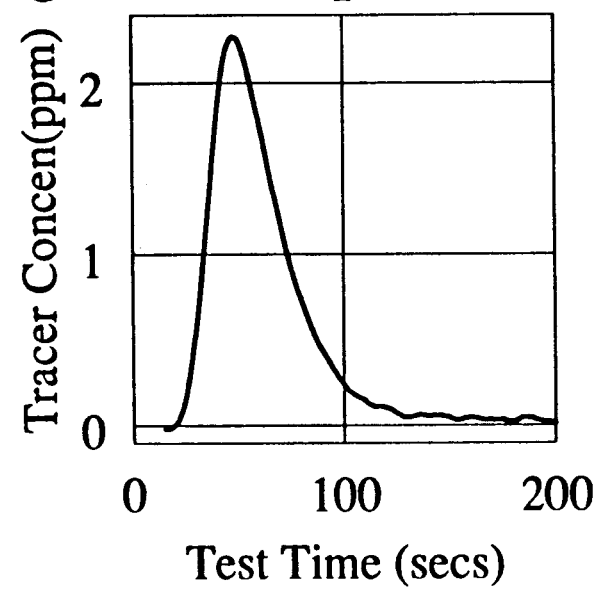
## Slug Test Response 8.7 cc/m



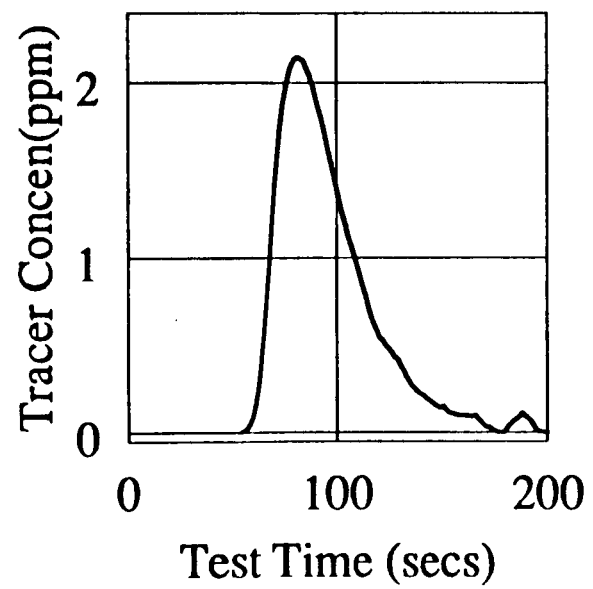
## Slug Test Response 9.7 cc/m



## Slug Test Response 16 cc/m



## Slug Test Response 16.3 cc/m



**APPENDIX B: Derivation of the Matrix Diffusion Model Solution with an  
Error Function Inlet Boundary Condition**

The system of governing differential equations is,

$$\left. \frac{\partial C_f}{\partial t} - \frac{2D_e}{\delta} \frac{\partial C_p}{\partial y} \right]_{y=0} + u \frac{\partial C_f}{\partial x} = 0 \quad (B1)$$

$$D_a \frac{\partial^2 C_p}{\partial y^2} = \frac{\partial C_p}{\partial t} \quad (B2)$$

The boundary and initial conditions are,

$$C_f = C_p = 0 \quad \text{at} \quad t = 0$$

$$\frac{C_f}{C_o} = erfc \left( \frac{100 - u t}{2\sqrt{\eta t}} \right) \quad \text{at } x=0 \text{ for } t>0$$

$$C_p = C_f \quad \text{at} \quad y = 0$$

$$C_p \rightarrow 0 \quad \text{as} \quad y \rightarrow \infty$$

The general solution to this system of partial differential equations is obtained by transforming the problem into Laplace space. The Laplace space solution is,

$$\bar{C}_f = A e^{-\frac{s}{\beta}} e^{-\frac{2\alpha}{\sqrt{\beta}}\sqrt{s}} \quad (B3)$$

To apply the boundary condition the error function inlet boundary condition must first be inverted into Laplace space. The resulting error function inversion is,

$$\frac{\bar{C}_f}{C_o} = e^{-2b \frac{\sqrt{s+a} - \sqrt{a}}{\sqrt{s+a}(\sqrt{s+a} - \sqrt{a})}} \quad (B4)$$

where

$$a = \frac{u^2}{4\eta}$$

$$b = \frac{100}{2\sqrt{\eta}}$$

Finally applying the boundary condition

$$\frac{\bar{C}_f}{C_o} = e^{-2b \frac{\sqrt{s+a} - \sqrt{a}}{\sqrt{s+a}(\sqrt{s+a} - \sqrt{a})}} \quad \text{at } x=0 \quad \text{implies } A = e^{-2b \frac{\sqrt{s+a} - \sqrt{a}}{\sqrt{s+a}(\sqrt{s+a} - \sqrt{a})}}$$

Thus, the solution for continuous injection is

$$\bar{C}_f = e^{-2b \frac{\sqrt{s+a} - \sqrt{a}}{\sqrt{s+a}(\sqrt{s+a} - \sqrt{a})}} e^{-\frac{s}{\beta}} e^{-2\alpha \frac{\sqrt{s}}{\sqrt{\beta}}} \quad (B5)$$

To find the solution for a slug injection, the Laplace solution is simply multiplied by the Laplace parameter  $s$ ,

$$\bar{C}_f = s e^{-2b \frac{\sqrt{s+a} - \sqrt{a}}{\sqrt{s+a}(\sqrt{s+a} - \sqrt{a})}} e^{-\frac{s}{\beta}} e^{-2\alpha \frac{\sqrt{s}}{\sqrt{\beta}}} \quad (B6)$$

Thus, the solution for the concentration within the porous matrix is

$$\bar{C}_f = s e^{-2b \frac{\sqrt{s+a} - \sqrt{a}}{\sqrt{s+a}(\sqrt{s+a} - \sqrt{a})}} e^{-\frac{s}{\beta}} e^{-2\alpha \frac{\sqrt{s}}{\sqrt{\beta}}} e^{-z \sqrt{s} - D_a} \quad (B7)$$

There is no closed form real space inversion to this Laplace space solution, however, the Stehfest Algorithm gave a good approximation of the real space solution. This inversion method was subsequently used in data analysis.

Following the same methodology used above, the Laplace space solution for the Taylor Dispersion model with an error function inlet boundary condition was found to be,

$$\bar{C}_f = s e^{-2b \frac{\sqrt{s+a} - \sqrt{a}}{\sqrt{s+a}(\sqrt{s+a} - \sqrt{a})}} \frac{e^{\frac{r_1 - \sqrt{r_2}}{\sqrt{\alpha \beta}}}}{r_1^2 - r_1 \sqrt{r_2}} \quad (B8)$$

where

$$r_1 = (r_2 + s)^{0.5}$$

$$r_2 = \frac{\beta}{4 \alpha}$$

**APPENDIX C: FORTRAN Optimization Routine for Modified Matrix  
Diffusion Model with Sample Program Input  
and Output**

```

C PROGRAM TO FIT THE LABORATORY DATA TO THE MODIFIED MATRIX
C DIFFUSION MODEL AND ESTIMATE THE OPTIMUM MODEL MATCH PARAMETERS
C 1) FIRST THE DATA IS READ
C 2) NEXT THE INITIAL GUESSES FOR THE NON-LINEAR PARAMETERS
C ARE ENTERED
C 3) THE INLET DISPERSION CONSTANTS ARE READ IN
C 4) THE FITTING ROUTINE VARPRO IS CALLED
C 5) VARPRO CALLS THE SUBROUTINE ADA, WHICH CONTAINS
C THE MATRIX DIFFUSION MODEL AND ESTIMATES DERIVATIVES
C OF THE NON-LINEAR PARAMETERS
C
C
C

```

1002.

```

implicit real*8(a-b,d-h,o-z)
common /INP/ xip,uip,disip
common /V/ v(50),g(50),h(25)
dimension y(400),t(400),alf(14),beta(7),w(400),a(400,13),
*inc(14,8),c(400,8),ctitle(20),ct(400),cy(400),dim(7),out(7)
*,out1(7),t1(400)
double precision alf,xip,uip,disip
external ada
nmax=400
iprint=1
read (5,70) ctitle
70 format (20a4)
write(6,71) ctitle
71 format (1h0,10x,20a4)
read(5,*) nl
write (6,12) nl
12 format(1h0,10x,'number of nonlinear parameters'//(i3))
l=nl/3
read (5,*) (dim(i),out(i),out1(i),i=1,1)
do 80 i=1,1
ii=2*i-1
alf(ii+2)=1./out1(i)
alf(ii)=dim(i)
80 alf(ii+1)=1./out(i)
write(6,21) (alf(i),i=1,nl)
21 format(1h0,10x,'initial est. of nonlin. parameters'//(f7.3))
write(6,20) (dim(i),out(i),out1(i),i=1,1)
20 format(//,'0 dimensionless number tracer arrival time inletA',//,
*(5x,f9.5,22x,f7.3,x,f7.3))
lp=lp+1
lpp2=lp+nl+2
read(5,*) n
write(6,35) n
read(5,*) xip
read(5,*) uip
read(5,*) dissip
35 format(/1h0,10x,'number of observations'//(i4))
iv=1
read(5,*) (t(i),y(i),i=1,n)
do 695 i=1,n
t(i)=t(i)
695 y(i)=y(i)**-1000.0
write(6,60) (t(i),y(i),i=1,n)
60 format(1h0,'independent variables'//,(5x,f8.3,21x,f9.3))
wt=0.
do 1 i=1,n
1 w(i)=1.
jj=12
nn=10
call vector(jj,nn)
call varpro(l, nl, n, nmax, lpp2, iv, t, y, w, ada, a
*, iprint, alf, beta, ierr)

```

```

write(6,13)
lpl=l+1
call ada (lpl,nl,n,nmax,lpp2,iv,a,inc,t,alf,2)
do 8 i=1,n
t1(i)=t(i)-1./alf(3)
c(i,lpl)=0.
do 9 j=1,1
c(i,j)=beta(j)*a(i,j)
9 c(i,lpl)=c(i,lpl)+c(i,j)
write(6,14) t1(i),y(i),c(i,lpl),(c(i,j),j=1,1)
cy(i)=y(i)
ct(i)=t(i)
8 continue
do 888 i=1,n
c(i,lpl)=0.
do 999 j=1,1
c(i,j)=beta(j)*a(i,j)
999 c(i,lpl)=c(i,lpl)+c(i,j)
write(6,14) t1(i),y(i)
cy(i)=y(i)
ct(i)=t(i)
888 continue
do 887 i=1,n
c(i,lpl)=0.
do 998 j=1,1
c(i,j)=beta(j)*a(i,j)
998 c(i,lpl)=c(i,lpl)+c(i,j)
write(6,14) t1(i),c(i,lpl),(c(i,j),j=1,1)
cy(i)=y(i)
ct(i)=t(i)
887 continue
13 format(1h0,' time actual calc comp#1 comp#2',//)
14 format(1x,8f10.4)
do 22 i=1,1
ii=2*i-1
out1(i)=1./alf(ii+2)
dim(i)=alf(ii)
22 out(i)=1./alf(ii+1)
sum=0.
do 25 j=1,1
25 sum=sum+beta(j)
do 93 i=1,1
93 beta(i)=beta(i)/sum
write(6,38) (beta(i),dim(i),out(i),out1(i),i=1,1)
919 format(e12.5)
38 format(,'0 fraction dimensionless number arrival time
* inlet A fit ',/(5x,f7.3,5x,f7.3,22x,f7.3,10x,f7.4))
stop
end
subroutine ada(lp,nl,n,nmax,lpp2,iv,a,inc,t,alf,isel)
implicit real*8(a-h,o-z)
dimension alf(nl),a(nmax,lpp2),t(nmax),inc(14,8),d(400,7)
double precision alf,pwd,pwd1,pwd2,pwd3,dalf,old
l=lp-1
if(isel.eq.2) go to 90
if(isel.eq.3) go to 165
inc(1,1)=1.0
inc(2,1)=1.0
inc(3,1)=1.0
90 do 81 i=1,n
do 81 j=1,1
k1=2*j-1
k2=2*j
if(alf(2)*t(i)*alf(3)/(alf(3)+alf(2)).gt.1.0) go to 82
a(i,j)=0.0
d(i,j)=0.

```

```

      go to 81
82  nn1=12
     mm1=10
     a(i,j)=PWD(T(i),NN1,MM1,ALF,n1,nmax)
     d(i,j)=a(i,j)
81  continue
     if(isel.eq.2) go to 200
165  do 170 i=1,n
     do 170 j=1,n1
     k1=(j+1)/2
     k2=2*k1
     k3=k2-1
     jj=1+j+1
     if(alf(2)*t(i)*alf(3)/(alf(2)+alf(3)).gt.1.0) go to 171
     a(i,jj)=0.
     go to 170
171  if(j.eq.2) go to 300
     if(J.eq.3) go to 310
     nn1=12
     mm1=10
     a(i,jj)=PWD1(T(i),Nn1,Mm1,ALF,n1,nmax)
     go to 170
300  nn1=12
     mm1=10
     a(i,jj)=PWD2(T(i),Nn1,Mm1,ALF,n1,nmax)
     go to 170
310  nn1=12
     mm1=10
     a(i,jj)=PWD3(T(i),Nn1,Mm1,ALF,n1,nmax)
     go to 170
170  continue
     write(6,111) a(50,3),a(50,4),a(50,5),a(50,6),a(50,7)
111  format(e12.5,3x,e12.5,3x,e12.5,3x,e12.5)
200  continue
     return
     END
     function vector(n,m)
     IMPLICIT REAL*8 (A-H,O-Z)
     common /V/ v(50),g(50),h(25)
     M=N
     DLOGTW=0.6931471805599
     NH=N/2
C
C      THE FACTORIALS OF 1 TO N ARE CALCULATED INTO ARRAY G.
C
     G(1)=1
     DO 1 I=2,N
       G(I)=G(I-1)*I
1    CONTINUE
C
C      TERMS WITH K ONLY ARE CALCULATED INTO ARRAY H.
C
     H(1)=2./G(NH-1)
     DO 6 I=2,NH
       FI=I
       IF(I-NH) 4,5,6
4      H(I)=FI**NH*G(2*I)/(G(NH-I)*G(I)*G(I-1))
       GO TO 6
5      H(I)=FI**NH*G(2*I)/(G(I)*G(I-1))
6    CONTINUE
C
C      THE TERMS (-1)**NH+1 ARE CALCULATED.
C      FIRST THE TERM FOR I=1
     SN=2*(NH-NH/2*2)-1
C
C      THE REST OF THE SN'S ARECALCULATED IN THE MAIN RUTINE.
C
C

```

```

C      THE ARRAY V(I) IS CALCULATED.
C      DO 7 I=1,N
C
C      FIRST SET V(I)=0
C      V(I)=0.
C
C      THE LIMITS FOR K ARE ESTABLISHED.
C      THE LOWER LIMIT IS K1=INTEG((I+1/2))
C      K1=(I+1)/2
C
C      THE UPPER LIMIT IS K2=MIN(I,N/2)
C      K2=I
C      IF (K2-NH) 8,8,9
C      K2=NH
C
C      THE SUMMATION TERM IN V(I) IS CALCULATED.
C      DO 10 K=K1,K2
C          IF (2*K-I) 12,13,12
C          IF (I-K) 11,14,11
C          V(I)=V(I)+H(K)/(G(I-K)*G(2*K-I))
C          GO TO 10
C          V(I)=V(I)+H(K)/G(I-K)
C          GO TO 10
C          V(I)=V(I)+H(K)/G(2*K-I)
C      CONTINUE
C
C      THE V(I) ARRAY IS FINALLY CALCULATED BY WEIGHTING
C      ACCORDING TO SN.
C      V(I)=SN*V(I)
C
C      THE TERM SN CHANGES ITS SIGN EACH ITERATION.
C      SN--SN
C      CONTINUE
C      Return
C      end
C      THE STEHFEST ALGORITHM
C      ****
C
C      FUNCTION PWD(TD,N,M,ALF,nl,nmax)
C          THIS FUNTION COMPUTES NUMERICALLY THE LAPLACE TRNSFORM
C          INVERSE OF F(S).
C          IMPLICIT REAL*8 (A-H,O-Z)
C          common /V/ v(50),g(50),h(25)
C          DIMENSION ALF(nl)
C          double precision alf,arg,pwd1,pwd
C
C          NOW IF THE ARRAY V(I) WAS COMPUTED BEFORE THE PROGRAM
C          GOES DIRECTLY TO THE END OF THE SUBROUTINE TO CALCULATE
C          F(S).
C          DLOGTW=0.6931471805599
C
C
C      THE NUMERICAL APPROXIMATION IS CALCULATED.
C      A=DLOGTW/TD
C      PWD=0
C      DO 15 I=1,N
C          ARG=A*I
C          PWD=PWD+V(I)*PWD1(ARG,ALF,NL,NMAX,kk1,kk2)
C      CONTINUE
C      PWD=PWD*A
C      RETURN
C      END
C
C      FUNCTION PWD1(ARG,ALF,NL,NMAX)

```

```

common /INP/ xip,uip,disip
DIMENSION ALF(nl)
double precision alf,arg,pwdl,u,x,ds,b,a,rts,xip,uip,disip
u=uip/(60.*0.0325)
x=xip
ds=disip
b=x/(2.*(ds**0.5))
a=u/(2.*(ds**0.5))
rts=(arg+a**2.)**0.5
bc1=(arg*dexp(-2.*b*(rts-a)))/(rts*(rts-a))
bc=bc1
PWDL=dexp(-arg/alf(2))*dexp(-2.*alf(1)*((arg/alf(2))**0.5))*  

*dexp(-arg/alf(3))*bc
return
end

c
c
c          THE STEHFEST ALGORITHM
c ****
c
c
FUNCTION PWD1(TD,N,M,ALF, nl, nmax)
C      THIS FUNTION COMPUTES NUMERICALLY THE LAPLACE TRNSFORM
C      INVERSE OF F(S).
IMPLICIT REAL*8 (A-H,O-Z)
common /V/ v(50),g(50),h(25)
DIMENSION ALF(nl)
double precision alf,arg,pwdl1,pwdl
C
C      NOW IF THE ARRAY V(I) WAS COMPUTED BEFORE THE PROGRAM
C      GOES DIRECTLY TO THE END OF THE SUBRUTINE TO CALCULATE
C      F(S).
DLOGTW=0.6931471805599
C
C      THE NUMERICAL APPROXIMATION IS CALCULATED.
A=DLOGTW/TD
PWD1=0
DO 15 I=1,N
    ARG=A*I
    PWD1=PWD1+V(I)*PWDL1(ARG,ALF,NL,NMAX)
15 CONTINUE
PWD1=PWD1*A
RETURN
END

c
c
FUNCTION PWDL1(ARG,ALF,NL,NMAX)
common /INP/ xip,uip,disip
DIMENSION ALF(nl)
double precision alf,arg,pwdl1,u,x,ds,b,a,rts,xip,uip,disip
u=uip/(60.*0.0325)
x=xip
ds=disip
b=x/(2.*(ds**0.5))
a=u/(2.*(ds**0.5))
rts=(arg+a**2.)**0.5
bc1=(arg*dexp(-2.*b*(rts-a)))/(rts*(rts-a))
bc=bc1
PWDL1=(-2.*((arg/alf(2))**0.5))*dexp(-arg/alf(3))*  

*dexp(-arg/alf(2))*dexp(-2.*alf(1)*((arg/alf(2))**0.5))*  

*bc
return
end

c
c
c          THE STEHFEST ALGORITHM

```

```

C ****
C
C FUNCTION PWD2(TD,N,M,ALF,n1,nmax)
C   THIS FUNTION COMPUTES NUMERICALLY THE LAPLACE TRNSFORM
C   INVERSE OF F(S).
C IMPLICIT REAL*8 (A-H,O-Z)
C common /V/ v(50),g(50),h(25)
C DIMENSION ALF(n1)
C double precision alf,arg,pwd12,pwd2
C
C   NOW IF THE ARRAY V(I) WAS COMPUTED BEFORE THE PROGRAM
C   GOES DIRECTLY TO THE END OF THE SUBRUTINE TO CALCULATE
C   F(S).
C DLOGTW=0.6931471805599
C
C   THE NUMERICAL APPROXIMATION IS CALCULATED.
C A=DLOGTW/TD
C PWD2=0
C DO 15 I=1,N
C   ARG=A*I
C   PWD2=PWD2+V(I)*PWDL2(ARG,ALF,NL,NMAX)
15  CONTINUE
C PWD2=PWD2*A
18  RETURN
C END
C
C
C FUNCTION PWDL2(ARG,ALF,NL,NMAX)
C common /INP/ xip,uip,disip
C DIMENSION ALF(n1)
C double precision alf,arg,pwd12,u,x,ds,b,a,rts,xip,uip,disip
C u=uip/(60.*0.0325)
C x=xip
C ds=disip
C b=x/(2.* (ds**0.5))
C a=u/(2.* (ds**0.5))
C rts=(arg+a**2.)**0.5
C bcl=(arg*dexp(-2.*b*(rts-a)))/(rts*(rts-a))
C bc=bc1
C PWDL2=((arg/(alf(2)**2.))+(alf(1)*(arg**0.5))/(alf(2)**1.5))*  

* dexp(-arg/alf(3))*bc*  

* dexp(-arg/alf(2))*dexp(-2.*alf(1)*((arg/alf(2))**0.5))
C return
C end
C
C   THE STEHFEST ALGORITHM
C ****
C
C FUNCTION PWD3(TD,N,M,ALF,n1,nmax)
C   THIS FUNTION COMPUTES NUMERICALLY THE LAPLACE TRNSFORM
C   INVERSE OF F(S).
C IMPLICIT REAL*8 (A-H,O-Z)
C common /V/ v(50),g(50),h(25)
C DIMENSION ALF(n1)
C double precision alf,arg,pwd13,pwd3
C
C   NOW IF THE ARRAY V(I) WAS COMPUTED BEFORE THE PROGRAM
C   GOES DIRECTLY TO THE END OF THE SUBRUTINE TO CALCULATE
C   F(S).
C DLOGTW=0.6931471805599
C
C   THE NUMERICAL APPROXIMATION IS CALCULATED.
C A=DLOGTW/TD
C PWD3=0
C DO 15 I=1,N
C   ARG=A*I

```

```

      PWD3=PWD3+V(I)*PWDL3(ARG,ALF,NL,NMAX)
15    CONTINUE
      PWD3=PWD3*A
18    RETURN
      END
C
C
      FUNCTION PWDL3(ARG,ALF,NL,NMAX)
      common /INP/ xip,uip,disip
      DIMENSION ALF(nl)
      double precision alf,arg,pwdl3,u,x,ds,b,a,rts,xip,uip,disip
      u=uip/(60.*0.0325)
      x=xip
      ds=disip
      b=x/(2.*ds**0.5)
      a=u/(2.*ds**0.5)
      rts=(arg+a**2.)**0.5
      bc1=(arg*dexp(-2.*b*(rts-a)))/(rts*(rts-a))
      bc=bc1
      pwdl3=dexp(-arg/alf(3))*(arg/(alf(3)**2.))*bc*
      *dexp(-arg/alf(2))*dexp(-2.*alf(1)*((arg/alf(2))**0.5))
      return
      end
C
      SUBROUTINE VARPRO (L, NL, N, NMAX, LPP2, IV, T, Y, W, ADA, A,
X IPRINT, ALF, BETA, IERR)
C
C
      GIVEN A SET OF N OBSERVATIONS, CONSISTING OF VALUES Y(1),
C      Y(2), ..., Y(N) OF A DEPENDENT VARIABLE Y, WHERE Y(I)
C      CORRESPONDS TO THE IV INDEPENDENT VARIABLE(S) T(I,1), T(I,2),
C      ..., T(I,IV), VARPRO ATTEMPTS TO COMPUTE A WEIGHTED LEAST
C      SQUARES FIT TO A FUNCTION ETA (THE 'MODEL') WHICH IS A LINEAR
C      COMBINATION
C
C
      L
      ETA(ALF, BETA; T) = SUM BETA * PHI (ALF; T) + PHI (ALF; T)
      J=1      J      J           L+1
C
C
      OF NONLINEAR FUNCTIONS PHI(J) (E.G., A SUM OF EXPONENTIALS AND/
C      OR GAUSSIANS). THAT IS, DETERMINE THE LINEAR PARAMETERS
C      BETA(J) AND THE VECTOR OF NONLINEAR PARAMETERS ALF BY MINIMIZ-
C      ING
C
C
      2      N
      NORM(RESIDUAL) = SUM W * (Y - ETA(ALF, BETA; T )) .
      I=1      I      I           I
C
C
      THE (L+1)-ST TERM IS OPTIONAL, AND IS USED WHEN IT IS DESIRED
      TO FIX ONE OR MORE OF THE BETA'S (RATHER THAN LET THEM BE
      DETERMINED). VARPRO REQUIRES FIRST DERIVATIVES OF THE PHI'S.
C
C
      NOTES:
C
C
      A) THE ABOVE PROBLEM IS ALSO REFERRED TO AS 'MULTIPLE
      NONLINEAR REGRESSION'. FOR USE IN STATISTICAL ESTIMATION,
      VARPRO RETURNS THE RESIDUALS, THE COVARIANCE MATRIX OF THE
      LINEAR AND NONLINEAR PARAMETERS, AND THE ESTIMATED VARIANCE OF
      THE OBSERVATIONS.
C
C
      B) AN ETA OF THE ABOVE FORM IS CALLED 'SEPARABLE'. THE
      CASE OF A NONSEPARABLE ETA CAN BE HANDLED BY SETTING L = 0
      AND USING PHI(L+1).
C
C
      C) VARPRO MAY ALSO BE USED TO SOLVE LINEAR LEAST SQUARES
      PROBLEMS (IN THAT CASE NO ITERATIONS ARE PERFORMED). SET
      NL = 0.
C

```

D) THE MAIN ADVANTAGE OF VARPRO OVER OTHER LEAST SQUARES  
 PROGRAMS IS THAT NO INITIAL GUESSES ARE NEEDED FOR THE LINEAR  
 PARAMETERS. NOT ONLY DOES THIS MAKE IT EASIER TO USE, BUT IT  
 OFTEN LEADS TO FASTER CONVERGENCE.

DESCRIPTION OF PARAMETERS

L	NUMBER OF LINEAR PARAMETERS BETA (MUST BE .GE. 0).	51.
NL	NUMBER OF NONLINEAR PARAMETERS ALF (MUST BE .GE. 0).	52.
N	NUMBER OF OBSERVATIONS. N MUST BE GREATER THAN L + NL <i>(I.E., THE NUMBER OF OBSERVATIONS MUST EXCEED THE    NUMBER OF PARAMETERS).</i>	53.
IV	NUMBER OF INDEPENDENT VARIABLES T.	54.
T	REAL N BY IV MATRIX OF INDEPENDENT VARIABLES. T(I, J) <i>CONTAINS THE VALUE OF THE I-TH OBSERVATION OF THE J-TH    INDEPENDENT VARIABLE.</i>	55.
Y	N-VECTOR OF OBSERVATIONS, ONE FOR EACH ROW OF T.	56.
W	N-VECTOR OF NONNEGATIVE WEIGHTS. SHOULD BE SET TO 1'S <i>IF WEIGHTS ARE NOT DESIRED. IF VARIANCES OF THE    INDIVIDUAL OBSERVATIONS ARE KNOWN, W(I) SHOULD BE SET    TO 1./VARIANCE(I).</i>	57.
INC	NL X (L+1) INTEGER INCIDENCE MATRIX. INC(K, J) = 1 IF <i>NON-LINEAR PARAMETER ALF(K) APPEARS IN THE J-TH    FUNCTION PHI(J). (THE PROGRAM SETS ALL OTHER INC(K, J)    TO ZERO.) IF PHI(L+1) IS INCLUDED IN THE MODEL,    THE APPROPRIATE ELEMENTS OF THE (L+1)-ST COLUMN SHOULD    BE SET TO 1'S. INC IS NOT NEEDED WHEN L = 0 OR NL = 0.</i> <i>CAUTION: THE DECLARED ROW DIMENSION OF INC (IN ADA)    MUST CURRENTLY BE SET TO 12. SEE 'RESTRICTIONS' BELOW.</i>	58.
NMAX	THE DECLARED ROW DIMENSION OF THE MATRICES A AND T.	59.
LPP2	IT MUST BE AT LEAST MAX(N, 2*NL+3). <i>L+P+2, WHERE P IS THE NUMBER OF ONES IN THE MATRIX INC.    THE DECLARED COLUMN DIMENSION OF A MUST BE AT LEAST    LPP2. (IF L = 0, SET LPP2 = NL+2. IF NL = 0, SET LPP2    L+2.)</i>	60.
A	REAL MATRIX OF SIZE MAX(N, 2*NL+3) BY L+P+2. ON INPUT <i>IT CONTAINS THE PHI(J)'S AND THEIR DERIVATIVES (SEE    BELOW). ON OUTPUT, THE FIRST L+NL ROWS AND COLUMNS OF    A WILL CONTAIN AN APPROXIMATION TO THE (WEIGHTED)    COVARIANCE MATRIX AT THE SOLUTION (THE FIRST L ROWS    CORRESPOND TO THE LINEAR PARAMETERS, THE LAST NL TO THE    NONLINEAR ONES), COLUMN L+NL+1 WILL CONTAIN THE    WEIGHTED RESIDUALS (Y - ETA), A(1, L+NL+2) WILL CONTAIN    THE (EUCLIDEAN) NORM OF THE WEIGHTED RESIDUAL, AND    A(2, L+NL+2) WILL CONTAIN AN ESTIMATE OF THE (WEIGHTED)    VARIANCE OF THE OBSERVATIONS, NORM(RESIDUAL)**2/    (N - L - NL).</i>	61.
IPRINT	INPUT INTEGER CONTROLLING PRINTED OUTPUT. IF IPRINT IS <i>POSITIVE, THE NONLINEAR PARAMETERS, THE NORM OF THE    RESIDUAL, AND THE MARQUARDT PARAMETER WILL BE OUTPUT    EVERY IPRINT-TH ITERATION (AND INITIALLY, AND AT THE    FINAL ITERATION). THE LINEAR PARAMETERS WILL BE    PRINTED AT THE FINAL ITERATION. ANY ERROR MESSAGES    WILL ALSO BE PRINTED. (IPRINT = 1 IS RECOMMENDED AT    FIRST.) IF IPRINT = 0, ONLY THE FINAL QUANTITIES WILL    BE PRINTED, AS WELL AS ANY ERROR MESSAGES. IF IPRINT =    -1, NO PRINTING WILL BE DONE. THE USER IS THEN    RESPONSIBLE FOR CHECKING THE PARAMETER IERR FOR ERRORS.</i>	62.
ALF	NL-VECTOR OF ESTIMATES OF NONLINEAR PARAMETERS <i>(INPUT). ON OUTPUT IT WILL CONTAIN OPTIMAL VALUES OF    THE NONLINEAR PARAMETERS.</i>	63.
BETA	L-VECTOR OF LINEAR PARAMETERS (OUTPUT ONLY).	64.
IERR	INTEGER ERROR FLAG (OUTPUT): <i>.GT. 0 - SUCCESSFUL CONVERGENCE, IERR IS THE NUMBER OF    ITERATIONS TAKEN.</i>	65.

C -1 TERMINATED FOR TOO MANY ITERATIONS. 109.  
 C -2 TERMINATED FOR ILL-CONDITIONING (MARQUARDT 110.  
 C PARAMETER TOO LARGE.) ALSO SEE IERR = -8 BELOW. 111.  
 C -4 INPUT ERROR IN PARAMETER N, L, NL, LPP2, OR NMAX. 112.  
 C -5 INC MATRIX IMPROPERLY SPECIFIED, OR P DISAGREES 113.  
 C WITH LPP2. 114.  
 C -6 A WEIGHT WAS NEGATIVE. 115.  
 C -7 'CONSTANT' COLUMN WAS COMPUTED MORE THAN ONCE. 116.  
 C -8 CATASTROPHIC FAILURE - A COLUMN OF THE A MATRIX HAS 117.  
 C BECOME ZERO. SEE 'CONVERGENCE FAILURES' BELOW. 118.  
 C 119.  
 C (IF IERR .LE. -4, THE LINEAR PARAMETERS, COVARIANCE 120.  
 C MATRIX, ETC. ARE NOT RETURNED.) 121.  
 C 122.  
 C SUBROUTINES REQUIRED 123.  
 C 124.  
 C NINE SUBROUTINES, DPA, ORFAC1, ORFAC2, BACSUB, POSTPR, COV, 125.  
 C XNORM, INIT, AND VARERR ARE PROVIDED. IN ADDITION, THE USER 126.  
 C MUST PROVIDE A SUBROUTINE (CORRESPONDING TO THE ARGUMENT ADA) 127.  
 C WHICH, GIVEN ALF, WILL EVALUATE THE FUNCTIONS PHI(J) AND THEIR 128.  
 C PARTIAL DERIVATIVES D PHI(J)/D ALF(K), AT THE SAMPLE POINTS 129.  
 C T(I). THIS ROUTINE MUST BE DECLARED 'EXTERNAL' IN THE CALLING 130.  
 C PROGRAM. ITS CALLING SEQUENCE IS 131.  
 C 132.  
 C SUBROUTINE ADA (L+1, NL, N, NMAX, LPP2, IV, A, INC, T, ALF, 133.  
 C ISEL) 134.  
 C 135.  
 C THE USER SHOULD MODIFY THE EXAMPLE SUBROUTINE 'ADA' (GIVEN 136.  
 C ELSEWHERE) FOR HIS OWN FUNCTIONS. 137.  
 C 138.  
 C THE VECTOR SAMPLED FUNCTIONS PHI(J) SHOULD BE STORED IN THE 139.  
 C FIRST N ROWS AND FIRST L+1 COLUMNS OF THE MATRIX A, I.E., 140.  
 C A(I, J) SHOULD CONTAIN PHI(J, ALF; T(I,1), T(I,2), ..., 141.  
 C T(I,IV)), I = 1, ..., N; J = 1, ..., L (OR L+1). THE (L+1)-ST 142.  
 C COLUMN OF A CONTAINS PHI(L+1) IF PHI(L+1) IS IN THE MODEL, 143.  
 C OTHERWISE IT IS RESERVED FOR WORKSPACE. THE 'CONSTANT' FUNC- 144.  
 C TIONS (THESE ARE FUNCTIONS PHI(J) WHICH DO NOT DEPEND UPON ANY 145.  
 C NONLINEAR PARAMETERS ALF, E.G., T(I)\*\*J) (IF ANY) MUST APPEAR 146.  
 C FIRST, STARTING IN COLUMN 1. THE COLUMN N-VECTORS OF NONZERO 147.  
 C PARTIAL DERIVATIVES D PHI(J) / D ALF(K) SHOULD BE STORED 148.  
 C SEQUENTIALLY IN THE MATRIX A IN COLUMNS L+2 THROUGH L+P+1. 149.  
 C THE ORDER IS 150.  
 C 151.  
 C D PHI(1) D PHI(2) D PHI(L) D PHI(L+1) D PHI(1) 152.  
 C -----, -----, ..., -----, -----, -----, -----, 153.  
 C D ALF(1) D ALF(1) D ALF(1) D ALF(1) D ALF(2) 154.  
 C 155.  
 C D PHI(2) D PHI(L+1) D PHI(1) D PHI(L+1) 156.  
 C -----, ..., -----, ..., -----, ..., -----, 157.  
 C D ALF(2) D ALF(2) D ALF(NL) D ALF(NL) 158.  
 C 159.  
 C OMITTING COLUMNS OF DERIVATIVES WHICH ARE ZERO, AND OMITTING 160.  
 C PHI(L+1) COLUMNS IF PHI(L+1) IS NOT IN THE MODEL. NOTE THAT 161.  
 C THE LINEAR PARAMETERS BETA ARE NOT USED IN THE MATRIX A. 162.  
 C COLUMN L+P+2 IS RESERVED FOR WORKSPACE. 163.  
 C 164.  
 C THE CODING OF ADA SHOULD BE ARRANGED SO THAT: 165.  
 C 166.  
 C ISEL = 1 (WHICH OCCURS THE FIRST TIME ADA IS CALLED) MEANS: 167.  
 C A. FILL IN THE INCIDENCE MATRIX INC 168.  
 C B. STORE ANY CONSTANT PHI'S IN A. 169.  
 C C. COMPUTE NONCONSTANT PHI'S AND PARTIAL DERIVA- 170.  
 C TIVES. 171.  
 C - 2 MEANS COMPUTE ONLY THE NONCONSTANT FUNCTIONS PHI 172.  
 C - 3 MEANS COMPUTE ONLY THE DERIVATIVES 173.  
 C 174.

C (WHEN THE PROBLEM IS LINEAR (NL = 0) ONLY ISEL = 1 IS USED, AND 175.  
 C DERIVATIVES ARE NOT NEEDED.) 176.  
 C 177.  
 C 178.  
 C 179.  
 C RESTRICTIONS 180.  
 C 181.  
 C 182.  
 C 183.  
 C 184.  
 C 185.  
 C 186.  
 C 187.  
 C 188.  
 C 189.  
 C 190.  
 C 191.  
 C 192.  
 C 193.  
 C 194.  
 C 195.  
 C 196.  
 C 197.  
 C 198.  
 C 199.  
 C 200.  
 C 201.  
 C 202.  
 C 203.  
 C 204.  
 C 205.  
 C 206.  
 C 207.  
 C 208.  
 C 209.  
 C 210.  
 C 211.  
 C 212.  
 C 213.  
 C 214.  
 C 215.  
 C 216.  
 C 217.  
 C 218.  
 C 219.  
 C 220.  
 C 221.  
 C 222.  
 C 223.  
 C 224.  
 C 225.  
 C 226.  
 C 227.  
 C 228.  
 C 229.  
 C 230.  
 C 231.  
 C 232.  
 C 233.  
 C 234.  
 C 235.  
 C 236.  
 C 237.  
 C 238.  
 C 239.  
 C 240.

THE SUBROUTINES DPA, INIT (AND ADA) CONTAIN THE LOCALLY  
 DIMENSIONED MATRIX INC, WHOSE DIMENSIONS ARE CURRENTLY SET FOR  
 MAXIMA OF L+1 = 8, NL = 12. THEY MUST BE CHANGED FOR LARGER  
 PROBLEMS. DATA PLACED IN ARRAY A IS OVERWRITTEN ('DESTROYED').  
 DATA PLACED IN ARRAYS T, Y AND INC IS LEFT INTACT. THE PROGRAM  
 RUNS IN WATFIV, EXCEPT WHEN L = 0 OR NL = 0.

IT IS ASSUMED THAT THE MATRIX PHI(J, ALF; T(I)) HAS FULL  
 COLUMN RANK. THIS MEANS THAT THE FIRST L COLUMNS OF THE MATRIX  
 A MUST BE LINEARLY INDEPENDENT.

OPTIONAL NOTE: AS WILL BE NOTED FROM THE SAMPLE SUBPROGRAM  
 ADA, THE DERIVATIVES D PHI(J)/D ALF(K) (ISEL = 3) MUST BE  
 COMPUTED INDEPENDENTLY OF THE FUNCTIONS PHI(J) (ISEL = 2),  
 SINCE THE FUNCTION VALUES ARE OVERWRITTEN AFTER ADA IS CALLED  
 WITH ISEL = 2. THIS IS DONE TO MINIMIZE STORAGE, AT THE POS-  
 SIBLE EXPENSE OF SOME RECOMPUTATION (SINCE THE FUNCTIONS AND  
 DERIVATIVES FREQUENTLY HAVE SOME COMMON SUBEXPRESSIONS). TO  
 REDUCE THE AMOUNT OF COMPUTATION AT THE EXPENSE OF SOME  
 STORAGE, CREATE A MATRIX B OF DIMENSION NMAX BY L+1 IN ADA, AND  
 AFTER THE COMPUTATION OF THE PHI'S (ISEL = 2), COPY THE VALUES  
 INTO B. THESE VALUES CAN THEN BE USED TO CALCULATE THE DERIV-  
 ATIVES (ISEL = 3). (THIS MAKES USE OF THE FACT THAT WHEN A  
 CALL TO ADA WITH ISEL = 3 FOLLOWS A CALL WITH ISEL = 2, THE  
 ALFS ARE THE SAME.)

TO CONVERT TO OTHER MACHINES, CHANGE THE OUTPUT UNIT IN THE  
 DATA STATEMENTS IN VARPRO, DPA, POSTPR, AND VARERR. THE  
 PROGRAM HAS BEEN CHECKED FOR PORTABILITY BY THE BELL LABS PPORT  
 VERIFIER. FOR MACHINES WITHOUT DOUBLE PRECISION HARDWARE, IT  
 MAY BE DESIRABLE TO CONVERT TO SINGLE PRECISION. THIS CAN BE  
 DONE BY CHANGING (A) THE DECLARATIONS 'DOUBLE PRECISION' TO  
 'REAL', (B) THE PATTERN '.D' TO '.E' IN THE 'DATA' STATEMENT IN  
 VARPRO, (C) DSIGN, DSQRT AND DABS TO SIGN, SQRT AND ABS,  
 RESPECTIVELY, AND (D) DEXP TO EXP IN THE SAMPLE PROGRAMS ONLY.

NOTE ON INTERPRETATION OF COVARIANCE MATRIX

FOR USE IN STATISTICAL ESTIMATION (MULTIPLE NONLINEAR  
 REGRESSION) VARPRO RETURNS THE COVARIANCE MATRIX OF THE LINEAR  
 AND NONLINEAR PARAMETERS. THIS MATRIX WILL BE USEFUL ONLY IF  
 THE USUAL STATISTICAL ASSUMPTIONS HOLD: AFTER WEIGHTING, THE  
 ERRORS IN THE OBSERVATIONS ARE INDEPENDENT AND NORMALLY DISTRI-  
 BUTED, WITH MEAN ZERO AND THE SAME VARIANCE. IF THE ERRORS DO  
 NOT HAVE MEAN ZERO (OR ARE UNKNOWN), THE PROGRAM WILL ISSUE A  
 WARNING MESSAGE (UNLESS IPRINT .LT. 0) AND THE COVARIANCE  
 MATRIX WILL NOT BE VALID. IN THAT CASE, THE MODEL SHOULD BE  
 ALTERED TO INCLUDE A CONSTANT TERM (SET PHI(1) = 1.).

NOTE ALSO THAT, IN ORDER FOR THE USUAL ASSUMPTIONS TO HOLD,  
 THE OBSERVATIONS MUST ALL BE OF APPROXIMATELY THE SAME  
 MAGNITUDE (IN THE ABSENCE OF INFORMATION ABOUT THE ERROR OF  
 EACH OBSERVATION), OTHERWISE THE VARIANCES WILL NOT BE THE  
 SAME. IF THE OBSERVATIONS ARE NOT THE SAME SIZE, THIS CAN BE  
 CURED BY WEIGHTING.

IF THE USUAL ASSUMPTIONS HOLD, THE SQUARE ROOTS OF THE  
 DIAGONALS OF THE COVARIANCE MATRIX A GIVE THE STANDARD ERROR  
 S(I) OF EACH PARAMETER. DIVIDING A(I,J) BY S(I)\*S(J) YIELDS  
 THE CORRELATION MATRIX OF THE PARAMETERS. PRINCIPAL AXES AND  
 CONFIDENCE ELLIPSOIDS CAN BE OBTAINED BY PERFORMING AN EIGEN-

C VALUE/EIGENVECTOR ANALYSIS ON A. ONE SHOULD CALL THE EISPACK 241.  
 C PROGRAM TRED2, FOLLOWED BY TQL2 (OR USE THE EISPACK CONTROL 242.  
 C PROGRAM). 243.  
 C 244.  
 C CONVERGENCE FAILURES 245.  
 C 246.  
 C IF CONVERGENCE FAILURES OCCUR, FIRST CHECK FOR INCORRECT 247.  
 C CODING OF THE SUBROUTINE ADA. CHECK ESPECIALLY THE ACTION OF 248.  
 C ISEL, AND THE COMPUTATION OF THE PARTIAL DERIVATIVES. IF THESE 249.  
 C ARE CORRECT, TRY SEVERAL STARTING GUESSES FOR ALF. IF ADA 250.  
 C IS CODED CORRECTLY, AND IF ERROR RETURNS IERR = -2 OR -8 251.  
 C PERSISTENTLY OCCUR, THIS IS A SIGN OF ILL-CONDITIONING, WHICH 252.  
 C MAY BE CAUSED BY SEVERAL THINGS. ONE IS POOR SCALING OF THE 253.  
 C PARAMETERS; ANOTHER IS AN UNFORTUNATE INITIAL GUESS FOR THE 254.  
 C PARAMETERS, STILL ANOTHER IS A POOR CHOICE OF THE MODEL. 255.  
 C 256.  
 C ALGORITHM 257.  
 C 258.  
 C THE RESIDUAL R IS MODIFIED TO INCORPORATE, FOR ANY FIXED 259.  
 C ALF, THE OPTIMAL LINEAR PARAMETERS FOR THAT ALF. IT IS THEN 260.  
 C POSSIBLE TO MINIMIZE ONLY ON THE NONLINEAR PARAMETERS. AFTER 261.  
 C THE OPTIMAL VALUES OF THE NONLINEAR PARAMETERS HAVE BEEN DETER- 262.  
 C MINED, THE LINEAR PARAMETERS CAN BE RECOVERED BY LINEAR LEAST 263.  
 C SQUARES TECHNIQUES (SEE REF. 1). 264.  
 C 265.  
 C THE MINIMIZATION IS BY A MODIFICATION OF OSBORNE'S (REF. 3) 266.  
 C MODIFICATION OF THE LEVENBERG-MARQUARDT ALGORITHM. INSTEAD OF 267.  
 C SOLVING THE NORMAL EQUATIONS WITH MATRIX 268.  
 C 269.  
 C 
$$(J^T J + \nu^2 D), \quad \text{WHERE } J = D(\text{ETA})/D(\text{ALF}),$$
 270.  
 C 271.  
 C STABLE ORTHOGONAL (HOUSEHOLDER) REFLECTIONS ARE USED ON A 272.  
 C MODIFICATION OF THE MATRIX 273.  
 C 274.  
 C 
$$\begin{pmatrix} J \\ \hline \dots \\ \nu^2 D \end{pmatrix},$$
 275.  
 C 276.  
 C 277.  
 C 278.  
 C WHERE D IS A DIAGONAL MATRIX CONSISTING OF THE LENGTHS OF THE 279.  
 C COLUMNS OF J. THIS MARQUARDT STABILIZATION ALLOWS THE ROUTINE 280.  
 C TO RECOVER FROM SOME RANK DEFICIENCIES IN THE JACOBIAN. 281.  
 C OSBORNE'S EMPIRICAL STRATEGY FOR CHOOSING THE MARQUARDT PARAM- 282.  
 C ETER HAS PROVEN REASONABLY SUCCESSFUL IN PRACTICE. (GAUSS- 283.  
 C NEWTON WITH STEP CONTROL CAN BE OBTAINED BY MAKING THE CHANGE 284.  
 C INDICATED BEFORE THE INSTRUCTION LABELED 5). A DESCRIPTION CAN 285.  
 C BE FOUND IN REF. (3), AND A FLOW CHART IN (2), P. 22. 286.  
 C 287.  
 C FOR REFERENCE, SEE 288.  
 C 289.  
 C 1. GENE H. GOLUB AND V. PEREYRA, 'THE DIFFERENTIATION OF 290.  
 C PSEUDO-INVERSES AND NONLINEAR LEAST SQUARES PROBLEMS WHOSE 291.  
 C VARIABLES SEPARATE,' SIAM J. NUMER. ANAL. 10, 413-432 292.  
 C (1973). 293.  
 C 2. -----, SAME TITLE, STANFORD C.S. REPORT 72-261, FEB. 1972. 294.  
 C 3. OSBORNE, MICHAEL R., 'SOME ASPECTS OF NON-LINEAR LEAST 295.  
 C SQUARES CALCULATIONS,' IN LOOTSMA, ED., 'NUMERICAL METHODS 296.  
 C FOR NON-LINEAR OPTIMIZATION,' ACADEMIC PRESS, LONDON, 1972. 297.  
 C 4. KROGH, FRED, 'EFFICIENT IMPLEMENTATION OF A VARIABLE PRO- 298.  
 C JECTION ALGORITHM FOR NONLINEAR LEAST SQUARES PROBLEMS,' 299.  
 C COMM. ACM 17, PP. 167-169 (MARCH, 1974). 300.  
 C 5. KAUFMAN, LINDA, 'A VARIABLE PROJECTION METHOD FOR SOLVING 301.  
 C SEPARABLE NONLINEAR LEAST SQUARES PROBLEMS', B.I.T. 15, 302.  
 C 49-57 (1975). 303.  
 C 6. DRAPER, N., AND SMITH, H., APPLIED REGRESSION ANALYSIS, 304.  
 C WILEY, N.Y., 1966 (FOR STATISTICAL INFORMATION ONLY). 305.  
 C 7. C. LAWSON AND R. HANSON, SOLVING LEAST SQUARES PROBLEMS, 306.

```

C PRENTICE-HALL, ENGLEWOOD CLIFFS, N. J., 1974. 307.
C C JOHN BOLSTAD 308.
C C COMPUTER SCIENCE DEPT., SERRA HOUSE 309.
C C STANFORD UNIVERSITY 310.
C C JANUARY, 1977 311.
C C ..... 312.
C C ..... 313.
C C ..... 314.
C C ..... 315.
C C DOUBLE PRECISION A(NMAX, LPP2), BETA(L), ALF(NL), T(NMAX, IV), 316.
C 2 W(N), Y(N), ACUM, EPS1, GNSTEP, NU, PRJRES, R, RNEW, XNORM 317.
C INTEGER B1, OUTPUT 318.
C LOGICAL SKIP 319.
C EXTERNAL ADA 320.
C DATA EPS1 /1.D-6/, ITMAX /40/, OUTPUT /6/ 321.
C
C THE FOLLOWING TWO PARAMETERS ARE USED IN THE CONVERGENCE 322.
C TEST: EPS1 IS AN ABSOLUTE AND RELATIVE TOLERANCE FOR THE 323.
C NORM OF THE PROJECTION OF THE RESIDUAL ONTO THE RANGE OF THE 324.
C JACOBIAN OF THE VARIABLE PROJECTION FUNCTIONAL. 325.
C ITMAX IS THE MAXIMUM NUMBER OF FUNCTION AND DERIVATIVE 326.
C EVALUATIONS ALLOWED. CAUTION: EPS1 MUST NOT BE 327.
C SET SMALLER THAN 10 TIMES THE UNIT ROUND-OFF OF THE MACHINE. 328.
C
C----- 329.
C----- 330.
C----- 330.005
C----- CALL LIB MONITOR FROM VARPRO, MAINTENANCE NUMBER 509, DATE 77178 330.006
C----- ****PLEASE DON'T REMOVE OR CHANGE THE ABOVE CALL. IT IS YOUR ONLY 330.008
C----- ****PROTECTION AGAINST YOUR USING AN OUT-OF-DATE OR INCORRECT 330.009
C----- ****VERSION OF THE ROUTINE. THE LIBRARY MONITOR REMOVES THIS CALL, 330.01
C----- ****SO IT ONLY OCCURS ONCE, ON THE FIRST ENTRY TO THIS ROUTINE. 330.011
C----- 330.012
C----- IERR = 1 331.
C----- ITER = 0 332.
C----- LP1 = L + 1 333.
C----- B1 = L + 2 334.
C----- LNL2 = L + NL + 2 335.
C----- NLP1 = NL + 1 336.
C----- SKIP = .FALSE. 337.
C----- MODIT = IPRINT 338.
C----- IF (IPRINT .LE. 0) MODIT = ITMAX + 2 339.
C----- NU = 0. 340.
C----- IF GAUSS-NEWTON IS DESIRED REMOVE THE NEXT STATEMENT. 341.
C----- NU = 1. 342.
C----- BEGIN OUTER ITERATION LOOP TO UPDATE ALF. 343.
C----- CALCULATE THE NORM OF THE RESIDUAL AND THE DERIVATIVE OF 344.
C----- THE MODIFIED RESIDUAL THE FIRST TIME, BUT ONLY THE 345.
C----- DERIVATIVE IN SUBSEQUENT ITERATIONS. 346.
C----- 347.
C----- 348.
C----- 5 CALL DPA (L, NL, N, NMAX, LPP2, IV, T, Y, W, ALF, ADA, IERR, 349.
C----- X IPRINT, A, BETA, A(1, LP1), R) 350.
C----- GNSTEP = 1.0 351.
C----- ITERIN = 0 352.
C----- IF (ITER .GT. 0) GO TO 10 353.
C----- IF (NL .EQ. 0) GO TO 90 354.
C----- IF (IERR .NE. 1) GO TO 99 355.
C----- IF (IPRINT .LE. 0) GO TO 10 356.
C----- WRITE (OUTPUT, 207) ITERIN, R 357.
C----- WRITE (OUTPUT, 200) NU 358.
C----- BEGIN TWO-STAGE ORTHOGONAL FACTORIZATION 359.
C----- 360.
C----- 10 CALL ORFAC1(NLP1, NMAX, N, L, IPRINT, A(1, B1), PRJRES, IERR) 361.
C----- IF (IERR .LT. 0) GO TO 99 362.
C----- IERR = 2 363.
C----- IF (NU .EQ. 0.) GO TO 30 364.
C----- 365.

```

```

C      BEGIN INNER ITERATION LOOP FOR GENERATING NEW ALF AND      366.
C      TESTING IT FOR ACCEPTANCE.                                     367.
C
C      25      CALL ORFAC2(NLP1, NMAX, NU, A(1, B1))                  368.
C
C      SOLVE A NL X NL UPPER TRIANGULAR SYSTEM FOR DELTA-ALF.      369.
C      THE TRANSFORMED RESIDUAL (IN COL. LNL2 OF A) IS OVER-      370.
C      WRITTEN BY THE RESULT DELTA-ALF.                                371.
C
C      30      CALL BACSUB (NMAX, NL, A(1, B1), A(1, LNL2))          372.
C      DO 35 K = 1, NL
C          A(K, B1) = ALF(K) + A(K, LNL2)                            373.
C          NEW ALF(K) = ALF(K) + DELTA ALF(K)                          374.
C
C      STEP TO THE NEW POINT NEW ALF, AND COMPUTE THE NEW      375.
C      NORM OF RESIDUAL.  NEW ALF IS STORED IN COLUMN B1 OF A.  376.
C
C      40      CALL DPA (L, NL, N, NMAX, LPP2, IV, T, Y, W, A(1, B1), ADA, 377.
C      X      IERR, IPRINT, A, BETA, A(1, LP1), RNEW)                  378.
C      IF (IERR .NE. 2) GO TO 99
C          ITER = ITER + 1
C          ITERIN = ITERIN + 1
C          SKIP = MOD(ITER, MODIT) .NE. 0
C          IF (SKIP) GO TO 45
C              WRITE (OUTPUT, 203) ITER
C              WRITE (OUTPUT, 216) (A(K, B1), K = 1, NL)
C              WRITE (OUTPUT, 207) ITERIN, RNEW
C
C      45      IF (ITER .LT. ITMAX) GO TO 50
C          IERR = -1
C          CALL VARERR (IPRINT, IERR, 1)
C          GO TO 95
C      50      IF (RNEW - R .LT. EPS1*(R + 1.D0)) GO TO 75
C
C          RETRACT THE STEP JUST TAKEN
C
C          IF (NU .NE. 0.) GO TO 60
C
C          GAUSS-NEWTON OPTION ONLY
C          GNSTEP = 0.5*GNSTEP
C          IF (GNSTEP .LT. EPS1) GO TO 95
C          DO 55 K = 1, NL
C              A(K, B1) = ALF(K) + GNSTEP*A(K, LNL2)
C          GO TO 40
C
C          ENLARGE THE MARQUARDT PARAMETER
C          60      NU = 1.5*NU
C          IF (.NOT. SKIP) WRITE (OUTPUT, 206) NU
C          IF (NU .LE. 110.) GO TO 65
C              IERR = -2
C              CALL VARERR (IPRINT, IERR, 1)
C              GO TO 95
C
C          RETRIEVE UPPER TRIANGULAR FORM
C          AND RESIDUAL OF FIRST STAGE.
C
C          65      DO 70 K = 1, NL
C              KSUB = LP1 + K
C              DO 70 J = K, NLP1
C                  JSUB = LP1 + J
C                  ISUB = NLP1 + J
C              70      A(K, JSUB) = A(ISUB, KSUB)
C              GO TO 25
C
C          END OF INNER ITERATION LOOP
C
C          ACCEPT THE STEP JUST TAKEN
C
C          75 R = RNEW
C          DO 80 K = 1, NL
C              80      ALF(K) = A(K, B1)
C
C          CALC. NORM(DELTA ALF)/NORM(ALF) 431.

```



```

C COLUMN WAS ZERO 498.
C IERR = -8 499.
C CALL VARERR (IPRINT, IERR, LP1 + K) 500.
C GO TO 99 501.
C APPLY REFLECTIONS TO REMAINING COLUMNS 502.
C OF B AND TO RESIDUAL VECTOR. 503.
C
C 13  KP1 = K + 1 504.
C DO 25 J = KP1, NLP1 505.
C ACUM = 0.0 506.
C DO 20 I = LPK, N 507.
C ACUM = ACUM + B(I, K) * B(I, J) 508.
C ACUM = ACUM / BETA 509.
C DO 25 I = LPK, N 510.
C B(I, J) = B(I, J) - B(I, K) * ACUM 511.
C 30  B(LPK, K) = -ALPHA 512.
C
C PRJRES = XNORM(NL, B(LP1, NLP1)) 513.
C
C SAVE UPPER TRIANGULAR FORM AND TRANSFORMED RESIDUAL, FOR USE 514.
C IN CASE A STEP IS RETRACTED. ALSO COMPUTE COLUMN LENGTHS. 515.
C
C IF (IERR .EQ. 4) GO TO 99 516.
C DO 50 K = 1, NL 517.
C LPK = L + K 518.
C DO 40 J = K, NLP1 519.
C JSUB = NLP1 + J 520.
C B(K, J) = B(LPK, J) 521.
C 40  B(JSUB, K) = B(LPK, J) 522.
C 50  B(NL23, K) = XNORM(K, B(LP1, K)) 523.
C
C 99 RETURN 524.
C END 525.
C
C SUBROUTINE ORFAC2(NLP1, NMAX, NU, B) 526.
C
C STAGE 2: SPECIAL HOUSEHOLDER REDUCTION OF 527.
C
C NL ( DR' . R3 ) (DR'' . R5 ) 528.
C (----- . -- ) (----- . -- ) 529.
C N-L-NL ( 0 . R4 ) TO ( 0 . R4 ) 530.
C (----- . -- ) (----- . -- ) 531.
C NL (NU*D . 0 ) ( 0 . R6 ) 532.
C
C NL 1 NL 1 533.
C
C WHERE DR', R3, AND R4 ARE AS IN ORFAC1, NU IS THE MARQUARDT 534.
C PARAMETER, D IS A DIAGONAL MATRIX CONSISTING OF THE LENGTHS OF 535.
C THE COLUMNS OF DR', AND DR'' IS IN UPPER TRIANGULAR FORM. 536.
C DETAILS IN (1), PP. 423-424. NOTE THAT THE (N-L-NL) BAND OF 537.
C ZEROES, AND R4, ARE OMITTED IN STORAGE. 538.
C
C ..... 539.
C
C DOUBLE PRECISION ACUM, ALPHA, B(NMAX, NLP1), BETA, DSIGN, NU, U, 540.
C X NORM 541.
C
C NL = NLP1 - 1 542.
C NL2 = 2*NL 543.
C NL23 = NL2 + 3 544.
C DO 30 K = 1, NL 545.
C KP1 = K + 1 546.
C NLPK = NL + K 547.
C NLPKM1 = NLPK - 1 548.
C B(NLPK, K) = NU * B(NL23, K) 549.
C B(NL, K) = B(K, K) 550.
C ALPHA = DSIGN(XNORM(K+1, B(NL, K)), B(K, K)) 551.

```

```

U = B(K, K) + ALPHA      564.
BETA = ALPHA * U         565.
B(K, K) = -ALPHA         566.
C           THE K-TH REFLECTION MODIFIES ONLY ROWS K,      567.
C           NL+1, NL+2, ..., NL+K, AND COLUMNS K TO NL+1. 568.
C           DO 30 J = KP1, NLP1      569.
C             B(NLPK, J) = 0.      570.
C             ACUM = U * B(K, J) 571.
C             DO 20 I = NLP1, NLPKM1 572.
C               ACUM = ACUM + B(I, K) * B(I, J) 573.
C               ACUM = ACUM / BETA 574.
C               B(K, J) = B(K, J) - U * ACUM 575.
C               DO 30 I = NLP1, NLPK 576.
C                 B(I, J) = B(I, J) - B(I, K) * ACUM 577.
C
C           RETURN 578.
C           END 579.
C
C           SUBROUTINE DPA (L, NL, N, NMAX, LPP2, IV, T, Y, W, ALF, ADA, ISEL, 582.
C X IPRINT, A, U, R, RNORM) 583.
C
C           COMPUTE THE NORM OF THE RESIDUAL (IF ISEL = 1 OR 2), OR THE 584.
C (N-L) X NL DERIVATIVE OF THE MODIFIED RESIDUAL (N-L) VECTOR 585.
C Q2*Y (IF ISEL = 1 OR 3). HERE Q * PHI = S, I.E., 586.
C
C           L      ( Q1 ) (      . . .      ) ( S . R1 . F1 ) 587.
C           (---) ( PHI : Y : D(PHI) ) = (--- . -- . --- ) 588.
C           N-L ( Q2 ) (      . . .      ) ( 0 . R2 . F2 ) 589.
C
C           N       L       1       P       L       1       P 590.
C
C           WHERE Q IS N X N ORTHOGONAL, AND S IS L X L UPPER TRIANGULAR. 591.
C           THE NORM OF THE RESIDUAL = NORM(R2), AND THE DESIRED DERIVATIVE 592.
C           ACCORDING TO REF. (5), IS 593.
C
C           D(Q2 * Y) = -Q2 * D(PHI) * S-1 * Q1* Y. 594.
C
C           .....
C
C           DOUBLE PRECISION A(NMAX, LPP2), ALF(NL), T(NMAX, IV), W(N), Y(N), 603.
C X ACUM, ALPHA, BETA, RNORM, DSIGN, DSQRT, SAVE, R(N), U(L), XNORM 604.
C INTEGER FIRSTC, FIRSTR, INC(12, 8) 605.
C LOGICAL NOWATE, PHILP1 606.
C EXTERNAL ADA 607.
C
C           IF (ISEL .NE. 1) GO TO 3 608.
C             LP1 = L + 1 609.
C             LNL2 = L + 2 + NL 610.
C             LP2 = L + 2 611.
C             LPP1 = LPP2 - 1 612.
C             FIRSTC = 1 613.
C             LASTC = LPP1 614.
C             FIRSTR = LP1 615.
C             CALL INIT(L, NL, N, NMAX, LPP2, IV, T, W, ALF, ADA, ISEL, 616.
C X IPRINT, A, INC, NCON, NCONP1, PHILP1, NOWATE) 617.
C             IF (ISEL .NE. 1) GO TO 99 618.
C             GO TO 30 619.
C
C           3 CALL ADA (LP1, NL, N, NMAX, LPP2, IV, A, INC, T, ALF, MIN0(ISEL, 620.
C X 3)) 621.
C             IF (ISEL .EQ. 2) GO TO 6 622.
C
C             FIRSTC = LP2 623.
C             LASTC = LPP1 624.
C             FIRSTR = (4 - ISEL)*L + 1 625.
C             GO TO 50 626.
C
C           ISEL = 3 OR 4 627.
C
C             FIRSTC = LP2 628.
C             LASTC = LPP1 629.
C             FIRSTR = (4 - ISEL)*L + 1

```

```

C           ISEL = 2          630.
6 FIRSTC = NCONP1          631.
LASTC = LP1                632.
IF (NCON .EQ. 0) GO TO 30  633.
IF (A(1, NCON) .EQ. SAVE) GO TO 30  634.
ISEL = -7                  635.
CALL VARERR (IPRINT, ISEL, NCON)  636.
GO TO 99                  637.

C           ISEL = 1 OR 2      638.
30 IF (PHILP1) GO TO 40    639.
DO 35 I = 1, N             640.
35   R(I) = Y(I)           641.
GO TO 50                  642.
40   DO 45 I = 1, N        643.
45   R(I) = Y(I) - R(I)   644.

C           WEIGHT APPROPRIATE COLUMNS 645.
50 IF (NOWATE) GO TO 58    646.
DO 55 I = 1, N             647.
ACUM = W(I)                648.
DO 55 J = FIRSTC, LASTC   649.
55   A(I, J) = A(I, J) * ACUM  650.

C           COMPUTE ORTHOGONAL FACTORIZATIONS BY HOUSEHOLDER 651.
C           REFLECTIONS. IF ISEL = 1 OR 2, REDUCE PHI (STORED IN THE 652.
C           FIRST L COLUMNS OF THE MATRIX A) TO UPPER TRIANGULAR FORM, 653.
C           (Q*PHI = S), AND TRANSFORM Y (STORED IN COLUMN L+1), GETTING 654.
C           Q*Y = R. IF ISEL = 1, ALSO TRANSFORM J = D PHI (STORED IN 655.
C           COLUMNS L+2 THROUGH L+P+1 OF THE MATRIX A), GETTING Q*J = F. 656.
C           IF ISEL = 3 OR 4, PHI HAS ALREADY BEEN REDUCED, TRANSFORM 657.
C           ONLY J, S, R, AND F OVERWRITE PHI, Y, AND J, RESPECTIVELY, 658.
C           AND A FACTORED FORM OF Q IS SAVED IN U AND THE LOWER 659.
C           TRIANGLE OF PHI. 660.

C           58 IF (L .EQ. 0) GO TO 75          661.
DO 70 K = 1, L             662.
    KP1 = K + 1             663.
    IF (ISEL .GE. 3 .OR. (ISEL .EQ. 2 .AND. K .LT. NCONP1)) GO TO 66 664.
    ALPHA = DSIGN(XNORM(N+1-K, A(K, K)), A(K, K))  665.
    U(K) = A(K, K) + ALPHA  666.
    A(K, K) = -ALPHA       667.
    FIRSTC = KP1            668.
    IF (ALPHA .NE. 0.0) GO TO 66  669.
    ISEL = -8               670.
    CALL VARERR (IPRINT, ISEL, K)  671.
    GO TO 99               672.

C           APPLY REFLECTIONS TO COLUMNS 673.
C           FIRSTC TO LASTC. 674.

C           66   BETA = -A(K, K) * U(K)          675.
DO 70 J = FIRSTC, LASTC   676.
    ACUM = U(K)*A(K, J)      677.
    DO 68 I = KP1, N         678.
        ACUM = ACUM + A(I, K)*A(I, J)  679.
    ACUM = ACUM / BETA      680.
    A(K, J) = A(K, J) - U(K)*ACUM  681.
    DO 70 I = KP1, N         682.
        A(I, J) = A(I, J) - A(I, K)*ACUM  683.
    C           75 IF (ISEL .GE. 3) GO TO 85  684.
    RNORM = XNORM(N-L, R(LP1))  685.
    IF (ISEL .EQ. 2) GO TO 99  686.
    IF (NCON .GT. 0) SAVE = A(1, NCON)  687.

C           F2 IS NOW CONTAINED IN ROWS L+1 TO N AND COLUMNS L+2 TO 688.
C           L+P+1 OF THE MATRIX A. NOW SOLVE THE L X L UPPER TRIANGULAR 689.
C           SYSTEM S*BETA = R1 FOR THE LINEAR PARAMETERS BETA. BETA  690.
C           OVERWRITES R1. 691.

C           692.
C           693.
C           694.
C           695.

```

```

C 85 IF (L .GT. 0) CALL BACSUB (NMAX, L, A, R) 696.
C 697.
C 698.
C MAJOR PART OF KAUFMAN'S SIMPLIFICATION OCCURS HERE. COMPUTE 699.
C THE DERIVATIVE OF ETA WITH RESPECT TO THE NONLINEAR 700.
C PARAMETERS 701.
C 702.
C T D ETA T L D PHI(J) D PHI(L+1) 703.
C Q * ----- = Q * (SUM BETA(J) ----- + -----) = F2*BETA 704.
C D ALF(K) J=1 D ALF(K) D ALF(K) 705.
C 706.
C AND STORE THE RESULT IN COLUMNS L+2 TO L+NL+1. IF ISEL NOT 707.
C = 4, THE FIRST L ROWS ARE OMITTED. THIS IS -D(Q2)*Y. IF 708.
C ISEL NOT = 4 THE RESIDUAL R2 = Q2*Y (IN COL. L+1) IS COPIED 709.
C TO COLUMN L+NL+2. OTHERWISE ALL OF COLUMN L+1 IS COPIED. 710.
C 711.
C DO 95 I = FIRSTR, N 712.
C IF (L .EQ. NCON) GO TO 95 713.
C M = LP1 714.
C DO 90 K = 1, NL 715.
C ACUM = 0. 716.
C DO 88 J = NCONP1, L 717.
C IF (INC(K, J) .EQ. 0) GO TO 88 718.
C M = M + 1 719.
C ACUM = ACUM + A(I, M) * R(J) 720.
C 88 CONTINUE 721.
C KSUB = LP1 + K 722.
C IF (INC(K, LP1) .EQ. 0) GO TO 90 723.
C M = M + 1 724.
C ACUM = ACUM + A(I, M) 725.
C 90 A(I, KSUB) = ACUM 726.
C 95 A(I, LNL2) = R(I) 727.
C 728.
C 99 RETURN 729.
C END 730.
C 731.
C SUBROUTINE INIT(L, NL, N, NMAX, LPP2, IV, T, W, ALF, ADA, ISEL, 732.
C X IPRINT, A, INC, NCON, NCONP1, PHILP1, NOWATE) 733.
C 734.
C CHECK VALIDITY OF INPUT PARAMETERS, AND DETERMINE NUMBER OF 735.
C CONSTANT FUNCTIONS. 736.
C 737.
C 738.
C 739.
C DOUBLE PRECISION A(NMAX, LPP2), ALF(NL), T(NMAX, IV), W(N), 740.
C X DSQRT 741.
C INTEGER OUTPUT, P, INC(12, 8) 742.
C LOGICAL NOWATE, PHILP1 743.
C DATA OUTPUT /6/ 744.
C 745.
C LP1 = L + 1 746.
C LNL2 = L + 2 + NL 747.
C 748.
C CHECK FOR VALID INPUT
C IF (L .GE. 0 .AND. NL .GE. 0 .AND. L+NL .LT. N .AND. LNL2 .LE. 749.
C X LPP2 .AND. 2*NL + 3 .LE. NMAX .AND. N .LE. NMAX .AND. 750.
C X IV .GT. 0 .AND. .NOT. (NL .EQ. 0 .AND. L .EQ. 0)) GO TO 1 751.
C ISEL = -4 752.
C CALL VARERR (IPRINT, ISEL, 1) 753.
C GO TO 99 754.
C 755.
C 1 IF (L .EQ. 0 .OR. NL .EQ. 0) GO TO 3 756.
C DO 2 J = 1, LP1 757.
C DO 2 K = 1, NL 758.
C 2 INC(K, J) = 0 759.
C 760.
C 3 CALL ADA (LP1, NL, N, NMAX, LPP2, IV, A, INC, T, ALF, ISEL) 761.

```

```

C
      NOWATE = .TRUE.
      DO 9 I = 1, N
          NOWATE = NOWATE .AND. (W(I) .EQ. 1.0)
          IF (W(I) .GE. 0.) GO TO 9
C
      ISEL = -6
      CALL VARERR (IPRINT, ISEL, I)
      GO TO 99
      9   W(I) = DSQRT(W(I))
C
      NCON = L
      NCONP1 = LP1
      PHILP1 = L .EQ. 0
      IF (PHILP1 .OR. NL .EQ. 0) GO TO 99
C
      11  CONTINUE
C
      NCON = NCONP1 - 1
      IF (IPRINT .GE. 0) WRITE (OUTPUT, 210) NCON
      IF (L+P+2 .EQ. LPP2) GO TO 20
C
      15  ISEL = -5
          CALL VARERR (IPRINT, ISEL, 1)
          GO TO 99
C
      20  DO 25 K = 1, NL
          25  IF (INC(K, LP1) .EQ. 1) PHILP1 = .TRUE.
C
      99  RETURN
      210 FORMAT (33H0  NUMBER OF CONSTANT FUNCTIONS =, I4 /)
      END
      SUBROUTINE BACSUB (NMAX, N, A, X)
C
      C
          BACKSOLVE THE N X N UPPER TRIANGULAR SYSTEM A*X = B.
          THE SOLUTION X OVERWRITES THE RIGHT SIDE B.
C
      DOUBLE PRECISION A(NMAX, N), X(N), ACUM
C
      X(N) = X(N) / A(N, N)
      IF (N .EQ. 1) GO TO 30
      NP1 = N + 1
      DO 20 IBACK = 2, N
          I = NP1 - IBACK
          C
              I = N-1, N-2, ..., 2, 1
              IP1 = I + 1
              ACUM = X(I)
              DO 10 J = IP1, N
                  10  ACUM = ACUM - A(I,J)*X(J)
              20  X(I) = ACUM / A(I,I)
C
      30  RETURN
      END
      SUBROUTINE POSTPR(L, NL, N, NMAX, LNL2, EPS, RNORM, IPRINT, ALF,
      X W, A, R, U, IERR)
C
      C
          CALCULATE RESIDUALS, SAMPLE VARIANCE, AND COVARIANCE MATRIX.
          ON INPUT, U CONTAINS INFORMATION ABOUT HOUSEHOLDER REFLECTIONS

```

```

C      FROM DPA.  ON OUTPUT, IT CONTAINS THE LINEAR PARAMETERS.      828.
C
C      DOUBLE PRECISION A(NMAX, LNL2), ALF(NL), R(N), U(L), W(N), ACUM,      829.
C      X EPS, PRJRES, RNORM, SAVE, DABS      830.
C      INTEGER OUTPUT      831.
C      DATA OUTPUT /6/      832.
C
C      LP1 = L + 1      833.
C      LPNL = LNL2 - 2      834.
C      LNL1 = LPNL + 1      835.
C      DO 10 I = 1, N      836.
C      10    W(I) = W(I)**2      837.
C
C      UNWIND HOUSEHOLDER TRANSFORMATIONS TO GET RESIDUALS,      838.
C      AND MOVE THE LINEAR PARAMETERS FROM R TO U.      839.
C
C      IF (L .EQ. 0) GO TO 30      840.
C      DO 25 KBACK = 1, L      841.
C          K = LP1 - KBACK      842.
C          KP1 = K + 1      843.
C          ACUM = 0.      844.
C          DO 20 I = KP1, N      845.
C              ACUM = ACUM + A(I, K) * R(I)      846.
C              SAVE = R(K)      847.
C              R(K) = ACUM / A(K, K)      848.
C              ACUM = -ACUM / (U(K) * A(K, K))      849.
C              U(K) = SAVE      850.
C              DO 25 I = KP1, N      851.
C                  R(I) = R(I) - A(I, K)*ACUM      852.
C
C      25          COMPUTE MEAN ERROR      853.
C
C      30 ACUM = 0.      854.
C      DO 35 I = 1, N      855.
C      35    ACUM = ACUM + R(I)      856.
C      SAVE = ACUM / N      857.
C
C      THE FIRST L COLUMNS OF THE MATRIX HAVE BEEN REDUCED TO      858.
C      UPPER TRIANGULAR FORM IN DPA.  FINISH BY REDUCING ROWS      859.
C      L+1 TO N AND COLUMNS L+2 THROUGH L+NL+1 TO TRIANGULAR      860.
C      FORM.  THEN SHIFT COLUMNS OF DERIVATIVE MATRIX OVER ONE      861.
C      TO THE LEFT TO BE ADJACENT TO THE FIRST L COLUMNS.      862.
C
C      IF (NL .EQ. 0) GO TO 45      863.
C      CALL ORFAC1(NL+1, NMAX, N, L, IPRINT, A(1, L+2), PRJRES, 4)      864.
C      DO 40 I = 1, N      865.
C          A(I, LNL2) = R(I)      866.
C          DO 40 K = LP1, LNL1      867.
C              A(I, K) = A(I, K+1)      868.
C
C      40          COMPUTE COVARIANCE MATRIX      869.
C
C      45 A(1, LNL2) = RNORM      870.
C      ACUM = RNORM*RNORM/(N - L - NL)      871.
C      A(2, LNL2) = ACUM      872.
C      CALL COV(NMAX, LPNL, ACUM, A)      873.
C
C      IF (IPRINT .LT. 0) GO TO 99      874.
C      WRITE (OUTPUT, 209)      875.
C      IF (L .GT. 0) WRITE (OUTPUT, 210) (U(J), J = 1, L)      876.
C      IF (NL .GT. 0) WRITE (OUTPUT, 211) (ALF(K), K = 1, NL)      877.
C      WRITE (OUTPUT, 214) RNORM, SAVE, ACUM      878.
C      IF (DABS(SAVE) .GT. EPS) WRITE (OUTPUT, 215)      879.
C      WRITE (OUTPUT, 209)      880.
C
C      99 RETURN      881.
C
C      209 FORMAT (1H0, 50(1H'))      882.
C      210 FORMAT (20H0  LINEAR PARAMETERS // (7E15.7))      883.
C      211 FORMAT (23H0  NONLINEAR PARAMETERS // (7E15.7))      884.
C      214 FORMAT (21H0  NORM OF RESIDUAL =, E15.7, 33H EXPECTED ERROR OF OBS 885.
C

```

```

XERVATIONS =, E15.7, / 39H ESTIMATED VARIANCE OF OBSERVATIONS =, 894.
X E15.7 ) 895.
215 FORMAT (95H WARNING -- EXPECTED ERROR OF OBSERVATIONS IS NOT ZERO 896.
X. COVARIANCE MATRIX MAY BE MEANINGLESS. /) 897.
END 898.
SUBROUTINE COV(NMAX, N, SIGMA2, A) 899.

C 900.
C COMPUTE THE SCALED COVARIANCE MATRIX OF THE L + NL 901.
C PARAMETERS. THIS INVOLVES COMPUTING 902.
C 903.
C 2 -1 -T
C SIGMA * T * T 904.
C 905.
C WHERE THE (L+NL) X (L+NL) UPPER TRIANGULAR MATRIX T IS 906.
C DESCRIBED IN SUBROUTINE POSTPR. THE RESULT OVERWRITES THE 907.
C FIRST L+NL ROWS AND COLUMNS OF THE MATRIX A. THE RESULTING 908.
C MATRIX IS SYMMETRIC. SEE REF. 7, PP. 67-70, 281. 909.
C 910.
C ..... 911.
C 912.
C DOUBLE PRECISION A(NMAX, N), SUM, SIGMA2 913.
C 914.
C 10 DO 10 J = 1, N 915.
C 10 A(J, J) = 1./A(J, J) 916.
C 917.
C INVERT T UPON ITSELF 918.
C 919.
C IF (N .EQ. 1) GO TO 70 920.
C NM1 = N - 1 921.
C DO 60 I = 1, NM1 922.
C IP1 = I + 1 923.
C DO 60 J = IP1, N 924.
C JM1 = J - 1 925.
C SUM = 0. 926.
C DO 50 M = I, JM1 927.
C SUM = SUM + A(I, M) * A(M, J) 928.
C 50 A(I, J) = -SUM * A(J, J) 929.
C 60 930.
C 931.
C NOW FORM THE MATRIX PRODUCT 932.
C 933.
C 70 DO 90 I = 1, N 934.
C DO 90 J = I, N 935.
C SUM = 0. 936.
C DO 80 M = J, N 937.
C SUM = SUM + A(I, M) * A(J, M) 938.
C SUM = SUM * SIGMA2 939.
C A(I, J) = SUM 940.
C 90 A(J, I) = SUM 941.

C 942.
C RETURN 943.
C END 944.
C SUBROUTINE VARERR (IPRINT, IERR, K) 945.

C 946.
C PRINT ERROR MESSAGES 947.

C 948.
C INTEGER ERRNO, OUTPUT 949.
C DATA OUTPUT /6/ 950.

C 951.
C IF (IPRINT .LT. 0) GO TO 99 952.
C ERRNO = IABS(IERR) 953.
C GO TO (1, 2, 99, 4, 5, 6, 7, 8), ERRNO 954.

C 955.
C 1 WRITE (OUTPUT, 101) 956.
C GO TO 99 957.
C 2 WRITE (OUTPUT, 102) 958.
C GO TO 99 959.

```

```

4 WRITE (OUTPUT, 104) 960.
  GO TO 99 961.
5 WRITE (OUTPUT, 105) 962.
  GO TO 99 963.
6 WRITE (OUTPUT, 106) K 964.
  GO TO 99 965.
7 WRITE (OUTPUT, 107) K 966.
  GO TO 99 967.
8 WRITE (OUTPUT, 108) K 968.
C 99 RETURN 969.
101 FORMAT (46H0 PROBLEM TERMINATED FOR EXCESSIVE ITERATIONS //) 970.
102 FORMAT (49H0 PROBLEM TERMINATED BECAUSE OF ILL-CONDITIONING //) 971.
104 FORMAT (/ 50H INPUT ERROR IN PARAMETER L, NL, N, LPP2, OR NMAX. /) 972.
105 FORMAT (68H0 ERROR -- INC MATRIX IMPROPERLY SPECIFIED, OR DISAGRE 973.
  XES WITH LPP2. /) 974.
106 FORMAT (19H0 ERROR -- WEIGHT(, I4, 14H) IS NEGATIVE. /) 975.
107 FORMAT (28H0 ERROR -- CONSTANT COLUMN , I3, 37H MUST BE COMPUTED 976.
  XONLY WHEN ISEL = 1. /) 977.
108 FORMAT (33H0 CATASTROPHIC FAILURE -- COLUMN , I4, 28H IS ZERO, SE 978.
  XE DOCUMENTATION. /) 979.
  END 980.
  DOUBLE PRECISION FUNCTION XNORM(N, X) 981.
C
C      COMPUTE THE L2 (EUCLIDEAN) NORM OF A VECTOR, MAKING SURE TO 982.
C      AVOID UNNECESSARY UNDERFLOWS.  NO ATTEMPT IS MADE TO SUPPRESS 983.
C      OVERFLOWS. 984.
C
C      DOUBLE PRECISION X(N), RMAX, SUM, TERM, DABS, DSQRT 985.
C
C      FIND LARGEST (IN ABSOLUTE VALUE) ELEMENT 986.
C      RMAX = 0. 987.
C      DO 10 I = 1, N 988.
C          IF (DABS(X(I)) .GT. RMAX) RMAX = DABS(X(I)) 989.
C 10      CONTINUE 990.
C
C      SUM = 0. 991.
C      IF (RMAX .EQ. 0.) GO TO 30 992.
C      DO 20 I = 1, N 993.
C          TERM = 0. 994.
C          IF (RMAX + DABS(X(I)) .NE. RMAX) TERM = X(I)/RMAX 995.
C 20      SUM = SUM + TERM*TERM 996.
C
C 30 XNORM = RMAX*DSQRT(SUM) 997.
C 99 RETURN 998.
  END 999.

```

0 Match 1118 Erfc  
 0 number of nonlinear parameters  
 3  
 0 initial est. of nonlin. parameters  
 1.600  
 0.025  
 0.004  
 0 dimensionless number tracer arrival time inletA  
 1.60000 40.000 280.000  
 0 number of observations  
 316  
 0 independent variables dependent variables  
 294.775 1.824  
 300.102 1.849  
 305.327 1.899  
 310.530 2.055  
 315.807 2.362  
 321.068 2.823  
 326.347 3.393  
 331.609 4.170  
 336.833 5.206  
 342.119 6.454  
 347.321 7.937  
 352.583 9.716  
 357.938 11.930  
 363.220 14.566  
 368.557 17.537  
 373.840 20.874  
 379.044 24.524  
 384.381 28.645  
 389.586 33.119  
 394.847 38.042  
 400.134 43.190  
 405.414 48.553  
 410.762 54.168  
 415.963 60.181  
 421.224 66.212  
 423.855 69.216  
 426.502 72.162  
 429.115 75.101  
 431.726 77.877  
 434.338 80.628  
 436.929 83.414  
 439.594 86.179  
 442.207 88.846  
 444.819 91.714  
 447.410 94.446  
 450.022 97.114  
 452.694 99.659  
 455.343 102.223  
 457.955 104.728  
 460.569 107.065  
 463.239 109.381  
 465.979 111.867  
 468.591 114.393  
 471.239 117.177  
 473.849 119.988  
 476.461 122.985  
 479.074 125.954  
 481.742 128.813

484.409	131.440
487.022	134.065
489.671	136.156
492.284	137.900
494.951	139.686
497.563	141.449
500.176	143.297
502.822	145.169
505.435	147.244
508.106	149.143
510.717	150.940
513.329	152.701
515.927	154.215
518.601	155.610
521.252	157.081
523.934	158.310
526.551	159.583
529.199	161.202
531.814	162.520
534.428	163.891
537.096	165.658
539.768	167.318
542.440	169.055
545.053	169.870
547.645	170.469
550.315	170.890
552.928	171.473
555.598	171.937
558.270	172.941
560.942	174.281
563.612	175.402
566.285	176.483
568.957	177.960
571.627	179.952
574.241	181.394
576.835	182.991
579.577	184.431
582.250	185.647
584.901	186.930
587.515	187.469
590.130	187.772
592.800	188.326
595.471	188.806
598.142	188.880
600.814	188.678
603.485	188.365
606.099	187.601
608.767	187.070
611.418	186.710
614.031	187.017
616.644	186.876
619.314	186.753
621.988	186.516
624.658	186.244
627.328	186.823
629.999	187.219
632.614	187.632
635.328	188.266
637.942	189.289
640.556	190.455
643.224	190.989
645.895	191.359
648.567	191.367
651.237	190.752
653.851	189.262
656.445	189.032

659.059	186.992
661.652	185.304
664.321	184.196
666.936	183.359
669.585	182.283
672.200	181.586
674.816	181.366
677.489	180.957
680.083	180.343
682.755	180.217
685.369	180.352
687.962	179.986
690.634	179.587
693.376	179.118
696.046	179.220
698.719	179.292
701.391	178.696
704.004	177.447
706.673	175.875
709.323	173.561
711.939	172.621
714.554	169.967
717.147	168.054
719.814	166.812
722.428	165.911
725.078	164.259
727.694	163.461
730.309	163.002
732.957	162.463
735.632	162.336
738.246	162.013
740.861	162.500
743.511	161.293
746.124	159.991
748.802	158.004
751.474	156.756
754.144	155.686
756.758	154.331
759.352	152.618
762.023	150.879
764.638	148.584
767.232	147.084
769.905	144.500
772.576	142.619
775.190	141.147
777.859	140.230
780.452	139.616
783.067	141.367
785.661	141.952
788.333	142.943
791.006	144.441
793.677	145.099
796.349	146.515
799.021	146.398
801.636	146.069
804.435	145.509
807.048	144.820
809.640	144.062
812.312	143.387
814.927	142.438
817.519	141.320
820.189	140.478
822.804	139.682
825.397	138.527
828.011	136.211
830.604	133.982

833.272	132.179
835.887	129.988
838.537	129.839
841.153	128.974
843.765	127.315
846.438	125.036
849.088	122.921
851.702	120.883
854.315	118.550
856.986	117.190
859.656	116.269
862.335	115.138
864.983	113.867
867.599	113.438
870.213	111.194
872.861	109.774
875.552	109.224
878.222	108.545
880.836	109.166
883.429	106.975
886.042	105.347
888.710	103.282
891.360	101.436
893.975	99.498
896.588	100.110
899.238	99.235
901.855	97.252
904.526	95.509
907.140	92.961
909.789	91.615
912.403	90.030
917.758	88.765
923.098	89.377
928.306	89.975
933.587	92.481
938.849	93.528
944.134	90.984
954.680	86.460
959.967	84.275
965.174	82.785
970.382	81.951
975.709	82.155
980.975	82.157
986.203	81.492
996.750	77.633
1002.090	73.991
1007.370	74.014
1012.648	74.171
1025.799	75.604
1031.149	75.945
1036.429	75.704
1041.687	72.546
1046.907	69.705
1052.186	65.971
1057.518	60.805
1062.796	58.738
1068.055	58.329
1073.280	57.720
1078.538	59.034
1083.762	61.015
1089.107	61.249
1094.364	59.109
1099.585	54.895
1104.864	51.004
1110.142	47.685
1115.474	45.548

1120.698	47.959
1125.957	46.999
1131.241	47.106
1136.499	50.121
1141.853	53.607
1147.077	55.784
1152.337	52.231
1157.616	47.310
1162.897	46.946
1168.179	44.714
1173.513	42.272
1178.772	40.242
1184.056	39.348
1189.282	39.679
1199.756	43.575
1205.038	42.788
1210.297	36.491
1215.518	32.145
1220.856	31.948
1226.134	31.035
1231.337	27.821
1236.597	26.934
1241.880	26.704
1255.106	32.282
1260.388	35.521
1278.802	37.034
1284.026	35.551
1289.231	34.686
1294.491	32.162
1299.776	28.506
1305.058	29.774
1307.671	28.031
1310.404	27.790
1313.016	27.530
1315.663	26.644
1318.275	24.993
1320.888	25.120
1323.557	24.256
1326.224	24.363
1328.835	25.744
1331.505	28.699
1334.117	28.309
1336.764	28.248
1339.453	27.273
1342.065	25.106
1344.713	23.637
1347.325	21.117
1349.938	19.048
1352.611	16.929
1355.279	15.536
1357.893	16.210
1360.485	17.426
1363.097	17.249
1365.745	18.359
1368.487	19.239
1371.100	18.570
1373.713	19.100
1376.383	18.891
1379.052	18.019
1381.718	17.822
1384.331	18.976
1387.000	22.009
1389.613	22.740
1392.261	24.490
1394.950	25.255
1397.620	25.938

1400.232	25.192
1402.878	25.647
1405.490	24.644
1408.102	23.246
0 NUMBER OF CONSTANT FUNCTIONS = 0	
0 0 NORM OF RESIDUAL = 0.6945794e+03	
NU = 0.1000000e+01	
0 ITERATION 1 NONLINEAR PARAMETERS	
0 0.1601724e+01 0.3664138e-01 0.4109866e-02	
0 1 NORM OF RESIDUAL = 0.1622322e+03	
NU = 0.5000000e+00	
NORM(DELTA-ALF) / NORM(ALF) = 0.735e-02	
0 ITERATION 2 NONLINEAR PARAMETERS	
0 0.1594719e+01 0.4457335e-01 0.4002702e-02	
0 1 NORM OF RESIDUAL = 0.9674819e+02	
NU = 0.2500000e+00	
NORM(DELTA-ALF) / NORM(ALF) = 0.663e-02	
0 ITERATION 3 NONLINEAR PARAMETERS	
0 0.1596320e+01 0.4828995e-01 0.3928502e-02	
0 1 NORM OF RESIDUAL = 0.9298198e+02	
NU = 0.1250000e+00	
NORM(DELTA-ALF) / NORM(ALF) = 0.253e-02	
0 ITERATION 4 NONLINEAR PARAMETERS	
0 0.1613556e+01 0.4985469e-01 0.3914612e-02	
0 1 NORM OF RESIDUAL = 0.9289213e+02	
NU = 0.6250000e-01	
NORM(DELTA-ALF) / NORM(ALF) = 0.107e-01	
0 ITERATION 5 NONLINEAR PARAMETERS	
0 0.1663352e+01 0.5289702e-01 0.3897484e-02	
0 1 NORM OF RESIDUAL = 0.9289590e+02	
STEP RETRACTED, NU = 0.9375000e-01	
0 ITERATION 6 NONLINEAR PARAMETERS	
0 0.1636594e+01 0.5124610e-01 0.3907576e-02	
0 2 NORM OF RESIDUAL = 0.9289102e+02	
NU = 0.9375000e-01	
NORM(DELTA-ALF) / NORM(ALF) = 0.141e-01	
0 ITERATION 7 NONLINEAR PARAMETERS	
0 0.1674215e+01 0.5366816e-01 0.3892669e-02	
0 1 NORM OF RESIDUAL = 0.9289297e+02	
STEP RETRACTED, NU = 0.1406250e+00	
0 ITERATION 8 NONLINEAR PARAMETERS	
0 0.1653582e+01 0.5237304e-01 0.3900245e-02	
0 2 NORM OF RESIDUAL = 0.9289135e+02	
STEP RETRACTED, NU = 0.2109375e+00	
0 ITERATION 9 NONLINEAR PARAMETERS	
0 0.1644180e+01 0.5178155e-01 0.3903733e-02	
0 3 NORM OF RESIDUAL = 0.9289130e+02	
STEP RETRACTED, NU = 0.3164063e+00	
0 ITERATION 10 NONLINEAR PARAMETERS	
0 0.1639956e+01 0.5151327e-01 0.3905372e-02	
0 4 NORM OF RESIDUAL = 0.9289126e+02	
STEP RETRACTED, NU = 0.4746094e+00	
0 ITERATION 11 NONLINEAR PARAMETERS	
0 0.1638074e+01 0.5138938e-01 0.3906222e-02	
0 5 NORM OF RESIDUAL = 0.9289119e+02	
STEP RETRACTED, NU = 0.7119141e+00	
0 ITERATION 12 NONLINEAR PARAMETERS	
0 0.1637241e+01 0.5132898e-01 0.3906751e-02	
0 6 NORM OF RESIDUAL = 0.9289109e+02	
NU = 0.7119141e+00	
NORM(DELTA-ALF) / NORM(ALF) = 0.398e-03	
0 ITERATION 13 NONLINEAR PARAMETERS	
0 0.1637443e+01 0.5131336e-01 0.3907253e-02	
0 1 NORM OF RESIDUAL = 0.9289085e+02	
NU = 0.3559570e+00	

```

NORM(DELTA-ALF) / NORM(ALF) = 0.124e-03
0 ITERATION 14 NONLINEAR PARAMETERS
0 0.1637217e+01 0.5125649e-01 0.3908455e-02
0 1 NORM OF RESIDUAL = 0.9289066e+02
NU = 0.1779785e+00
NORM(DELTA-ALF) / NORM(ALF) = 0.142e-03
0 ITERATION 15 NONLINEAR PARAMETERS
0 0.1638332e+01 0.5130045e-01 0.3908949e-02
0 1 NORM OF RESIDUAL = 0.9289066e+02
NU = 0.8898926e-01
NORM(DELTA-ALF) / NORM(ALF) = 0.681e-03
0 ITERATION 16 NONLINEAR PARAMETERS
0 0.1663297e+01 0.5290327e-01 0.3898719e-02
0 1 NORM OF RESIDUAL = 0.9289106e+02
STEP RETRACTED, NU = 0.1334839e+00
0 ITERATION 17 NONLINEAR PARAMETERS
0 0.1649630e+01 0.5204870e-01 0.3903667e-02
0 2 NORM OF RESIDUAL = 0.9289069e+02
NU = 0.1334839e+00
NORM(DELTA-ALF) / NORM(ALF) = 0.686e-02
0 ITERATION 18 NONLINEAR PARAMETERS
0 0.1653957e+01 0.5235399e-01 0.3901368e-02
0 1 NORM OF RESIDUAL = 0.9289084e+02
STEP RETRACTED, NU = 0.2002258e+00
0 ITERATION 19 NONLINEAR PARAMETERS
0 0.1651561e+01 0.5220181e-01 0.3902244e-02
0 2 NORM OF RESIDUAL = 0.9289084e+02
STEP RETRACTED, NU = 0.3003387e+00
0 ITERATION 20 NONLINEAR PARAMETERS
0 0.1650480e+01 0.5213151e-01 0.3902683e-02
0 3 NORM OF RESIDUAL = 0.9289082e+02
STEP RETRACTED, NU = 0.4505081e+00
0 ITERATION 21 NONLINEAR PARAMETERS
0 0.1649999e+01 0.5209743e-01 0.3902954e-02
0 4 NORM OF RESIDUAL = 0.9289079e+02
STEP RETRACTED, NU = 0.6757622e+00
0 ITERATION 22 NONLINEAR PARAMETERS
0 0.1649787e+01 0.5207874e-01 0.3903175e-02
0 5 NORM OF RESIDUAL = 0.9289076e+02
NU = 0.6757622e+00
NORM(DELTA-ALF) / NORM(ALF) = 0.968e-04
0 ITERATION 23 NONLINEAR PARAMETERS
0 0.1650156e+01 0.5207729e-01 0.3903726e-02
0 1 NORM OF RESIDUAL = 0.9289066e+02
NU = 0.3378811e+00
NORM(DELTA-ALF) / NORM(ALF) = 0.223e-03
0 ITERATION 24 NONLINEAR PARAMETERS
0 0.1650193e+01 0.5200836e-01 0.3905514e-02
0 1 NORM OF RESIDUAL = 0.9289081e+02
STEP RETRACTED, NU = 0.5068216e+00
0 ITERATION 25 NONLINEAR PARAMETERS
0 0.1650198e+01 0.5202016e-01 0.3905200e-02
0 2 NORM OF RESIDUAL = 0.9289074e+02
NU = 0.5068216e+00
NORM(DELTA-ALF) / NORM(ALF) = 0.430e-04
0 ITERATION 26 NONLINEAR PARAMETERS
0 0.1650371e+01 0.5204088e-01 0.3904920e-02
0 1 NORM OF RESIDUAL = 0.9289070e+02
NU = 0.2534108e+00
NORM(DELTA-ALF) / NORM(ALF) = 0.105e-03
0 ITERATION 27 NONLINEAR PARAMETERS
0 0.1652047e+01 0.5216982e-01 0.3903733e-02
0 1 NORM OF RESIDUAL = 0.9289064e+02
NU = 0.1267054e+00
NORM(DELTA-ALF) / NORM(ALF) = 0.102e-02
0 ITERATION 28 NONLINEAR PARAMETERS

```

```

0 0.1664336e+01 0.5295119e-01 0.3899315e-02
0 1 NORM OF RESIDUAL = 0.9289064e+02
  NU = 0.6335270e-01
  NORM(DELTA-ALF) / NORM(ALF) = 0.740e-02
0 ITERATION 29 NONLINEAR PARAMETERS
0 0.1709641e+01 0.5593425e-01 0.3881342e-02
0 1 NORM OF RESIDUAL = 0.9289444e+02
  STEP RETRACTED, NU = 0.9502906e-01
0 ITERATION 30 NONLINEAR PARAMETERS
0 0.1685012e+01 0.5436086e-01 0.3889965e-02
0 2 NORM OF RESIDUAL = 0.9289119e+02
  STEP RETRACTED, NU = 0.1425436e+00
0 ITERATION 31 NONLINEAR PARAMETERS
0 0.1673604e+01 0.5363090e-01 0.3893991e-02
0 3 NORM OF RESIDUAL = 0.9289106e+02
  STEP RETRACTED, NU = 0.2138154e+00
0 ITERATION 32 NONLINEAR PARAMETERS
0 0.1668441e+01 0.5329797e-01 0.3895881e-02
0 4 NORM OF RESIDUAL = 0.9289103e+02
  STEP RETRACTED, NU = 0.3207231e+00
0 ITERATION 33 NONLINEAR PARAMETERS
0 0.1666131e+01 0.5314415e-01 0.3896856e-02
0 5 NORM OF RESIDUAL = 0.9289097e+02
  STEP RETRACTED, NU = 0.4810846e+00
0 ITERATION 34 NONLINEAR PARAMETERS
0 0.1665108e+01 0.5306783e-01 0.3897506e-02
0 6 NORM OF RESIDUAL = 0.9289088e+02
  STEP RETRACTED, NU = 0.7216269e+00
0 ITERATION 35 NONLINEAR PARAMETERS
0 0.1664663e+01 0.5302400e-01 0.3898071e-02
0 7 NORM OF RESIDUAL = 0.9289078e+02
  STEP RETRACTED, NU = 0.1082440e+01
0 ITERATION 36 NONLINEAR PARAMETERS
0 0.1664473e+01 0.5299581e-01 0.3898564e-02
0 8 NORM OF RESIDUAL = 0.9289071e+02
  NU = 0.1082440e+01
  NORM(DELTA-ALF) / NORM(ALF) = 0.864e-04
0 ITERATION 37 NONLINEAR PARAMETERS
0 0.1664408e+01 0.5296275e-01 0.3899089e-02
0 1 NORM OF RESIDUAL = 0.9289064e+02
  NU = 0.5412202e+00
  NORM(DELTA-ALF) / NORM(ALF) = 0.436e-04
0 ITERATION 38 NONLINEAR PARAMETERS
0 0.1664089e+01 0.5290563e-01 0.3900271e-02
0 1 NORM OF RESIDUAL = 0.9289072e+02
  NU = 0.2706101e+00
  NORM(DELTA-ALF) / NORM(ALF) = 0.195e-03
0 ITERATION 39 NONLINEAR PARAMETERS
0 0.1664677e+01 0.5303803e-01 0.3897548e-02
0 1 NORM OF RESIDUAL = 0.9289087e+02
  STEP RETRACTED, NU = 0.4059151e+00
0 ITERATION 40 NONLINEAR PARAMETERS
0 0.1664313e+01 0.5300315e-01 0.3897986e-02
0 2 NORM OF RESIDUAL = 0.9289078e+02
0 PROBLEM TERMINATED FOR EXCESSIVE ITERATIONS

```

0'-----'

0 LINEAR PARAMETERS

0.1336236e+06

0 NONLINEAR PARAMETERS

0.1664089e+01 0.5290563e-01 0.3900271e-02

0 NORM OF RESIDUAL = 0.9289072e+02 EXPECTED ERROR OF OBSERVATIONS = 0.4932102  
 ESTIMATED VARIANCE OF OBSERVATIONS = 0.2765604e+02

WARNING -- EXPECTED ERROR OF OBSERVATIONS IS NOT ZERO. COVARIANCE MATRIX N

0	time	actual	calc	comp#1	comp#2
	38.3827	1.8235	-19.6515	-19.6515	
	43.7097	1.8485	-19.4165	-19.4165	
	48.9346	1.8990	-18.8172	-18.8172	
	54.1380	2.0546	-17.8456	-17.8456	
	59.4145	2.3619	-16.4626	-16.4626	
	64.6751	2.8230	-14.7231	-14.7231	
	69.9542	3.3934	-12.5847	-12.5847	
	75.2166	4.1699	-10.0791	-10.0791	
	80.4402	5.2062	-7.2663	-7.2663	
	85.7262	6.4545	-4.0410	-4.0410	
	90.9285	7.9373	-0.5443	-0.5443	
	96.1907	9.7157	3.2686	3.2686	
	101.5460	11.9302	7.4539	7.4539	
	106.8276	14.5660	11.8324	11.8324	
	112.1647	17.5365	16.4919	16.4919	
	117.4472	20.8742	21.3063	21.3063	
	122.6511	24.5239	26.2550	26.2550	
	127.9887	28.6451	31.5493	31.5493	
	133.1932	33.1190	36.8047	36.8047	
	138.4546	38.0416	42.1726	42.1726	
	143.7419	43.1900	47.6998	47.6998	
	149.0213	48.5530	53.3131	53.3131	
	154.3692	54.1679	58.9761	58.9761	
	159.5709	60.1808	64.6133	64.6133	
	164.8315	66.2116	70.2242	70.2242	
	167.4629	69.2158	73.0212	73.0212	
	170.1091	72.1615	75.8602	75.8602	
	172.7227	75.1012	78.6278	78.6278	
	175.3339	77.8774	81.3673	81.3673	
	177.9454	80.6284	84.0878	84.0878	
	180.5365	83.4144	86.8315	86.8315	
	183.2016	86.1787	89.6495	89.6495	
	185.8148	88.8456	92.2686	92.2686	
	188.4266	91.7140	94.9484	94.9484	
	191.0172	94.4462	97.5540	97.5540	
	193.6300	97.1135	100.1855	100.1855	
	196.3016	99.6587	102.8656	102.8656	
	198.9501	102.2227	105.4882	105.4882	
	201.5626	104.7279	108.0162	108.0162	
	204.1762	107.0649	110.5140	110.5140	
	206.8465	109.3806	113.0904	113.0904	
	209.5870	111.8670	115.6854	115.6854	
	212.1989	114.3932	117.9985	117.9985	
	214.8461	117.1770	120.4276	120.4276	
	217.4571	119.9880	122.6455	122.6455	
	220.0687	122.9847	125.0285	125.0285	
	222.6812	125.9543	127.3167	127.3167	
	225.3496	128.8129	129.5283	129.5283	
	228.0170	131.4396	131.7604	131.7604	
	230.6291	134.0652	133.9063	133.9063	
	233.2782	136.1555	136.0021	136.0021	
	235.8915	137.9003	137.9954	137.9954	
	238.5582	139.6857	140.2126	140.2126	
	241.1706	141.4489	142.1093	142.1093	
	243.7841	143.2968	143.9917	143.9917	
	246.4299	145.1695	145.9161	145.9161	
	249.0423	147.2435	147.7991	147.7991	
	251.7140	149.1434	149.5606	149.5606	
	254.3248	150.9403	151.3486	151.3486	
	256.9362	152.7013	153.1387	153.1387	

259.5341	154.2151	154.7001	154.7001
262.2082	155.6101	156.1596	156.1596
264.8599	157.0810	157.8764	157.8764
267.5418	158.3104	159.2651	159.2651
270.1587	159.5834	160.7646	160.7646
272.8069	161.2017	162.1602	162.1602
275.4217	162.5199	163.5924	163.5924
278.0356	163.8914	164.9672	164.9672
280.7036	165.6580	166.3875	166.3875
283.3752	167.3184	167.5735	167.5735
286.0474	169.0554	168.7519	168.7519
288.6603	169.8702	169.7838	169.7838
291.2527	170.4694	170.9051	170.9051
293.9225	170.8903	172.1285	172.1285
296.5356	171.4725	173.0262	173.0262
299.2052	171.9365	173.9401	173.9401
301.8777	172.9412	174.9304	174.9304
304.5491	174.2807	175.8568	175.8568
307.2192	175.4018	176.7502	176.7502
309.8927	176.4825	177.6919	177.6919
312.5641	177.9602	178.3747	178.3747
315.2347	179.9525	178.9825	178.9825
317.8487	181.3936	179.6428	179.6428
320.4422	182.9913	180.2796	180.2796
323.1849	184.4306	180.8622	180.8622
325.8572	185.6468	181.2784	181.2784
328.5082	186.9301	181.8872	181.8872
331.1227	187.4693	182.5038	182.5038
333.7381	187.7723	182.6564	182.6564
336.4076	188.3262	183.1446	183.1446
339.0786	188.8056	183.8735	183.8735
341.7497	188.8801	184.0369	184.0369
344.4211	188.6776	184.2899	184.2899
347.0926	188.3654	184.4442	184.4442
349.7066	187.6011	184.6327	184.6327
352.3751	187.0695	184.8844	184.8844
355.0261	186.7095	185.0851	185.0851
357.6387	187.0170	185.2810	185.2810
360.2516	186.8762	185.4096	185.4096
362.9214	186.7531	185.2772	185.2772
365.5952	186.5157	185.2939	185.2939
368.2656	186.2435	185.2267	185.2267
370.9357	186.8235	185.1730	185.1730
373.6066	187.2187	185.0812	185.0812
376.2219	187.6319	184.9059	184.9059
378.9357	188.2657	184.8094	184.8094
381.5495	189.2887	184.7125	184.7125
384.1636	190.4552	184.3968	184.3968
386.8320	190.9889	184.2835	184.2835
389.5024	191.3587	183.8231	183.8231
392.1751	191.3674	183.6956	183.6956
394.8444	190.7521	183.4767	183.4767
397.4584	189.2618	182.8467	182.8467
400.0530	189.0318	182.4107	182.4107
402.6671	186.9921	182.5278	182.5278
405.2600	185.3042	181.6877	181.6877
407.9287	184.1964	181.4369	181.4369
410.5435	183.3589	180.7336	180.7336
413.1922	182.2827	180.0509	180.0509
415.8079	181.5858	179.9125	179.9125
418.4235	181.3664	179.4642	179.4642
421.0967	180.9570	178.6277	178.6277
423.6902	180.3430	178.0924	178.0924
426.3629	180.2167	177.6105	177.6105
428.9768	180.3516	177.3008	177.3008
431.5696	179.9862	176.3284	176.3284

434.2417	179.5872	175.6392	175.6392
436.9833	179.1179	175.0811	175.0811
439.6537	179.2202	174.1795	174.1795
442.3262	179.2919	174.0948	174.0948
444.9981	178.6962	172.9648	172.9648
447.6121	177.4470	172.6150	172.6150
450.2809	175.8752	171.7519	171.7519
452.9309	173.5610	170.9424	170.9424
455.5461	172.6212	170.3399	170.3399
458.1612	169.9674	169.5974	169.5974
460.7546	168.0538	168.8795	168.8795
463.4219	166.8122	168.3873	168.3873
466.0357	165.9114	167.1640	167.1640
468.6859	164.2587	166.6424	166.6424
471.3017	163.4609	165.4285	165.4285
473.9169	163.0024	164.9401	164.9401
476.5649	162.4626	163.9931	163.9931
479.2391	162.3363	163.2228	163.2228
481.8540	162.0127	162.2241	162.2241
484.4689	162.5000	161.2600	161.2600
487.1183	161.2932	161.3127	161.3127
489.7318	159.9908	159.7881	159.7881
492.4101	158.0041	159.2700	159.2700
495.0820	156.7562	158.1557	158.1557
497.7520	155.6862	157.1763	157.1763
500.3656	154.3313	156.5488	156.5488
502.9599	152.6177	156.2839	156.2839
505.6307	150.8792	155.0039	155.0039
508.2452	148.5842	154.0197	154.0197
510.8397	147.0839	153.8511	153.8511
513.5129	144.5001	152.3297	152.3297
516.1835	142.6186	151.5382	151.5382
518.7975	141.1468	149.9920	149.9920
521.4670	140.2305	150.1364	150.1364
524.0592	139.6164	148.2687	148.2687
526.6741	141.3674	147.8773	147.8773
529.2686	141.9524	146.9919	146.9919
531.9405	142.9428	145.7171	145.7171
534.6138	144.4409	144.4457	144.4457
537.2843	145.0994	143.7948	143.7948
539.9564	146.5152	142.7938	142.7938
542.6287	146.3978	141.5581	141.5581
545.2435	146.0686	141.6913	141.6913
548.0423	145.5095	140.5435	140.5435
550.6554	144.8197	138.9692	138.9692
553.2472	144.0618	138.5317	138.5317
555.9199	143.3865	137.4518	137.4518
558.5341	142.4381	136.3805	136.3805
561.1271	141.3198	135.3958	135.3958
563.7967	140.4777	134.1985	134.1985
566.4114	139.6817	133.5657	133.5657
569.0044	138.5271	132.8240	132.8240
571.6184	136.2106	131.2397	131.2397
574.2120	133.9824	130.6805	130.6805
576.8797	132.1792	129.4308	129.4308
579.4944	129.9878	128.6840	128.6840
582.1442	129.8393	128.0924	128.0924
584.7602	128.9742	127.1613	127.1613
587.3726	127.3148	126.1870	126.1870
590.0454	125.0356	124.7999	124.7999
592.6954	122.9208	123.5807	123.5807
595.3097	120.8830	123.1119	123.1119
597.9228	118.5498	121.5194	121.5194
600.5935	117.1897	120.7794	120.7794
603.2637	116.2688	120.0666	120.0666
605.9422	115.1381	118.7771	118.7771

608.5908	113.8665	117.3811	117.3811
611.2061	113.4384	117.0150	117.0150
613.8202	111.1937	116.4186	116.4186
616.4685	109.7738	114.9616	114.9616
619.1598	109.2243	113.6988	113.6988
621.8294	108.5452	113.2048	113.2048
624.4438	109.1664	112.1189	112.1189
627.0366	106.9753	111.2646	111.2646
629.6500	105.3465	111.0712	111.0712
632.3177	103.2818	108.9701	108.9701
634.9674	101.4356	109.5511	109.5511
637.5823	99.4982	107.9271	107.9271
640.1961	100.1102	107.1721	107.1721
642.8460	99.2354	105.8094	105.8094
645.4629	97.2518	105.5612	105.5612
648.1340	95.5088	104.5390	104.5390
650.7472	92.9610	104.1234	104.1234
653.3967	91.6147	102.8556	102.8556
656.0107	90.0298	101.6042	101.6042
661.3652	88.7645	100.4630	100.4630
666.7053	89.3768	98.3606	98.3606
671.9135	89.9745	97.0109	97.0109
677.1944	92.4808	94.7621	94.7621
682.4569	93.5277	93.5596	93.5596
687.7413	90.9837	91.8691	91.8691
698.2877	86.4601	89.7127	89.7127
703.5747	84.2749	88.9175	88.9175
708.7817	82.7852	86.4864	86.4864
713.9892	81.9508	84.3947	84.3947
719.3165	82.1551	82.8624	82.8624
724.5826	82.1571	81.3761	81.3761
729.8104	81.4923	79.8106	79.8106
740.3575	77.6327	77.6827	77.6827
745.6976	73.9912	76.2762	76.2762
750.9776	74.0136	74.6502	74.6502
756.2556	74.1712	73.3995	73.3995
769.4066	75.6037	69.1196	69.1196
774.7566	75.9449	68.0986	68.0986
780.0366	75.7037	67.3316	67.3316
785.2946	72.5462	67.1097	67.1097
790.5146	69.7054	64.3117	64.3117
795.7936	65.9712	63.2520	63.2520
801.1255	60.8050	62.3054	62.3054
806.4036	58.7375	60.7731	60.7731
811.6627	58.3286	60.2851	60.2851
816.8876	57.7197	58.2631	58.2631
822.1456	59.0337	57.8806	57.8806
827.3696	61.0149	57.2286	57.2286
832.7147	61.2493	55.9266	55.9266
837.9716	59.1091	55.8183	55.8183
843.1926	54.8946	54.4666	54.4666
848.4716	51.0037	51.8594	51.8594
853.7496	47.6852	51.8046	51.8046
859.0816	45.5484	50.9492	50.9492
864.3056	47.9593	51.0342	51.0342
869.5646	46.9994	49.9051	49.9051
874.8486	47.1061	47.2613	47.2613
880.1066	50.1209	47.2773	47.2773
885.4606	53.6070	45.8223	45.8223
890.6846	55.7845	45.2751	45.2751
895.9446	52.2314	44.8765	44.8765
901.2236	47.3098	43.0840	43.0840
906.5046	46.9460	44.5544	44.5544
911.7866	44.7140	42.0871	42.0871
917.1205	42.2721	41.9071	41.9071
922.3796	40.2422	41.8761	41.8761

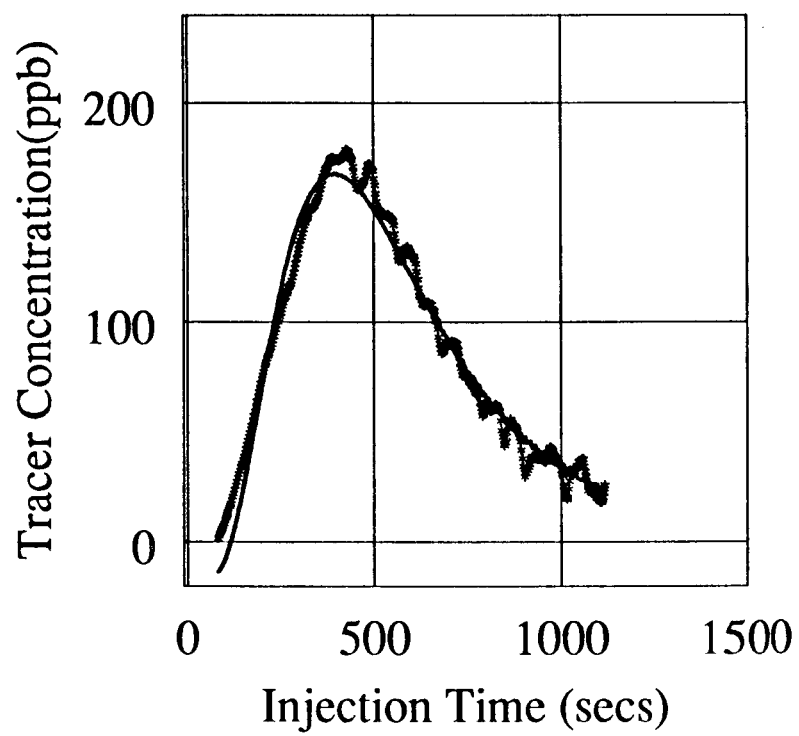
927.6636	39.3479	40.8414	40.8414
932.8896	39.6786	39.4891	39.4891
943.3636	43.5747	36.3387	36.3387
948.6456	42.7876	37.5535	37.5535
953.9046	36.4911	36.4697	36.4697
959.1255	32.1449	35.1967	35.1967
964.4636	31.9476	34.2865	34.2865
969.7416	31.0352	34.5297	34.5297
974.9446	27.8214	34.6187	34.6187
980.2046	26.9335	32.5561	32.5561
985.4876	26.7042	33.4520	33.4520
998.7136	32.2822	30.7285	30.7285
1003.9955	35.5211	32.6771	32.6771
1022.4096	37.0344	29.0456	29.0456
1027.6336	35.5505	26.2208	26.2208
1032.8386	34.6864	27.3412	27.3412
1038.0986	32.1623	26.7125	26.7125
1043.3836	28.5063	27.5415	27.5415
1048.6656	29.7738	26.3356	26.3356
1051.2786	28.0307	24.7366	24.7366
1054.0117	27.7896	27.5914	27.5914
1056.6236	27.5298	24.2819	24.2819
1059.2706	26.6440	24.0350	24.0350
1061.8826	24.9929	25.2757	25.2757
1064.4955	25.1205	24.0639	24.0639
1067.1646	24.2564	24.8365	24.8365
1069.8316	24.3626	24.2628	24.2628
1072.4426	25.7436	25.7201	25.7201
1075.1126	28.6990	24.9973	24.9973
1077.7245	28.3092	24.9385	24.9385
1080.3716	28.2476	24.1864	24.1864
1083.0606	27.2727	23.8891	23.8891
1085.6725	25.1065	22.9446	22.9446
1088.3206	23.6371	24.1602	24.1602
1090.9326	21.1173	22.4505	22.4505
1093.5456	19.0480	23.4984	23.4984
1096.2186	16.9293	22.0360	22.0360
1098.8867	15.5363	20.5462	20.5462
1101.5005	16.2103	20.8751	20.8751
1104.0926	17.4262	22.2364	22.2364
1106.7046	17.2487	22.3762	22.3762
1109.3526	18.3594	21.2054	21.2054
1112.0947	19.2389	20.3507	20.3507
1114.7076	18.5696	22.1273	22.1273
1117.3206	19.1002	20.5125	20.5125
1119.9907	18.8912	23.1070	23.1070
1122.6596	18.0187	20.7307	20.7307
1125.3256	17.8219	19.8335	19.8335
1127.9387	18.9757	21.7118	21.7118
1130.6076	22.0090	21.6331	21.6331
1133.2206	22.7401	20.0348	20.0348
1135.8686	24.4904	19.0220	19.0220
1138.5576	25.2554	19.6142	19.6142
1141.2276	25.9380	19.5932	19.5932
1143.8397	25.1919	20.1089	20.1089
1146.4857	25.6474	19.1089	19.1089
1149.0976	24.6439	18.2372	18.2372
1151.7097	23.2459	19.3862	19.3862

0 fraction dimensionless number arrival time  
 1.000 1.664 18.902

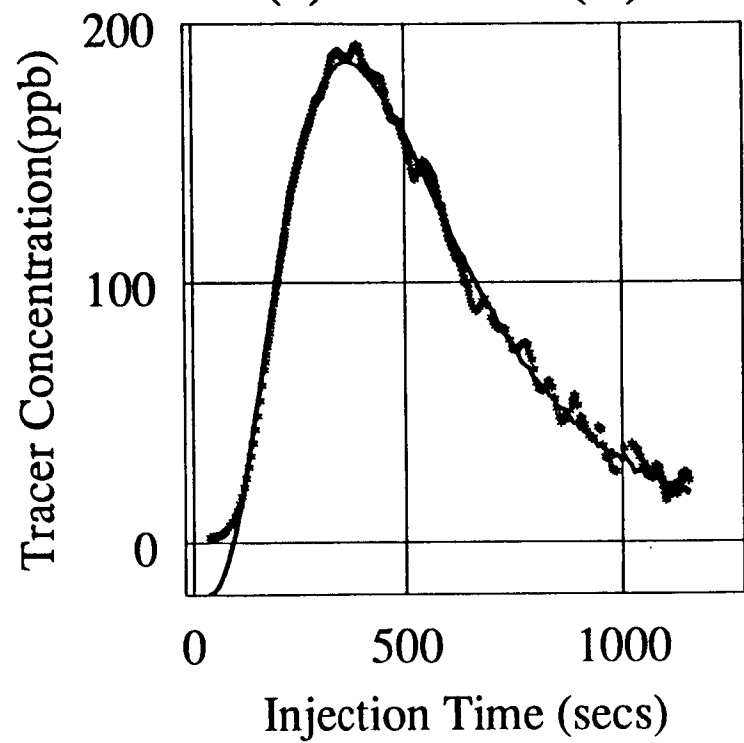
inlet A fit  
 \*\*\*\*\*

**APPENDIX D: Modified Matrix Diffusion Model Match of  
Laboratory "Step Up" Tracer Tests**

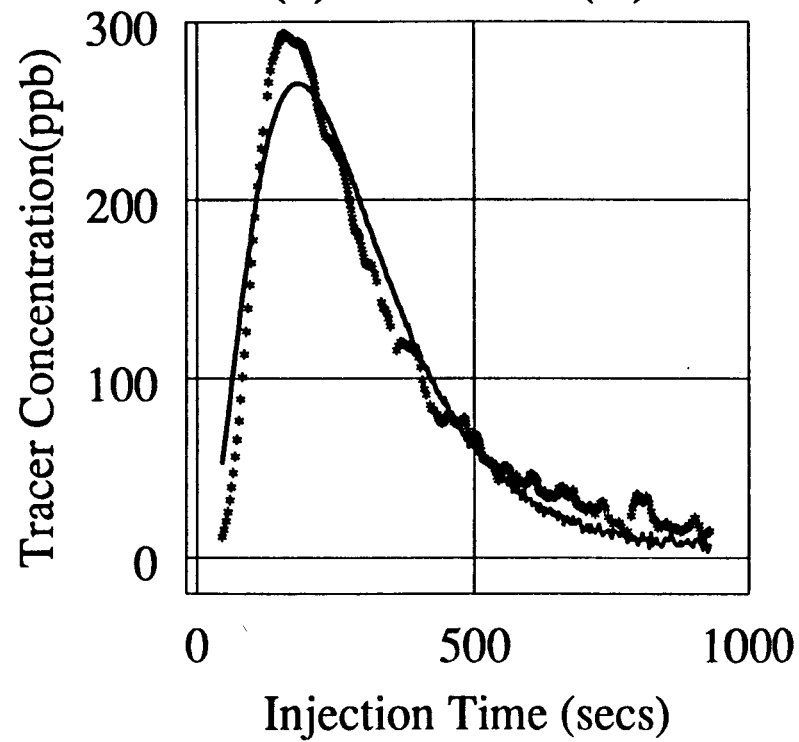
## Model Match(-) vs Data(\*) at 0.7 ml/min



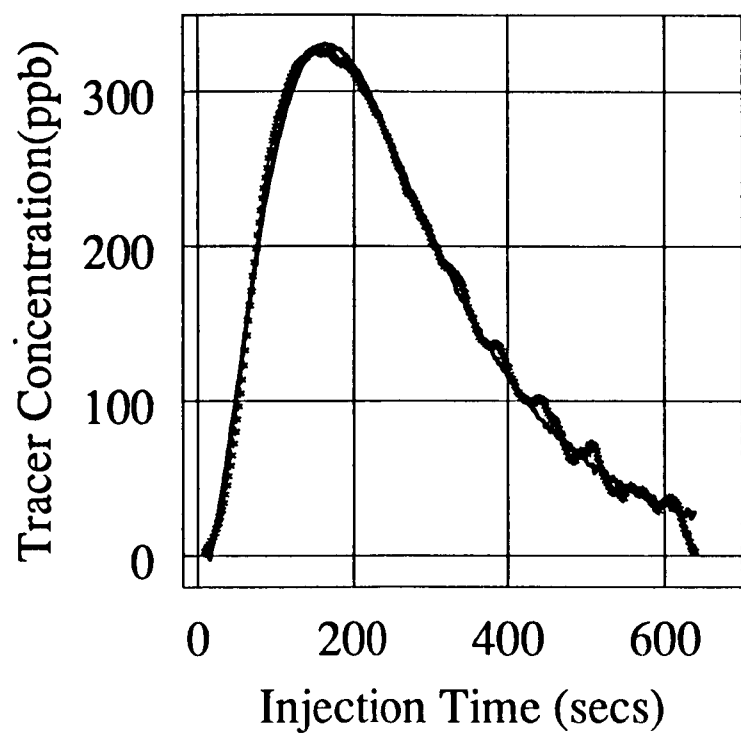
## Model Match(-) vs Data(\*) at 0.8 ml/min



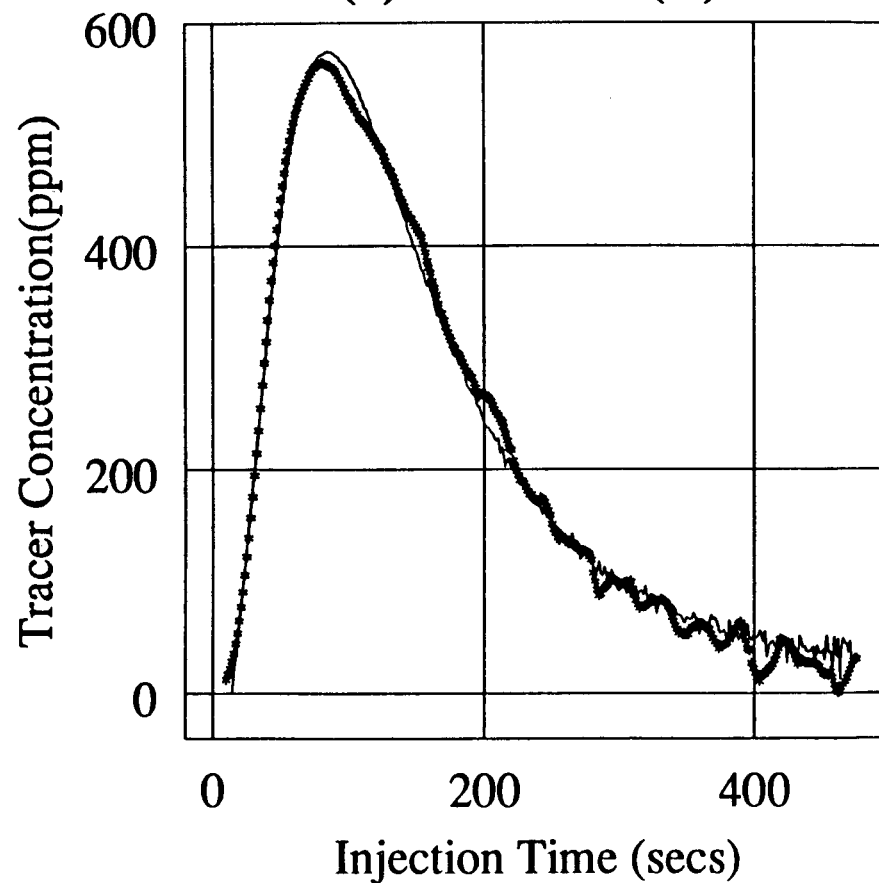
## Model Match(-) vs Data(\*) at 1.4 ml/min



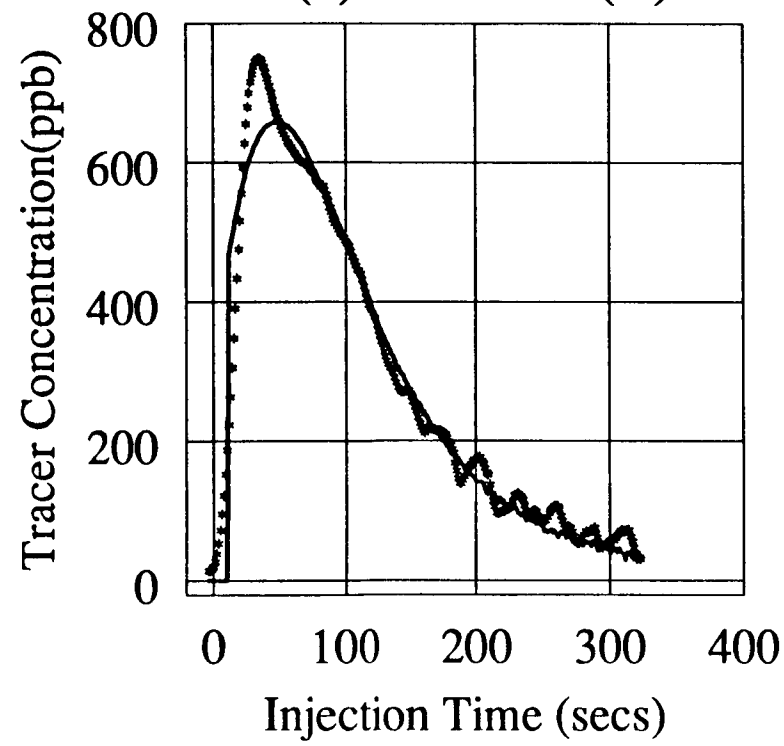
## Model Match(-) vs Data(\*) at 1.75 ml/min



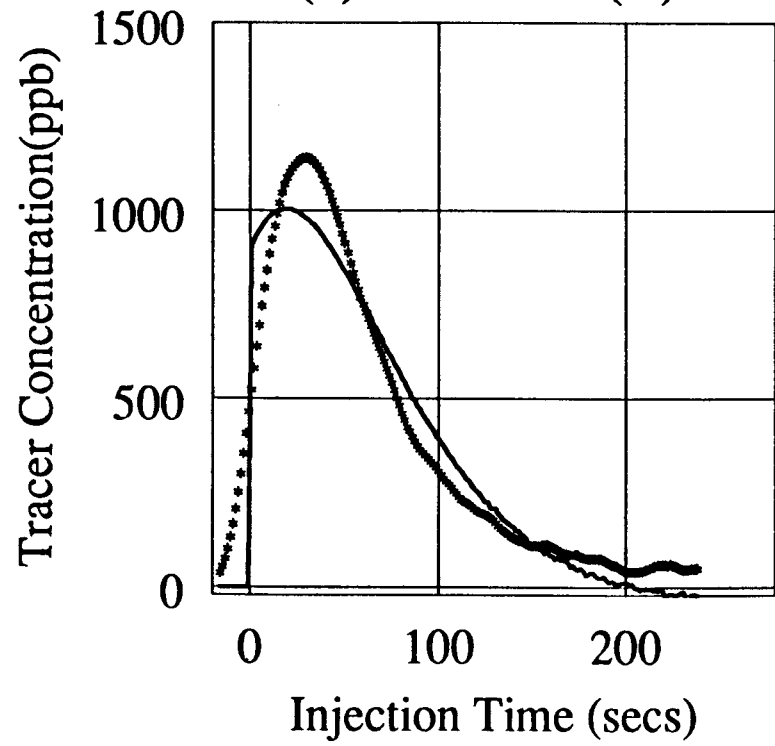
## Model Match(-) vs Data(\*) at 3.7 ml/min



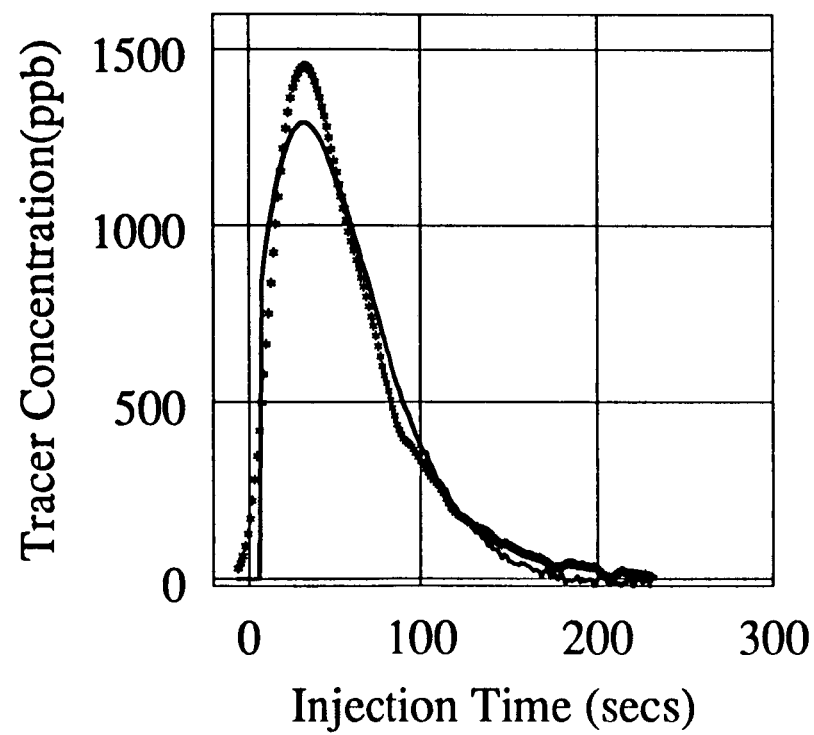
## Model Match(-) vs Data(\*) at 4 ml/min



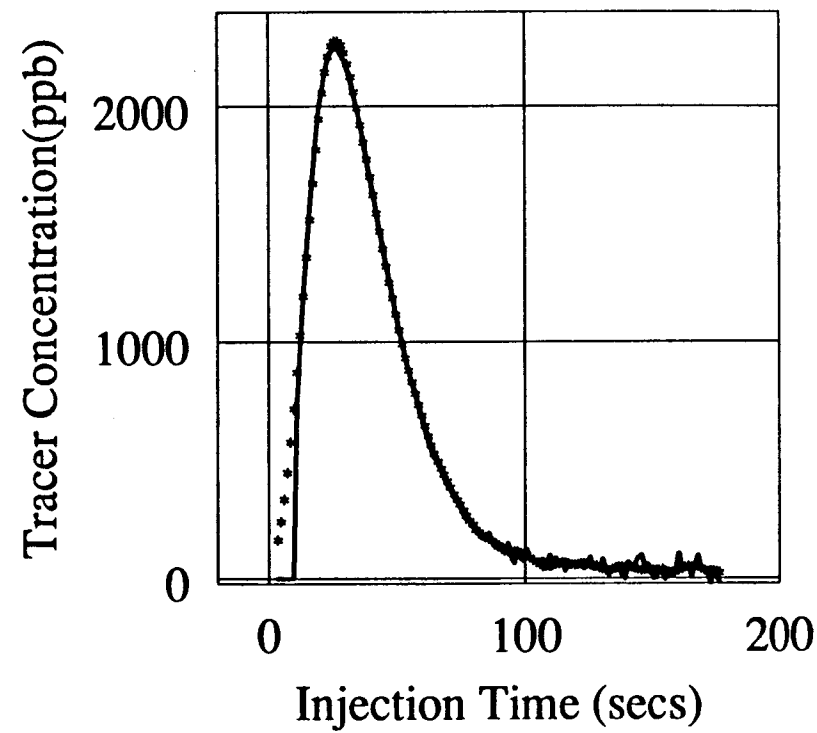
## Model Match(-) vs Data(\*) at 8.7 ml/min



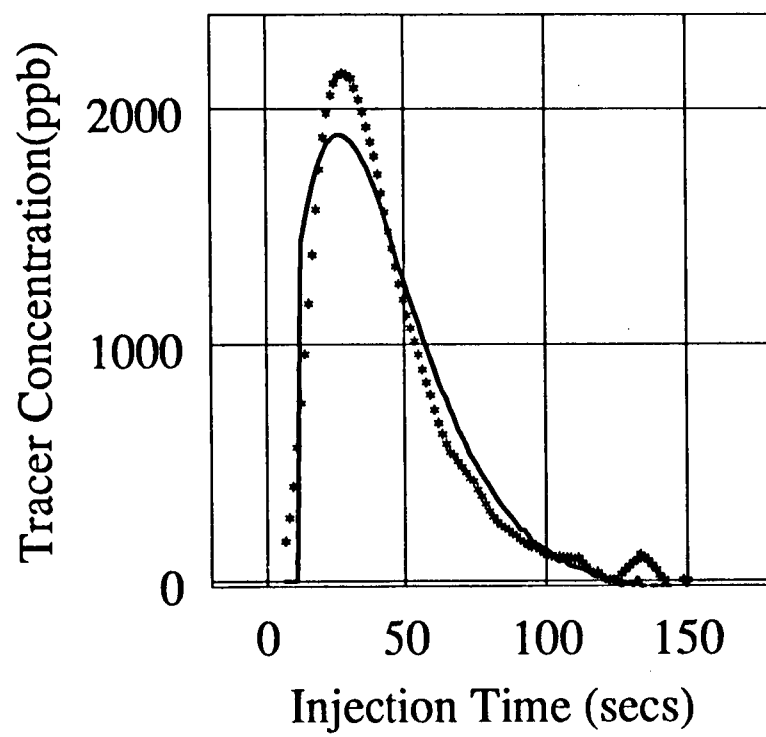
## Model Match(-) vs Data(\*) at 10 ml/min



## Model Match(-) vs Data(\*) at 16 ml/min



## Model Match(-) vs Data(\*) at 16.3 ml/min



## **APPENDIX E: Miscellaneous Computer Programs**

```
1000 REM PROGRAM FOR READING ELECTRODE RESPONSE
1010 DEF SEG=&HAFF0
1020 REM SET INTERVAL TIMER
1030 CO=65500!
1040 CZ=65500!
1043 CWRIT=0
1045 OPEN "C:INREFP.DAT" FOR OUTPUT AS #1
1046 OPEN "C:EXREFP.DAT" FOR OUTPUT AS #2
1047 OPEN "C:INLETP.DAT" FOR OUTPUT AS #3
1048 OPEN "C:EXITP.DAT" FOR OUTPUT AS #4
1050 OPEN "C:INREFN.DAT" FOR OUTPUT AS #5
1051 OPEN "C:EXREFN.DAT" FOR OUTPUT AS #6
1052 OPEN "C:INLETN.DAT" FOR OUTPUT AS #7
1053 OPEN "C:EXITN.DAT" FOR OUTPUT AS #8
1054 CWRIT=CWRIT+1
1055 IF CWRIT=5 GOTO 2100
1056 IF CWRIT=2 THEN PRINT CWRIT
1057 IF CWRIT=4 THEN PRINT CWRIT
1058 HZ=INT(CZ/256)
1060 LZ=CZ-(HZ*256)
1070 HO=INT(CO/256)
1080 LO=CO-(HO*256)
1090 POKE &HE0,1
1100 POKE &HC3,54
1110 POKE &HC0,LZ
1120 POKE &HC0,HZ
1130 POKE &HC3,116
1140 POKE &HC1,LO
1150 POKE &HC1,HO
1160 PT=0
1205 GOSUB 8010
1210 FOR I=1 TO 100:NEXT I
1225 GOSUB 8010
1300 BEG=TIME
1400 PT=PT+1
1401 GOSUB 8010
1500 BEG1=TIME
1600 ELAP=BEG1-BEG
1700 IF ELAP<.25 GOTO 1401
1800 IF PT>20 GOTO 1054
1900 GOSUB 4100
2000 GOTO 1400
2100 CLOSE
2200 END
4000 REM SUBROUTINE: SET VOLTAGE AND TAKE READINGS
4100 DEF SEG=&HAFF0
4200 HB1=15
4300 LB1=255
4310 POKE &H9A,0:REM SEL GAIN 1
4350 POKE &H9D,64
4400 POKE &H82,2:REM SEL SLOT2 CHAN 1
4500 POKE &H83,LB1
4600 POKE &H82,3
4700 POKE &H83,HB1
4750 POKE &H9D,1
4770 FOR I=1 TO 200:NEXT I
4800 GOSUB 9400
4900 IF(CWRIT=2)OR(CWRIT=4) THEN PRINT #1,
  USING "#####.##### ##.#####"; TIME,DVOLTS
5000 GOSUB 9600
5010 IF(CWRIT=2)OR(CWRIT=4) THEN PRINT #2,
  USING "#####.##### ##.#####"; TIME,DVOLTS
5020 GOSUB 6400
5030 IF(CWRIT=2)OR(CWRIT=4) THEN PRINT #3,
  USING "#####.##### ##.#####"; TIME,DVOLTS
5040 GOSUB 6600
```

```
5050 IF(CWRIT=2)OR(CWRIT=4) THEN PRINT #4,  
    USING "#####.###.###.#####"; TIME,DVOLTS  
5300 HB2=0  
5310 LB2=0  
5320 POKE &H82,2  
5330 POKE &H83,LB2  
5340 POKE &H82,3  
5350 POKE &H83,HB2  
5355 POKE &H9D,1  
5358 FOR I=1 TO 200:NEXT I  
5360 GOSUB 9400  
5370 IF(CWRIT=2)OR(CWRIT=4) THEN PRINT #5,  
    USING "#####.###.###.#####"; TIME,DVOLTS  
5375 GOSUB 9600  
5380 IF(CWRIT=2)OR(CWRIT=4) THEN PRINT #6,  
    USING "#####.###.###.#####"; TIME,DVOLTS  
5390 GOSUB 6400  
5400 IF(CWRIT=2)OR(CWRIT=4) THEN PRINT #7,  
    USING "#####.###.###.#####"; TIME,DVOLTS  
5410 GOSUB 6600  
5420 IF(CWRIT=2)OR(CWRIT=4) THEN PRINT #8,  
    USING "#####.###.###.#####"; TIME,DVOLTS  
5426 HB3=8  
5428 LB3=0  
5430 POKE &H82,2  
5440 POKE &H83,LB3  
5445 POKE &H82,3  
5450 POKE &H83,HB3  
5452 POKE &H9D,1  
5550 GOSUB 8010  
5560 BEG=TIME  
6000 RETURN  
6200 DEF SEG=&HAFF0  
6395 REM SUBROUTINE: READ INLET VOLTAGE  
6400 DEF SEG=&HAFF0  
6415 POKE &H9A,1:REM SEL GAIN 2  
6505 POKE &H80,1  
6510 POKE &H81,1:REM SEL SLT 1  
6520 POKE &H9B,255:REM STARTS A/D CONVER  
6522 IF PEEK(&H9B)<>127 GOTO 6522  
6525 DLOW=PEEK(&H80):REM READS LO BYTE  
6530 DHIGH=PEEK(&H81):REM READS HIGH BYTE  
6535 DHIGH=(DHIGH-240)*256:REM WTS HIGH BYTE  
6540 DRES=DLOW+DHIGH  
6545 DVOLTS=DRES*(5/4095)  
6550 RETURN  
6590 REM SUBROUTINE: READ OUTLET VOLTAGE  
6600 DEF SEG=&HAFF0  
6615 POKE &H80,2  
6620 POKE &H81,1:REM SEL SLOT 1  
6625 POKE &H9A,1:REM SETS GAIN 2  
6640 POKE &H9B,255  
6642 IF PEEK(&H9B)<>127 GOTO 6642  
6650 DLOW=PEEK(&H80)  
6660 DHIGH=PEEK(&H81)  
6670 DHIGH=(DHIGH-240)*256  
6680 DRES=DLOW+DHIGH  
6690 DVOLTS=DRES*(5/4095)  
6700 RETURN  
8000 REM SURROUTINE: READING THE INTERVAL TIMER  
8010 DEF SEG=&HAFF0  
8020 POKE &HC3,0  
8030 LZ=PEEK(&HC0)  
8040 HZ=PEEK(&HC0)  
8050 CCZ=LZ+(HZ*256)  
8060 POKE &HC3,64
```

```
8070 LO=PEEK(&HC1)
8080 HO=PEEK(&HC1)
8090 CCO=LO+(HO*256)
8100 CURRENTCOUNT#=(((CZ-CCZ)*CO)+(CO-CCO))/2
8110 TIME=CURRENTCOUNT#*.000001046#
8120 RETURN
9400 DEF SEG=&HAFF0
9415 POKE &H9A,1:REM SEL GAIN 2
9505 POKE &H80,3
9510 POKE &H81,1:REM SEL SLT 1
9520 POKE &H9B,255:REM STARTS A/D CONVER
9522 IF PEEK(&H9B)<>127 GOTO 9522
9525 DLOW=PEEK(&H80):REM READS LO BYTE
9530 DHIGH=PEEK(&H81):REM READS HIGH BYTE
9535 DHIGH=(DHIGH-240)*256:REM WTS HIGH BYTE
9540 DRES=DLOW+DHIGH
9545 DVOLTS=DRES*(5/4095)
9550 RETURN
9590 REM SUBROUTINE: READ OUTLET VOLTAGE
9600 DEF SEG=&HAFF0
9615 POKE &H80,4
9620 POKE &H81,1:REM SEL SLOT 1
9625 POKE &H9A,1:REM SETS GAIN 2
9640 POKE &H9B,255
9642 IF PEEK(&H9B)<>127 GOTO 9642
9650 DLOW=PEEK(&H80)
9660 DHIGH=PEEK(&H81)
9670 DHIGH=(DHIGH-240)*256
9680 DRES=DLOW+DHIGH
9690 DVOLTS=DRES*(5/4095)
9700 RETURN
```

```

program to differentiate continuous injection data into
slug test data using least squares method
dimension t(10000), x(10000)
read (5,100) np
read in number of points in file
and the number of points used for least
squares fit
read (5,100) nplus
nplot=np-2*nplus
write(6,100) nplot
do 3 i=1,np
read (5,101) t(i),x(i)
n3=2*nplus+1
do 1 i=nplus+1,np-nplus
sumx=0.0
sumy=0.0
sumxy=0.0
sumx2=0.0
do 2 j=i-nplus,i+nplus
sumx=sumx+t(j)
sumy=sumy+x(j)
sumxy=sumxy+x(j)*t(j)
sumx2=sumx2+t(j)*t(j)
continue
grad=-(sumx*sumy-n3*sumxy)/(sumx*sumx-n3*sumx2)
write (6,101) t(i),grad
continue
100 format(i5)
101 format(f10.4,x,f11.7)
-4-

```

```

Program to convert from electrode voltages to tracer concentration

```

```

read(5,103) ipt
write(6,103) ipt
do 6 k=1, ipt
read(5,102) t,x1
c=10.0** (4.024-x1)-9.75
6 write(6,102) t,c
102 format (i6)
102 format (f10.4,x,f11.7)
end

```

## **APPENDIX F: Complete Data Set for Test Number 11**

Entire data set for Run No. 11, November 6, 1986

Flowrate = 3.7cc/min Pressure Drop = 0.408 psi  
 Tracer Concentration = 102 ppm Step Up Cycle  
 Actual Test Start Time = 59.3 secs

Clock Time    Electrode    Tracer in    Equivalent  
 (seconds)    Voltage    Core Effluent Slug Test  
 (volts)    (ppm)    (ppm/sec)

16.8063	4.1575089	0.0151740	0.0000800
18.1735	4.1575089	0.0166443	-0.0000513
19.5406	4.1575089	0.0176342	-0.0001619
20.9080	4.1636138	0.0146735	-0.0002622
22.2721	4.1599512	0.0117314	-0.0003510
23.6601	4.1648359	0.0092464	-0.0004226
25.0271	4.1648359	0.0087560	-0.0004814
26.3934	4.1636138	0.0053347	-0.0005179
27.7600	4.1648359	0.0063130	-0.0005647
29.1272	4.1684980	0.0068020	-0.0005861
30.4973	4.1623931	0.0068001	-0.0005853
31.8637	4.1636138	0.0063111	-0.0005531
33.2522	4.1636138	0.0048208	-0.0004887
34.6185	4.1660562	0.0043710	-0.0004050
35.9855	4.1721611	0.0038719	-0.0003277
37.4170	4.1636138	0.0019307	-0.0002649
38.7841	4.1648359	0.0019288	-0.0002239
40.1732	4.1684980	0.0028803	-0.0001863
41.5396	4.1660562	0.0009641	-0.0001867
42.9061	4.1697192	0.0004556	-0.0001912
44.3477	4.1684980	0.0014539	-0.0002066
45.7145	4.1660562	0.0014596	-0.0002305
47.0814	4.1660562	0.0019240	-0.0002527
48.4488	4.1660562	0.0014378	-0.0003154
49.8165	4.1684980	0.0024107	-0.0003645
51.1846	4.1697192	0.0028899	-0.0004068
52.5707	4.1636138	0.0024192	-0.0004503
53.9372	4.1648359	0.0019222	-0.0004932
55.3030	4.1672769	0.0009527	-0.0004793
56.6698	4.1697192	-0.0009886	-0.0005001
58.0374	4.1721611	-0.0034063	-0.0005130
59.4077	4.1684980	-0.0053397	-0.0005033
60.7969	4.1709409	-0.0058275	-0.0004430
62.1639	4.1721611	-0.0096931	-0.0002918
63.5302	4.1709409	-0.0091869	-0.0000257
64.8968	4.1819291	-0.0092506	0.0004398
66.4142	4.1672769	-0.0086193	0.0011829
67.7842	4.1709409	-0.0096154	0.0022729
69.1541	4.1709409	-0.0058256	0.0038009
70.5242	4.1733818	-0.0082335	0.0058569
71.8933	4.1721611	-0.0077564	0.0085393
73.2625	4.1733818	-0.0073016	0.0119259
74.6858	4.1697192	-0.0028575	0.0162067
76.0558	4.1697192	0.0059072	0.0213947
77.4263	4.1623931	0.0191251	0.0275904

78.7957	4.1501832	0.0411468	0.0348346
80.1663	4.1404152	0.0741711	0.0433285
81.5549	4.1159959	0.1188998	0.0529421
82.9247	4.0915751	0.1779318	0.0639241
84.2950	4.0622711	0.2529412	0.0762564
85.6651	4.0231991	0.3468751	0.0898989
87.0351	3.9890110	0.4588909	0.1047354
88.4640	3.9389501	0.6013127	0.1207807
89.8342	3.8974359	0.7587447	0.1379174
91.2051	3.8473749	0.9451517	0.1559591
92.5747	3.7997561	1.1489518	0.1746171
93.9449	3.7509160	1.3936436	0.1938763
95.3155	3.7069600	1.6596735	0.2136417
96.7504	3.6459100	1.9736292	0.2339207
98.1207	3.6031749	2.3114529	0.2542504
99.4909	3.5543351	2.6846509	0.2746824
100.8620	3.5042739	3.0788414	0.2945090
102.2473	3.4627600	3.5135415	0.3142118
103.6650	3.4151411	3.9885652	0.3329909
105.0503	3.3760691	4.4759502	0.3511608
106.4137	3.3357761	4.9739547	0.3686733
107.7769	3.2967031	5.5065432	0.3848256
109.1631	3.2661779	6.0689902	0.4002737
110.6029	3.2222221	6.6872616	0.4149042
111.9650	3.1929181	7.2798247	0.4286213
113.3287	3.1575091	7.9130225	0.4413258
114.7130	3.1294260	8.5070095	0.4538881
116.0764	3.1013429	9.1756115	0.4650684
117.4404	3.0818069	9.8057308	0.4757837
118.8076	3.0427351	10.4792433	0.4855327
120.1940	3.0244200	11.1716032	0.4945955
121.5575	2.9963369	11.8123760	0.5032695
122.9213	2.9743590	12.5205660	0.5108534
124.3052	2.9682541	13.2483292	0.5175985
125.7956	2.9218559	14.0330725	0.5237576
127.1820	2.9084251	14.7552042	0.5295969
128.5462	2.8864470	15.5630245	0.5349529
129.9110	2.8705740	16.2581882	0.5390203
131.2971	2.8559220	17.0471287	0.5429287
132.7358	2.8302810	17.8195267	0.5465601
134.0997	2.8107450	18.5900021	0.5497385
135.4642	2.7985351	19.3937206	0.5533285
136.8290	2.7814410	20.1104488	0.5558663
138.2160	2.7667890	20.8679695	0.5584098
139.5805	2.7545791	21.6281548	0.5607560
141.0210	2.7338221	22.4595089	0.5619744
142.3845	2.7228329	23.2064648	0.5621282
143.7474	2.7057390	23.9373913	0.5640453
145.1325	2.6971920	24.7164078	0.5631891
146.4973	2.6886449	25.5231266	0.5622876
147.9418	2.6666670	26.3277302	0.5617395
149.3068	2.6544571	27.1873436	0.5612012
150.6720	2.6434679	27.9419460	0.5601251
152.0360	2.6288159	28.7532463	0.5588968

153.4223	2.6300371	29.5485039	0.5567831
154.8513	2.6056170	30.2817707	0.5543105
156.2163	2.5970700	30.9966316	0.5516585
157.6029	2.5934069	31.9069176	0.5487024
158.9680	2.5787549	32.4621201	0.5450063
160.3321	2.5689869	33.1965904	0.5411336
161.6963	2.5689869	34.0277977	0.5374206
163.0805	2.5494511	34.7906647	0.5332156
164.4452	2.5409040	35.4535141	0.5306333
165.8098	2.5323570	36.2345200	0.5290055
167.1953	2.5286939	36.9295845	0.5246505
168.5605	2.5225890	37.6482849	0.5214019
170.0012	2.5091579	38.3807411	0.5182681
171.3653	2.4993899	39.1024323	0.5145242
172.7298	2.4932849	39.7954369	0.5127546
174.1172	2.4884009	40.5111732	0.5111400
175.4809	2.4847381	41.2025261	0.5082256
176.9267	2.4713070	41.9040642	0.5060151
178.2922	2.4627600	42.6716652	0.5039353
179.6577	2.4590969	43.4772110	0.5006921
181.0236	2.4493289	43.8267441	0.4979700
182.3882	2.4444449	44.5721016	0.4952094
183.7748	2.4542129	45.3103371	0.4922138
185.2680	2.4261301	46.0187569	0.4892775
186.6545	2.4236879	46.7308540	0.4867835
188.0198	2.4188039	47.5979919	0.4848108
189.3852	2.4114780	48.1432571	0.4801459
190.7512	2.4139199	48.7796440	0.4758835
192.1345	2.4017100	49.4330177	0.4715013
193.4988	2.3956039	50.0283661	0.4680496
194.8638	2.3907199	50.6583366	0.4665695
196.2290	2.3858359	51.3224258	0.4614437
197.6161	2.3870580	51.9422569	0.4574807
199.0355	2.3736269	52.6170807	0.4530579
200.4239	2.3699639	53.2859039	0.4477556
201.7876	2.3638589	53.9782600	0.4419321
203.1515	2.3589749	54.3164330	0.4393954
204.5370	2.3589749	54.9712143	0.4352859
205.9000	2.3601961	55.5907631	0.4315856
207.3453	2.3443229	56.2321663	0.4284188
208.7101	2.3394389	56.8996582	0.4251587
210.0746	2.3357761	57.4438553	0.4238390
211.4380	2.3333340	58.0963097	0.4199675
212.8233	2.3394389	58.5960350	0.4168943
214.2516	2.3199029	59.1198845	0.4133633
215.6154	2.3211229	59.5830040	0.4107259
217.0015	2.3174601	60.2659760	0.4076176
218.3653	2.3162391	60.7477875	0.4008165
219.7298	2.3150189	61.3355103	0.3934437
221.1142	2.3028080	61.9418030	0.3864381
222.4774	2.3003671	62.5042419	0.3803550
223.8412	2.2967031	63.2541389	0.3755156
225.2269	2.2967031	63.5117531	0.3678637
226.5916	2.2893779	64.1301880	0.3621864

227.9563	2.2942619	64.5668793	0.3558511
229.3186	2.2796099	65.1189804	0.3478935
230.7051	2.2820511	65.4982681	0.3397265
232.0674	2.2783880	65.8688202	0.3391628
233.4314	2.2771671	66.2391968	0.3332739
234.8172	2.2820511	66.7301178	0.3268932
236.2401	2.2673991	67.2821426	0.3221210
237.6260	2.2661779	67.7831802	0.3177231
238.9891	2.2612939	67.9648743	0.3149710
240.3529	2.2612939	68.5016937	0.3103975
241.7386	2.2759471	68.9237976	0.3079519
243.2310	2.2503059	69.2770386	0.3044240
244.6165	2.2527471	69.7516022	0.3023368
245.9807	2.2515261	70.8095474	0.2996406
247.3453	2.2466421	70.7677689	0.2950883
248.7086	2.2429790	71.0479889	0.2912192
250.0955	2.2515261	71.5329056	0.2878646
251.5352	2.2442000	71.9170914	0.2852382
252.8998	2.2368741	72.1997223	0.2828719
254.2644	2.2356541	72.6032181	0.2816225
255.6288	2.2344320	73.0570526	0.2762232
257.0152	2.2393160	73.3463135	0.2722201
258.4556	2.2307701	73.7835846	0.2677104
259.8210	2.2283270	74.1559525	0.2642345
261.1863	2.2234430	74.4017258	0.2666882
262.5493	2.2234430	74.9071808	0.2667830
263.9354	2.2319901	75.2907944	0.2660675
265.3591	2.2161181	75.6475296	0.2646602
266.7461	2.2173381	75.9504623	0.2624951
268.1114	2.2136750	76.6793365	0.2600557
269.4766	2.2148960	76.5045776	0.2569215
270.8409	2.2112341	76.9804611	0.2532801
272.2270	2.2210021	77.3720779	0.2498048
273.6562	2.2039070	77.7873840	0.2473952
275.0209	2.2026861	78.0440140	0.2441671
276.4066	2.2039070	78.5757599	0.2417428
277.7722	2.2039070	78.9353943	0.2368542
279.1381	2.2063489	79.1134109	0.2308700
280.5000	2.1941390	79.3815079	0.2244951
281.8862	2.1978021	79.7941971	0.2183200
283.2511	2.1965809	80.0182953	0.2168260
284.6162	2.1929181	80.2001038	0.2072963
285.9803	2.2002439	80.6093063	0.2019395
287.3654	2.1892550	80.9820175	0.1974633
288.7311	2.1868131	81.2114410	0.1938195
290.0967	2.1868131	81.7187271	0.1895404
291.4617	2.1868131	81.6272430	0.1892596
292.8471	2.1868131	81.7651596	0.1869384
294.2123	2.1916969	81.9918747	0.1836542
295.6585	2.1831501	82.3375092	0.1799351
297.0244	2.1807079	82.6602402	0.1767890
298.3896	2.1782660	82.6061478	0.1771467
299.7557	2.1782660	83.1219635	0.1738061
301.1218	2.1929181	83.3980408	0.1716606

302.5795	2.1697190	83.6619339	0.1704840
303.9440	2.1733820	83.8935699	0.1703987
305.3083	2.1721611	84.3141174	0.1733260
306.6722	2.1721611	84.2664871	0.1723188
308.0567	2.1819291	84.5011368	0.1699571
309.4964	2.1709399	84.7089462	0.1661786
310.8603	2.1672771	84.8460846	0.1622870
312.2240	2.1672771	85.4690094	0.1582986
313.6099	2.1684980	85.4204941	0.1505205
314.9744	2.1660559	85.6159210	0.1457275
316.3375	2.1721611	85.8086929	0.1422189
317.7202	2.1623931	86.1546783	0.1382230
319.0846	2.1623931	86.3988876	0.1357896
320.4494	2.1599510	86.5452194	0.1399662
321.8121	2.1599510	86.7411728	0.1381622
323.1983	2.1684980	86.8394318	0.1366389
324.6204	2.1575091	86.9426270	0.1352107
326.0051	2.1599510	87.0439606	0.1328226
327.3693	2.1575091	87.1365662	0.1343361
328.7332	2.1575091	87.3325882	0.1331758
330.1200	2.1660559	87.5800552	0.1314086
331.5471	2.1526251	87.6892776	0.1295302
332.9098	2.1538460	87.9833374	0.1279731
334.2947	2.1550670	88.6345215	0.1272440
335.6592	2.1501830	88.4827271	0.1258071
337.0242	2.1501830	88.6817474	0.1260825
338.4094	2.1562879	88.8850021	0.1255498
339.8503	2.1489620	89.0440369	0.1242726
341.2153	2.1501830	89.1941071	0.1210917
342.5791	2.1465199	89.3411179	0.1179928
343.9435	2.1465199	89.4419479	0.1063074
345.3298	2.1526251	89.5948639	0.0989132
346.7703	2.1465199	89.6502075	0.0916440
348.1353	2.1465199	89.8032303	0.0863572
349.5007	2.1452990	89.9007874	0.0879206
350.8660	2.1428571	90.2042007	0.0911666
352.2518	2.1501830	90.3585587	0.0929132
353.6737	2.1391940	90.5177536	0.0948331
355.0591	2.1428571	90.5708389	0.0966070
356.4240	2.1416359	90.8233185	0.0991179
357.7889	2.1416359	90.0560379	0.1010378
359.1542	2.1440780	90.5124359	0.1006649
360.5412	2.1575091	90.7047119	0.0998190
362.0335	2.1318679	90.8995590	0.0984692
363.4183	2.1367519	91.2041321	0.0966555
364.7818	2.1379731	91.8074112	0.0968148
366.1471	2.1367519	91.7563477	0.0965769
367.5108	2.1428571	91.8593216	0.0979134
368.8951	2.1330891	91.9663239	0.0985153
370.2605	2.1343100	92.1753998	0.0972258
371.6248	2.1355309	92.2274628	0.0989631
372.9898	2.1318679	92.1763229	0.0913543
374.3766	2.1416359	92.2256241	0.0869057
375.8178	2.1343100	92.3880692	0.0821401

377.1831	2.1330891	92.4419937	0.0781718
378.5469	2.1318679	92.8036041	0.0752730
379.9125	2.1306469	92.6999512	0.0771906
381.3001	2.1330891	92.9620132	0.0761477
382.6646	2.1367519	92.9605713	0.0767929
384.0889	2.1269839	92.9644394	0.0784058
385.4757	2.1318679	93.2313232	0.0795958
386.8409	2.1306469	93.3314896	0.0834095
388.2062	2.1269839	93.4908447	0.0828756
389.5704	2.1343100	93.5437927	0.0820998
390.9445	2.1233211	93.7033997	0.0807551
392.3312	2.1306469	93.7590714	0.0808091
393.6957	2.1269839	93.8623428	0.0827317
395.0596	2.1257629	93.8095779	0.0819634
396.4237	2.1318679	94.0757446	0.0807566
397.8085	2.1245420	94.2921829	0.0790306
399.1731	2.1245420	94.2367706	0.0763944
400.5391	2.1221001	94.6653671	0.0742578
401.9236	2.1269839	94.5035629	0.0666492
403.2871	2.1221001	94.6656342	0.0640084
404.6496	2.1282051	94.6640625	0.0601258
406.0334	2.1208789	94.9897537	0.0563757
407.3976	2.1221001	95.0433960	0.0527756
408.7622	2.1196580	95.0970078	0.0553172
410.1261	2.1208789	94.9920197	0.0515832
411.5100	2.1269839	95.1502304	0.0514382
412.9541	2.1233211	95.2673645	0.0517085
414.3167	2.1184371	95.2629318	0.0514230
415.6812	2.1172161	94.7754593	0.0567330
417.0456	2.1208789	95.2624054	0.0583979
418.4310	2.1379731	95.2532272	0.0583979
419.9241	2.1123321	95.2785034	0.0578315
421.3103	2.1184371	95.3860245	0.0596745
422.6737	2.1172161	96.0722961	0.0611111
424.0359	2.1184371	95.6930847	0.0608353
425.4207	2.1221001	95.9645996	0.0604118
426.7837	2.1208789	95.9635849	0.0591781
428.1462	2.1123321	96.1243591	0.0577521
429.5309	2.1172161	96.4561539	0.0562613
430.8942	2.1147740	96.4001846	0.0525940
432.2580	2.1147740	96.2380981	0.0482069
433.6438	2.1221001	96.3457870	0.0456143
435.0823	2.1159949	96.4053116	0.0427289
436.4470	2.1147740	96.4596329	0.0387013
437.8116	2.1135530	96.3464279	0.0418936
439.1758	2.1135530	96.5654755	0.0409751
440.5610	2.1245420	96.4563675	0.0425408
441.9839	2.1111109	96.4571686	0.0428331
443.3701	2.1172161	96.5725327	0.0444113
444.7343	2.1135530	97.0036011	0.0481592
446.0989	2.1111109	96.6198883	0.0508310
447.4842	2.1147740	96.9485474	0.0528471
448.8491	2.1196580	97.0566406	0.0550925
450.2788	2.1098900	97.0076294	0.0575469

451.6637	2.1111109	97.1740646	0.0607068
453.0266	2.1123321	97.2781525	0.0622390
454.3897	2.1111109	97.3892059	0.0591159
455.7546	2.1172161	97.3888245	0.0535901
457.1370	2.1074481	97.5011902	0.0465391
458.5002	2.1111109	97.4998398	0.0390461
459.8650	2.1098900	97.5578537	0.0372939
461.2520	2.1111109	97.7788696	0.0263882
462.6149	2.1159949	97.8325500	0.0215427
463.9772	2.1025641	97.9412994	0.0173611
465.3633	2.1098900	98.1120911	0.0129929
466.7267	2.1074481	98.2216949	0.0102160
468.0905	2.1074481	97.6685715	0.0137084
469.4761	2.1135530	97.6677628	0.0158277
470.8416	2.1147740	97.6099548	0.0170381
472.2862	2.1098900	97.5639572	0.0190766
473.6507	2.1086690	97.7807693	0.0207204
475.0142	2.1086690	97.3364639	0.0227273
476.3788	2.1086690	97.6678696	0.0249677
477.7647	2.1245420	97.7142334	0.0293548
479.2575	2.1025641	97.7926254	0.0334539
480.6436	2.1074481	97.8494568	0.0389636
482.0065	2.1074481	98.4997177	0.0471503
483.3707	2.1074481	98.3332138	0.0466113
484.7354	2.1098900	98.3329391	0.0453068
486.1198	2.1062269	98.3895950	0.0450809
487.4852	2.1074481	98.4447479	0.0444517
488.8506	2.1062269	98.5011368	0.0436601
490.2366	2.1062269	98.3881760	0.0395151
491.5998	2.1086690	98.6125336	0.0372340
492.9636	2.1086690	98.5560303	0.0330350
494.3478	2.1025641	98.5573349	0.0290055
495.7118	2.1074481	98.7807083	0.0251444
497.0769	2.1062269	98.5007553	0.0300525
498.4418	2.1037850	98.5005951	0.0291918
499.8073	2.1147740	98.7787399	0.0282004
501.1965	2.1025641	98.8949966	0.0266780
502.5597	2.1013429	98.7806549	0.0261468
503.9223	2.1037850	99.0078735	0.0267881
505.3078	2.1062269	99.0054626	0.0259885
506.6723	2.1098900	98.8909454	0.0262297
508.1011	2.1025641	98.9524612	0.0261506
509.4866	2.1037850	99.0084229	0.0244970
510.8499	2.1025641	99.3422775	0.0232968
512.2125	2.1050060	99.0055771	0.0194314
513.5822	2.1025641	99.0612946	0.0160975
514.9509	2.1098900	99.0044250	0.0153886
516.3397	2.1025641	99.1178665	0.0163454
517.7101	2.1037850	99.2308350	0.0152995
519.0805	2.1025641	99.2859039	0.0184149
520.4510	2.1001220	99.2305603	0.0130208
521.8194	2.1086690	99.3425522	0.0071671
523.2425	2.1037850	99.2289658	0.0023438
524.6131	2.1013429	99.1180878	0.

525.9998	2.1050060	99.1720505	0.0013605
527.3655	2.1025641	99.2862930	0.0045266
528.7310	2.1074481	99.3358383	0.0071668
530.1786	2.1013429	99.4590225	0.0096749
531.5437	2.1001220	99.4003830	0.0126868
532.9090	2.1025641	99.6808929	0.0166538
534.2738	2.1037850	98.8396454	0.0205603
535.6402	2.1013429	98.8966370	0.0241770
537.0271	2.1196580	98.9430923	0.0275991
538.5213	2.0989010	99.1349945	0.0298354
539.8885	2.1013429	99.1843567	0.0296883
541.2771	2.1001220	99.7350540	0.0339300
542.6436	2.1001220	99.6816635	0.0328947
544.0100	2.1074481	99.7927780	0.0330835
545.4518	2.1001220	99.7984161	0.0339027
546.8188	2.0989010	99.8551331	0.0327157
548.1861	2.1001220	99.8504868	0.0339818
549.5522	2.0989010	99.9078369	0.0292436
550.9188	2.1074481	99.8506546	0.0236390
552.3050	2.0989010	99.9083328	0.0187990
553.6717	2.1001220	99.8516998	0.0160807
555.0373	2.0989010	100.3047180	0.0106660
556.4045	2.1001220	99.7390823	0.0099506
557.7716	2.0976801	99.8536377	0.0081861
559.1601	2.1111109	99.8500443	0.0056552
560.5865	2.0976801	99.7387543	0.0043484
561.9518	2.0989010	99.7385330	0.0064186
563.3396	2.1025641	100.0189285	0.0108273
564.7068	2.0976801	99.9644470	0.0138025
566.0741	2.1050060	100.1283722	0.0166451
567.5063	2.0989010	100.2501373	0.0194948
568.8743	2.0952380	100.0213089	0.0196891
570.2408	2.1001220	100.0234146	0.0246890
571.6281	2.1025641	99.9656067	0.0233524
572.9948	2.1050060	99.7918930	0.0235959
574.4367	2.1001220	99.9155807	0.0231892
575.8033	2.0989010	100.2534714	0.0217136
577.1697	2.0976801	100.5325165	0.0194415
578.5365	2.0952380	100.3617172	0.0157393
579.9031	2.0989010	100.4758682	0.0108582
581.2710	2.1037850	100.4758148	0.0080666
582.6560	2.0964589	100.3056107	0.0079801
584.0224	2.0976801	100.3622742	0.0077757
585.3886	2.0989010	100.3049393	0.0138453
586.7555	2.0976801	100.4185791	0.0156658
588.1234	2.1050060	100.4180298	0.0157393
589.4925	2.0940170	100.4745865	0.0145258
590.8813	2.0976801	100.4773178	0.0136719
592.2475	2.0976801	100.0749359	0.0158771
593.6153	2.0976801	100.0259094	0.0165107
594.9820	2.1135530	100.0719986	0.0178107
596.4981	2.0952380	100.2127304	0.0206816
597.8650	2.0964589	100.4393768	0.0223609
599.2320	2.0952380	101.1616287	0.0242187

600.6005	2.0927961	100.8748169	0.0216797
601.9652	2.0976801	100.9900513	0.0199531
603.3306	2.1013429	100.8192062	0.0193763
604.7160	2.0940170	100.5898666	0.0178105
606.0826	2.0989010	100.6470261	0.0163924
607.4493	2.0976801	100.6465836	0.0157558
608.8151	2.0964589	100.6461334	0.0098219
610.1825	2.1013429	100.8170853	0.0033429
611.5683	2.0940170	100.9337616	-0.0002621
612.9331	2.0952380	100.9329758	-0.0020288
614.2983	2.0952380	100.5919876	0.0041841
615.6640	2.0964589	100.5932693	0.0087982
617.0512	2.1086690	100.7016525	0.0145833
618.4761	2.0940170	100.5947723	0.0163411
619.8433	2.0927961	100.5906448	0.0171786
621.2331	2.0976801	101.1601715	0.0175039
622.5979	2.0964589	100.7595444	0.0173647
623.9639	2.0964589	100.7034378	0.0164062
625.3297	2.1025641	100.9264908	0.0179223
626.7820	2.0940170	100.9385681	0.0192157
628.1481	2.0927961	101.0509567	0.0208551
629.5159	2.0964589	101.1614609	0.0210725
630.8823	2.0940170	101.2192230	0.0172414
632.2486	2.1001220	100.9898834	0.0158377
633.6335	2.0927961	101.1623611	0.0134303
634.9995	2.0976801	101.1048508	0.0097062
636.3658	2.0927961	101.1044083	0.0114293
637.7335	2.0952380	101.0469284	0.0057147
639.0998	2.1001220	101.1620789	-0.0000658
640.4858	2.0940170	101.0477142	-0.0042172
641.8513	2.0952380	101.1049652	-0.0063125
643.2180	2.0952380	101.3339462	-0.0062303
644.5840	2.0940170	100.9898224	-0.0002615
645.9513	2.0952380	101.1616287	0.0054830
647.3191	2.1013429	101.2187195	0.0086724
648.6893	2.0915749	101.1607895	0.0121618
650.0777	2.0940170	101.1630859	0.0148129
651.4429	2.0952380	100.8155212	0.0185618
652.8088	2.0952380	100.8778305	0.0178015
654.1751	2.1086690	100.8124466	0.0201613
655.6926	2.0903540	101.0099564	0.0217109
657.0590	2.0952380	101.1204147	0.0230759
658.4266	2.0915749	101.6214981	0.0270639
659.7931	2.0927961	101.5639572	0.0264698
661.1600	2.0976801	101.6221695	0.0271767
662.5462	2.0915749	101.5066147	0.0279588
663.9124	2.0940170	101.5069504	0.0284950
665.2789	2.0940170	101.6792908	0.0273642
666.6452	2.0927961	101.3339462	0.0221859
668.0118	2.0940170	101.5636749	0.0164785
669.3791	2.0989010	101.6209869	0.0100000
670.7670	2.0891330	101.6229019	0.0021676
672.1331	2.0927961	101.6798553	-0.0032169

Entire data set for Run No. 11, November 6, 1986

Flowrate = 3.7cc/min Pressure Drop = 0.408 psi  
 Tracer Concentration = 104 ppm Step Down Cycle  
 Actual Test Start Time = 59.3 secs

Clock Time (sec)	Electrode Voltage Drop (volts)	Effluent Tracer Concentration (ppm)	Equivalent Slug Data (ppm/sec)
16.9425	2.0818069	103.9001465	0.0334543
18.3096	2.0818069	104.1334457	0.0195365
19.6771	2.0830281	104.5438461	0.0161277
21.0448	2.0805860	103.7779999	0.0148737
22.4113	2.0793650	104.0717926	0.0166593
23.7998	2.0976801	104.1283722	0.0209240
25.2949	2.0757020	104.0817566	0.0247546
26.6620	2.0818069	103.9625092	0.0251774
28.0288	2.0818069	104.5470276	0.0271925
29.4182	2.0818069	104.3661728	0.0233780
30.7859	2.0854700	104.3070297	0.0185140
32.2065	2.0793650	104.3076096	0.0139461
33.5956	2.0830281	104.3087616	0.0120274
34.9623	2.0818069	104.3061676	0.0136531
36.3292	2.0818069	104.4253464	0.0064718
37.6964	2.0854700	104.6032333	0.0020238
39.0620	2.0769229	104.6025925	-0.0030227
40.4297	2.0793650	104.5438461	-0.0084259
41.8185	2.0818069	104.7794495	-0.0144246
43.1854	2.0830281	104.3059921	-0.0128447
44.5522	2.0805860	104.2482147	-0.0139569
45.9190	2.0866909	104.2464294	-0.0148886
47.3671	2.0805860	104.3084793	-0.0151555
48.7348	2.0818069	104.2504120	-0.0164603
50.1015	2.0818069	104.1297607	-0.0142806
51.4681	2.0818069	104.1311417	-0.0133092
52.8349	2.0891330	104.0137939	-0.0080976
54.2880	2.0805860	104.0147171	-0.0022578
55.6548	2.0842490	104.0754776	0.0047360
57.0223	2.0818069	104.2478714	0.0117766
58.3894	2.0805860	104.1301041	0.0141870
59.7577	2.0854700	104.1912766	0.0147668
61.2010	2.0830281	104.2491989	0.0151847
62.5672	2.0830281	104.1316605	0.0150474
63.9341	2.0805860	104.4844894	0.0154533
65.3015	2.0830281	104.2479248	0.0105884
66.6700	2.0781441	104.4845505	0.0065199
68.0388	2.0879121	104.5426865	0.0006765
69.4286	2.0781441	104.7226334	-0.0060877
70.7991	2.0793650	104.4851837	-0.0131218
72.1689	2.0793650	104.4845505	-0.0125741
73.5391	2.0830281	104.3683701	-0.0189105
74.9092	2.0879121	104.3651352	-0.0263960
76.3385	2.0805860	104.2524872	-0.0347437

77.7092	2.0793650	104.3691177	-0.0472337
79.0781	2.0818069	103.9528961	-0.0603170
80.4483	2.0805860	104.0189209	-0.0797135
81.8178	2.0964589	103.9482956	-0.1011385
83.3378	2.0793650	103.8443756	-0.1271037
84.7081	2.0805860	103.7290115	-0.1556257
86.0786	2.0842490	104.3069153	-0.1896588
87.4488	2.0830281	103.7156906	-0.2260490
88.8193	2.0842490	103.4813690	-0.2652498
90.1682	2.0915749	103.2516861	-0.3037317
91.5575	2.0854700	102.8382416	-0.3428416
92.9274	2.0891330	102.2565689	-0.3800762
94.2980	2.0915749	101.6215515	-0.4188707
95.6684	2.0964589	100.8819122	-0.4599733
97.0385	2.1050060	99.9780121	-0.5008913
98.4622	2.1013429	99.0494995	-0.5392412
99.8329	2.1086690	98.1620407	-0.5751563
101.2037	2.1111109	97.2830582	-0.6022831
102.5889	2.1159949	96.4039764	-0.6295300
103.9533	2.1245420	95.7055969	-0.6535990
105.3976	2.1208789	94.8670197	-0.6738004
106.7614	2.1245420	94.0155106	-0.6910328
108.1252	2.1294260	93.2829437	-0.7047331
109.4890	2.1355309	91.9223557	-0.7158417
110.8751	2.1416359	90.8310242	-0.7247628
112.2386	2.1526251	89.8187103	-0.7339708
113.6881	2.1501830	88.7653046	-0.7422509
115.0516	2.1538460	87.5739899	-0.7505344
116.4140	2.1599510	86.5549164	-0.7565491
117.7996	2.1709399	85.4284515	-0.7655002
119.1642	2.1782660	84.3313751	-0.7714286
120.6043	2.1782660	83.1538239	-0.7760696
121.9677	2.1819291	82.2245865	-0.7785566
123.3313	2.1892550	81.2180176	-0.7784013
124.7167	2.1953599	80.2391434	-0.7841682
126.0807	2.2051280	79.1586456	-0.7898886
127.4427	2.2039070	78.1815872	-0.7955424
128.8290	2.2112341	77.0660629	-0.8011319
130.1942	2.2161181	76.1956024	-0.8076336
131.5566	2.2258861	74.7459183	-0.8106142
132.9206	2.2295480	73.7039642	-0.8148736
134.3061	2.2454219	72.4950104	-0.8187335
135.7293	2.2417581	71.4015121	-0.8228061
137.1157	2.2515261	70.2332001	-0.8263214
138.4802	2.2576311	68.8216171	-0.8283620
139.8448	2.2649579	67.7263718	-0.8308641
141.2315	2.2893779	66.5477600	-0.8318833
142.7231	2.2771671	65.2382584	-0.8310826
144.1090	2.2893779	64.1112442	-0.8291371
145.4735	2.2979240	63.2891350	-0.8225791
146.8383	2.3028080	62.0815315	-0.8184516
148.2032	2.3174601	61.0312004	-0.8139834
149.5868	2.3186820	59.9160233	-0.8091668
150.9522	2.3260069	58.7003555	-0.8034723

152.3162	2.3369961	57.6455765	-0.7982470
153.6803	2.3467641	56.3173599	-0.7959834
155.0664	2.3565321	55.2822762	-0.7929524
156.4316	2.3687429	54.1937332	-0.7894421
157.7939	2.3650801	53.1583748	-0.7870784
159.1807	2.3797319	52.2128105	-0.7845782
160.5455	2.3882790	51.1794930	-0.7767795
161.9097	2.3943839	50.0301819	-0.7705820
163.2740	2.4114780	49.0417709	-0.7635571
164.6630	2.4139199	47.9443855	-0.7547896
166.0261	2.4224670	46.8368187	-0.7455819
167.3906	2.4358981	45.7571983	-0.7348356
168.7555	2.4444449	44.7586327	-0.7259685
170.1426	2.4615390	43.7875099	-0.7166160
171.5716	2.4615390	42.6929665	-0.7071356
172.9350	2.4688649	41.6915054	-0.6979568
174.3215	2.4884009	40.9051247	-0.6875938
175.6857	2.4957271	39.8416672	-0.6764087
177.0508	2.5018320	38.8743134	-0.6649767
178.4142	2.5177050	38.0811310	-0.6522412
179.7976	2.5213680	37.2704201	-0.6389188
181.1634	2.5323570	36.4682388	-0.6265817
182.5281	2.5409040	35.6228561	-0.6143872
183.9141	2.5482299	34.7302361	-0.6044445
185.2784	2.5677660	33.8929977	-0.5935995
186.7191	2.5750921	32.9303284	-0.5833659
188.0833	2.5848601	32.0795364	-0.5724198
189.4488	2.5995121	31.3029366	-0.5591046
190.8149	2.6043961	30.6298504	-0.5464403
192.2014	2.6202691	29.9109001	-0.5350524
193.6246	2.6214900	29.2256699	-0.5231371
195.0098	2.6349211	28.4900208	-0.5109562
196.3752	2.6471310	27.8442421	-0.4985226
197.7393	2.6581199	26.9288197	-0.4857847
199.1052	2.6691091	26.3238354	-0.4737104
200.4927	2.6923079	25.6775436	-0.4613005
201.9846	2.6837609	25.0821152	-0.4503129
203.3701	2.6996341	24.5538349	-0.4403586
204.7325	2.7045181	24.0400963	-0.4301688
206.0965	2.7142861	23.4130993	-0.4198321
207.4829	2.7374849	22.8060188	-0.4092458
208.9016	2.7399271	22.1859474	-0.3984611
210.2878	2.7545791	21.5980339	-0.3877891
211.6513	2.7606840	21.0923920	-0.3768271
213.0144	2.7704520	20.5768642	-0.3688268
214.3997	2.7875459	20.1110935	-0.3606056
215.8394	2.7924299	19.6022644	-0.3524465
217.2023	2.8021979	19.1101875	-0.3441668
218.5659	2.8119659	18.7161713	-0.3351777
219.9517	2.8241761	18.2208252	-0.3252611
221.3164	2.8315020	17.8083096	-0.3159189
222.6774	2.8473749	17.3657990	-0.3072316
224.0439	2.8498170	16.9808426	-0.2990798
225.4293	2.8644691	16.5793800	-0.2914235

226.7926	2.8705740	16.1556034	-0.2838525
228.1569	2.8803420	15.7736931	-0.2768447
229.5429	2.9010990	15.4206066	-0.2693521
230.9720	2.8998780	15.0113897	-0.2621068
232.3355	2.9108670	14.6465702	-0.2553010
233.7211	2.9242980	14.3342237	-0.2476613
235.0851	2.9316239	13.9985046	-0.2406741
236.4487	2.9450550	13.6617146	-0.2337569
237.8326	2.9487181	13.3592272	-0.2272050
239.1969	2.9609280	13.0672522	-0.2205926
240.5619	2.9694750	12.7743511	-0.2140665
241.9254	2.9768009	12.4570808	-0.2082256
243.3112	2.9914529	12.1945095	-0.2023174
244.6735	3.0000000	11.9274282	-0.1960406
246.0553	3.0036631	11.6552830	-0.1902307
247.4194	3.0146520	11.4394999	-0.1849652
248.7836	3.0231991	11.1876163	-0.1792224
250.1484	3.0293040	10.9356422	-0.1739938
251.5341	3.0451770	10.6861649	-0.1689619
252.9574	3.0500610	10.4415216	-0.1639284
254.3434	3.0610499	10.2154703	-0.1587958
255.7077	3.0683761	9.9832859	-0.1537680
257.0721	3.0732601	9.7932158	-0.1494173
258.4367	3.0915749	9.6228647	-0.1452032
259.8944	3.0891330	9.4207230	-0.1412676
261.2586	3.0964589	9.2118740	-0.1376114
262.6217	3.1086690	9.0631618	-0.1338531
264.0062	3.1184371	8.8562746	-0.1301294
265.3690	3.1245420	8.6945448	-0.1266627
266.7337	3.1343100	8.5354328	-0.1234374
268.0963	3.1330891	8.3840761	-0.1204124
269.4834	3.1452990	8.2273130	-0.1174802
270.8475	3.1538460	8.0560532	-0.1147168
272.2106	3.1611731	7.8900752	-0.1122330
273.5952	3.1758239	7.7241359	-0.1094655
275.0356	3.1746030	7.5649638	-0.1067117
276.4007	3.1868131	7.4120584	-0.1042072
277.7659	3.1929181	7.2801242	-0.1015027
279.1318	3.2014649	7.1451173	-0.0989435
280.5170	3.2112341	7.0155578	-0.0965170
281.9400	3.2112341	6.8804545	-0.0940756
283.3248	3.2222221	6.7638178	-0.0915433
284.6899	3.2295489	6.6628242	-0.0889496
286.0553	3.2344320	6.5086308	-0.0865910
287.4208	3.2405379	6.4070716	-0.0843807
288.8079	3.2564099	6.2971520	-0.0823794
290.2384	3.2527471	6.1776605	-0.0803262
291.6028	3.2625151	6.0694356	-0.0785572
292.9677	3.2698419	5.9778390	-0.0766989
294.3547	3.2747259	5.8593454	-0.0749745
295.7203	3.2857151	5.7557697	-0.0732025
297.1611	3.2905991	5.6481647	-0.0716351
298.5262	3.2967031	5.5550408	-0.0699920
299.8918	3.3040299	5.4559212	-0.0682142

301.2576	3.3064711	5.3654780	-0.0669214
302.6420	3.3199029	5.2749615	-0.0654086
304.0815	3.3223441	5.1995769	-0.0639092
305.4444	3.3284500	5.1028476	-0.0624635
306.8070	3.3296709	5.0306153	-0.0610766
308.1914	3.3418801	4.9407096	-0.0595307
309.5555	3.3467650	4.8699274	-0.0583374
310.9191	3.3553121	4.7776737	-0.0571971
312.3075	3.3553121	4.7041616	-0.0561351
313.6715	3.3650801	4.6266689	-0.0549936
315.0343	3.3699639	4.5445633	-0.0538010
316.3982	3.3772900	4.4822764	-0.0526203
317.7830	3.3882790	4.4112587	-0.0513915
319.2757	3.3809519	4.3364868	-0.0500101
320.6623	3.3943839	4.2641282	-0.0487966
322.0248	3.3992679	4.2056055	-0.0475750
323.3873	3.4078150	4.1220565	-0.0464956
324.7717	3.4139199	4.0577884	-0.0453234
326.2102	3.4175830	3.9922822	-0.0442789
327.5743	3.4224670	3.9388945	-0.0431933
328.9394	3.4273510	3.8938725	-0.0421559
330.3264	3.4322350	3.8373611	-0.0412389
331.6902	3.4346769	3.7903602	-0.0402755
333.0538	3.4432240	3.7386544	-0.0393079
334.4373	3.4444449	3.6814435	-0.0384479
335.8017	3.4517710	3.6232097	-0.0376427
337.1661	3.4590969	3.5659244	-0.0367065
338.5299	3.4627600	3.5169022	-0.0361370
339.9171	3.4713070	3.4677565	-0.0356481
341.3410	3.4688649	3.4230106	-0.0352022
342.7265	3.4761910	3.3750236	-0.0347616
344.0898	3.4810750	3.3280866	-0.0342199
345.4547	3.4871800	3.2814353	-0.0336506
346.8182	3.4957271	3.2398818	-0.0330072
348.1918	3.4932849	3.1916492	-0.0322936
349.5792	3.4981689	3.1480882	-0.0316002
350.9448	3.5067160	3.1167574	-0.0309338
352.3090	3.5103791	3.0615208	-0.0302845
353.6731	3.5128210	3.0181730	-0.0296328
355.0580	3.5238099	2.9769435	-0.0289672
356.4984	3.5225890	2.9344318	-0.0282471
357.8640	3.5299151	2.8947356	-0.0275768
359.2291	3.5335779	2.8573618	-0.0268954
360.5942	3.5360200	2.8222933	-0.0264253
361.9801	3.5457880	2.7892313	-0.0258912
363.3983	3.5433459	2.7536709	-0.0254191
364.7847	3.5494511	2.7213387	-0.0249326
366.1500	3.5543351	2.6934462	-0.0243175
367.5146	3.5555561	2.6618187	-0.0237881
368.8793	3.5628819	2.6323104	-0.0233787
370.2692	3.5628819	2.6025164	-0.0229863
371.6338	3.5677660	2.5677359	-0.0226460
372.9984	3.5726500	2.5410573	-0.0223802
374.3636	3.5775340	2.4918351	-0.0220784

375.7508	3.5799761	2.4655931	-0.0217367
377.1147	3.5946281	2.4345667	-0.0213556
378.6080	3.5848601	2.4051926	-0.0209709
379.9950	3.5934069	2.3780782	-0.0205764
381.3597	3.5958490	2.3584073	-0.0201599
382.7236	3.5982909	2.3246198	-0.0198346
384.1094	3.6080589	2.2978005	-0.0195237
385.5281	3.6080589	2.2687764	-0.0191666
386.9149	3.6117220	2.2390084	-0.0187690
388.2800	3.6153851	2.2183537	-0.0182633
389.6440	3.6190481	2.1977844	-0.0179273
391.0096	3.6227109	2.1772275	-0.0175060
392.3939	3.6227109	2.1548724	-0.0171219
393.7585	3.6263740	2.1313317	-0.0167857
395.1235	3.6312580	2.1063733	-0.0164786
396.5103	3.6361420	2.0727377	-0.0161331
397.8753	3.6410260	2.0452721	-0.0158740
399.2398	3.6471310	2.0242739	-0.0156524
400.6867	3.6471310	2.0074182	-0.0154140
402.0496	3.6471310	1.9930983	-0.0152260
403.4121	3.6483519	1.9756935	-0.0149610
404.7973	3.6520150	1.9612963	-0.0147046
406.1615	3.6605620	1.9426246	-0.0144166
407.5904	3.6581199	1.9168353	-0.0141618
408.9755	3.6617830	1.8950272	-0.0138869
410.3406	3.6678879	1.8736439	-0.0136142
411.7041	3.6691091	1.8525827	-0.0134757
413.0880	3.6776559	1.8311927	-0.0133799
414.5277	3.6752141	1.8169880	-0.0132642
415.8925	3.6788771	1.7991753	-0.0131306
417.2572	3.6788771	1.7873809	-0.0129426
418.6208	3.6837609	1.7652140	-0.0127672
420.0069	3.6874239	1.7487102	-0.0125551
421.3705	3.6935289	1.7269077	-0.0123222
422.7319	3.6923079	1.7124820	-0.0121381
424.1174	3.6971920	1.6978991	-0.0120168
425.4816	3.6959710	1.6807296	-0.0118397
426.8450	3.6996341	1.6667001	-0.0117848
428.2317	3.7081809	1.6539249	-0.0117482
429.6550	3.7045181	1.6365974	-0.0116802
431.0413	3.7081809	1.6212175	-0.0115847
432.4047	3.7106230	1.6003940	-0.0113645
433.7686	3.7130649	1.5855596	-0.0111591
435.1320	3.7264960	1.5705979	-0.0109345
436.5904	3.7179489	1.5535307	-0.0106985
437.9536	3.7216120	1.5361392	-0.0104652
439.3170	3.7252750	1.5282223	-0.0102363
440.6817	3.7289381	1.5055356	-0.0100513
442.0674	3.7338221	1.4920132	-0.0098780
443.4317	3.7387061	1.4762611	-0.0097073
444.7938	3.7338221	1.4658051	-0.0095575
446.1794	3.7399271	1.4578910	-0.0094145
447.5441	3.7387061	1.4487543	-0.0092656
448.9075	3.7411480	1.4371617	-0.0091528

450.2726	3.7472529	1.4307261	-0.0090211
451.6562	3.7448111	1.4177556	-0.0089318
453.0207	3.7460320	1.4037459	-0.0088546
454.3839	3.7509160	1.3886471	-0.0087248
455.7700	3.7545791	1.3734660	-0.0086806
457.1347	3.7619050	1.3573351	-0.0086603
458.5802	3.7594631	1.3444135	-0.0086960
459.9441	3.7619050	1.3309371	-0.0087099
461.3094	3.7631259	1.3261302	-0.0086771
462.6945	3.7680099	1.3112607	-0.0086061
464.0589	3.7667890	1.3016953	-0.0084624
465.4234	3.7741151	1.2896898	-0.0082255
466.8731	3.7716730	1.2795064	-0.0079601
468.2370	3.7753360	1.2688887	-0.0077085
469.6023	3.7777779	1.2594423	-0.0074950
470.9676	3.7777779	1.2464824	-0.0074060
472.3545	3.7838831	1.2334633	-0.0073553
473.7728	3.7851040	1.2225506	-0.0073140
475.1580	3.7887671	1.2120934	-0.0072832
476.5215	3.7887671	1.2017133	-0.0071687
477.8854	3.7887671	1.1982813	-0.0071263
479.2731	3.7948720	1.1913888	-0.0070347
480.7133	3.7887671	1.1841743	-0.0069431
482.0763	3.7960930	1.1739452	-0.0068402
483.4407	3.7960930	1.1649427	-0.0067043
484.8055	3.7997561	1.1456957	-0.0064861
486.1923	3.8046401	1.1377592	-0.0063311
487.5563	3.8095241	1.1277337	-0.0062215
489.0024	3.8046401	1.1197158	-0.0061444
490.3678	3.8070819	1.1130557	-0.0061052
491.7324	3.8083031	1.0998650	-0.0060630
493.0968	3.8119659	1.0956274	-0.0060336
494.4835	3.8241761	1.0878589	-0.0059643
495.9769	3.8095241	1.0788891	-0.0058518
497.3427	3.8156290	1.0746171	-0.0057845
498.7302	3.8180709	1.0744832	-0.0057070
500.0955	3.8168499	1.0636983	-0.0056936
501.4575	3.8241761	1.0551103	-0.0056936
502.8391	3.8217340	1.0453186	-0.0056948
504.2015	3.8253970	1.0357488	-0.0056383
505.5643	3.8290601	1.0294143	-0.0055353
506.9508	3.8278389	1.0154870	-0.0055083
508.3140	3.8315020	1.0092344	-0.0054176
509.6781	3.8376069	1.0029720	-0.0053423
511.0622	3.8327229	0.9913812	-0.0053089
512.4256	3.8363860	0.9841325	-0.0052721
513.7946	3.8412700	0.9799960	-0.0051375
515.1651	3.8400490	0.9717750	-0.0050630
516.5340	3.8424909	0.9655997	-0.0049936
517.9835	3.8424909	0.9633852	-0.0049257
519.3543	3.8437121	0.9603761	-0.0048541
520.7242	3.8437121	0.9522067	-0.0047566
522.0933	3.8437121	0.9481924	-0.0047281
523.4624	3.8522589	0.9411719	-0.0046630

524.8968	3.8473749	0.9307016	-0.0045959
526.2638	3.8522589	0.9207729	-0.0045782
527.6307	3.8559220	0.9158559	-0.0045914
528.9961	3.8559220	0.9058957	-0.0046085
530.3843	3.8583641	0.8989260	-0.0046701
531.7507	3.8595850	0.8940606	-0.0047128
533.1919	3.8608060	0.8899381	-0.0047180
534.5574	3.8620269	0.8850418	-0.0046701
535.9229	3.8608060	0.8782163	-0.0046112
537.2885	3.8644691	0.8752961	-0.0045793
538.6549	3.8681321	0.8694597	-0.0044959
540.0406	3.8644691	0.8635690	-0.0044462
541.4060	3.8693531	0.8558181	-0.0043810
542.7706	3.8681321	0.8472125	-0.0042795
544.1373	3.8742371	0.8386576	-0.0041667
545.5256	3.8791211	0.8338150	-0.0040980
546.9503	3.8754580	0.8261012	-0.0040150
548.3177	3.8754580	0.8213815	-0.0039300
549.7058	3.8778999	0.8184983	-0.0038447
551.0728	3.8803420	0.8062420	-0.0037760
552.4380	3.8827839	0.8054228	-0.0036841
553.8032	3.8913310	0.7997935	-0.0035802
555.3186	3.8766789	0.7979658	-0.0034950
556.6861	3.8852260	0.7960525	-0.0034556
558.0537	3.8827839	0.7959952	-0.0034175
559.4202	3.8852260	0.7876365	-0.0034566
560.7860	3.8913310	0.7839535	-0.0034747
562.1705	3.8876679	0.7774255	-0.0035163
563.5375	3.8901100	0.7719139	-0.0035075
564.9045	3.8913310	0.7664067	-0.0034876
566.2703	3.8925519	0.7609412	-0.0035261
567.6362	3.8986571	0.7572929	-0.0035298
569.0218	3.8949940	0.7499712	-0.0035329
570.3881	3.8949940	0.7427434	-0.0035087
571.7536	3.9010990	0.7409784	-0.0034353
573.1190	3.9023199	0.7320216	-0.0033121
574.5073	3.9010990	0.7283754	-0.0032245
575.8733	3.9072039	0.7239538	-0.0031325
577.2988	3.8998780	0.7238937	-0.0030648
578.6872	3.9072039	0.7185325	-0.0030058
580.0538	3.9023199	0.7158653	-0.0029393
581.4203	3.9084251	0.7114794	-0.0029363
582.7868	3.9108670	0.7089223	-0.0029266
584.2186	3.9059830	0.7034948	-0.0029429
585.6067	3.9108670	0.7017316	-0.0029974
586.9724	3.9096460	0.6973310	-0.0030244
588.3389	3.9108670	0.6929726	-0.0030740
589.7053	3.9169719	0.6886187	-0.0030753
591.0708	3.9120879	0.6834039	-0.0030960
592.4582	3.9169719	0.6790251	-0.0030711
593.8243	3.9169719	0.6772861	-0.0030696
595.1908	3.9169719	0.6669424	-0.0031200
596.5584	3.9194140	0.6626396	-0.0031619
597.9245	3.9267399	0.6583748	-0.0031553

599.2904	3.9230771	0.6532449	-0.0031437
600.6790	3.9230771	0.6489798	-0.0030998
602.0436	3.9242980	0.6472597	-0.0029631
603.4086	3.9255190	0.6481257	-0.0028825
604.7734	3.9291821	0.6430477	-0.0028169
606.1414	3.9218559	0.6396667	-0.0027704
607.5282	3.9304030	0.6345555	-0.0027014
608.8936	3.9291821	0.6236283	-0.0026120
610.2596	3.9328451	0.6203609	-0.0025917
611.6245	3.9450550	0.6194962	-0.0025767
613.0613	3.9267399	0.6162304	-0.0025494
614.4480	3.9316239	0.6128926	-0.0025511
615.8146	3.9340661	0.6186416	-0.0025641
617.1801	3.9377289	0.6095340	-0.0025557
618.5458	3.9365079	0.6045857	-0.0024742
619.9131	3.9401710	0.5996411	-0.0024168
621.2987	3.9389501	0.5987917	-0.0023577
622.6638	3.9413919	0.5946965	-0.0022986
624.0303	3.9389501	0.5906064	-0.0022867
625.3962	3.9426129	0.5873534	-0.0023138
626.7622	3.9462759	0.5857312	-0.0023122
628.1478	3.9438341	0.5808193	-0.0022906
629.5153	3.9438341	0.5775803	-0.0022662
630.8823	3.9462759	0.5743611	-0.0021649
632.2472	3.9474969	0.5735690	-0.0021292
633.6341	3.9511600	0.5695192	-0.0021052
635.0586	3.9450550	0.5654315	-0.0020977
636.4241	3.9499390	0.5638730	-0.0020593
637.8118	3.9523809	0.5638503	-0.0020288
639.1777	3.9499390	0.5574626	-0.0019866
640.5441	3.9511600	0.5551051	-0.0019552
641.9102	3.9548230	0.5543539	-0.0019297
643.3616	3.9536021	0.5518492	-0.0019501
644.7281	3.9536021	0.5478956	-0.0019653
646.0938	3.9536021	0.5439537	-0.0019791
647.4602	3.9572649	0.5415940	-0.0019955
648.8261	3.9609280	0.5392280	-0.0020104
650.2133	3.9572649	0.5368585	-0.0020181
651.5795	3.9572649	0.5344906	-0.0020258
652.9454	3.9572649	0.5344891	-0.0020282
654.3112	3.9609280	0.5313640	-0.0021012
655.6770	3.9609280	0.5266852	-0.0021569
657.0625	3.9621489	0.5211706	-0.0021947
658.4300	3.9645910	0.5196276	-0.0022173
659.7973	3.9658120	0.5173033	-0.0022213
661.1641	3.9633701	0.5126626	-0.0021866
662.5295	3.9645910	0.5111519	-0.0021630
663.9173	3.9694750	0.5103719	-0.0021292
665.3439	3.9670329	0.5064341	-0.0020804
666.7101	3.9670329	0.5010814	-0.0020440
668.0761	3.9694750	0.4942777	-0.0019753
669.4643	3.9731381	0.4927432	-0.0019234
670.8309	3.9804640	0.4896497	-0.0018875
672.3250	3.9694750	0.4866604	-0.0018884